DEPARTMENT OF TRANSPORTATION

Establishing Fresh Properties of Fiber Reinforced Concrete for Performance Engineered Mixture (PEM)

Manik Barman, Principal Investigator
Department of Civil Engineering
University of Minnesota Duluth

JUNE 2022

Research Report
Final Report 2022-23

To request this document in an alternative format, such as braille or large print, call 651-366-4718 or 1-800-657-3774 (Greater Minnesota) or email your request to ADArequest.dot@state.mn.us. Please request at least one week in advance.

Technical Report Documentation Page

1. Report No. MN 2022-23	2.	3. Recipients Accession No.
4. Title and Subtitle Establishing Fresh Properties of Fiber Reinforced Concrete for Performance Engineered Mixture (PEM)		5. Report Date June 2022 6.
7. Author(s) Manik Barman, Alieu Kamara, Austin Janson		8. Performing Organization Report No.
9. Performing Organization Name and Address University of Minnesota Duluth Department of Civil Engineering 1405 Univ. Drive, Duluth, MN 55812		10. Project/Task/Work Unit No. CTS #2020007 11. Contract (C) or Grant (G) No. (c) 1003325 (wo) 112
12. Sponsoring Organization Name and Address Minnesota Department of Transportation Office of Research & Innovation 395 John Ireland Boulevard, MS 330 St. Paul, Minnesota 55155-1899		13. Type of Report and Period Covered 14. Sponsoring Agency Code
15. Supplementary Notes https://www.mndot.gov/research/reports/2022/202223.pdf		

16. Abstract (Limit: 250 words)

The addition of macro or structural fibers into concrete enhances its post-cracking performance. The objective of this study was to conduct a laboratory investigation to determine the influence of structural fibers on the fresh concrete test parameters (Super air meter (SAM) number, V-Kelly index, and Box test rating) recommended for the performance engineered mixture (PEM) procedure.

As many as fifty-seven different concrete mixes were designed and prepared, varying fiber types and dosages, aggregate types, and air contents of the concrete. Various fresh and hardened concrete tests were conducted on each of the mixes, and the results were used to determine the influence of the structural fibers on the fresh and hardened concrete properties. The study recommended the allowable range of the SAM number and provided necessary guidance on the box test rating and V-Kelly index for the fiber-reinforced concrete mixtures to be designed as per the PEM procedure.

17. Document Analysis/Descriptors Concrete pavements, Fiber reinforced concrete, Admixtures, Concrete tests		18. Availability Statement No restrictions. Document available from: National Technical Information Services, Alexandria, Virginia 22312	
19. Security Class (this report) Unclassified	20. Security Class (this page) Unclassified	21. No. of Pages 103	22. Price

Establishing Fresh Properties of Fiber Reinforced Concrete for Performance Engineered Mixture (PEM)

FINAL REPORT

Prepared by:

Manik Barman
Alieu Kamara
Austin Janson
Department of Civil Engineering
University of Minnesota Duluth

June 2022

Published by:

Minnesota Department of Transportation
Office of Research & Innovation
395 John Ireland Boulevard, MS 330
St. Paul, Minnesota 55155-1899

This report represents the results of research conducted by the authors and does not necessarily represent the views or policies of the Minnesota Department of Transportation or the University of Minnesota Duluth. This report does not contain a standard or specified technique.

The authors, the Minnesota Department of Transportation, and the University of Minnesota Duluth do not endorse products or manufacturers. Trade or manufacturers' names appear herein solely because they are considered essential to this report.

ACKNOWLEDGMENTS

The authors of this report gratefully acknowledge the financial support the Minnesota Department of Transportation provided for conducting this research. The research team is grateful to the Technical Advisory Panel (TAP) members, including the technical liaison Mr. Robert Golish, for providing valuable suggestions throughout this project. Also, special thanks go to the Project Coordinators, Mr. Leif Halverson, and the CTS colleagues for their time and administrative support.

The research team sincerely acknowledges the contribution of the post-doctoral associate Dr. Heena Dhasmana, several graduate and undergraduate students, faculties, and staff of the University of Minnesota Duluth (UMD), who helped the research team at different phases of this project.

TABLE OF CONTENTS

CHAPTER 1: INTRODUCTION **1**

CHAPTER 2: LITERATURE REVIEW **2**

2.1 INTRODUCTION 2

2.2 PERFORMANCE ENGINEERED CONCRETE MIXTURES 2

2.2.1 Aggregate Durability 2

2.2.2 Fluid Transport Property 2

2.2.3 Cold Weather Resistance 3

2.2.4 Shrinkage 6

2.2.5 Strength 8

2.2.6 Workability 10

2.3 FIBERS 10

2.3.1 Steel Fiber Reinforced Concrete (SFRC) 12

2.3.2 Synthetic Fiber Reinforced Concrete (SyFRC) 15

2.4 CONCLUSIONS 22

CHAPTER 3: MATERIALS AND MIXTURE DESIGNS **24**

3.1 FIBERS 24

3.2 CEMENTITIOUS MATERIALS 26

3.3 AGGREGATES 27

3.4 MIXTURE DESIGNS 31

3.5 MIXING PROCEDURE 32

3.6 CONCRETE TESTS 33

3.6.1 Slump Test 33

3.6.2 Air Content and SAM Test 34

3.6.3 Box Test 34

3.6.4 Vibrating Kelly Ball Test 36

3.6.5 Compressive Strength Test 36

3.6.6 Modulus of Elasticity Test 37

3.6.7 Beam Flexural Test 38

3.6.8 Electrical/Surface Resistivity Test 39

3.6.9 Rapid Freeze-Thaw Test 40

3.6.10 Formation Factor Bucket Test 41

CHAPTER 4: RESULTS AND DISCUSSIONS 42

4.1 RESULTS SUMMARY 42

4.2 DISCUSSIONS 48

4.2.1 Fresh Concrete Properties 48

4.2.2 Hardened Concrete Properties 58

CHAPTER 5: CONCLUSIONS AND RECOMMENDATIONS 74

5.1 CONCLUSIONS 74

5.2 RECOMMENDATIONS 75

5.2.1 SAM Number 75

5.2.2 Box Test Rating 76

5.2.3 V-Kelly Test 76

REFERENCES 77

APPENDIX A MISCELLENIOUS DATA

LIST OF FIGURES

Figure 2-1 Resistivity test in progress. 3

Figure 2-2 Illustration of the degree of saturation of concrete with time (Cackler et al., 2017). 4

Figure 2-3 Spacing factor vs. SAM number (Ley, 2015). 5

Figure 2-4 SAM number vs. durability factor (Ley, 2015). 5

Figure 2-5 SAM number vs. air content (Barman and Hansen, 2018). 6

Figure 2-6 Moisture warping and temperature curling of concrete slab (Mack, 2009). 7

Figure 2-7 Strain vs. time graph of drying shrinkage components (Mindess et al., 2008). 7

Figure 2-8 Long-term alternate wetting and drying shrinkage (Komatska and Wilson, 2016). 8

Figure 2-9 Tarantula curve showing recommended limits for aggregate gradation (Ley and Cook, 2014). 9

Figure 2-10 Influence of fly-ash in reducing calcium oxychloride content (Cackler et al., 2017). 10

Figure 2-11 Crack control and bridging effect of fibers (Gaddam, 2016). 11

Figure 2-12 Illustration of load vs deflection in plain concrete and FRC (after ACI Committee 544, 2009). 11

Figure 2-13 Stages of FRC failure (ACI.544.4R-18). 12

Figure 2-14 Strain softening and hardening behaviors (ACI.544.4R-18). 12

Figure 2-15 Various steel fiber geometries (Komatska and Wilson, 2016). 13

Figure 2-16 Photograph of steel fibers with hooked end (Barman, 2018). 13

Figure 2-17 Slump test output (Acikgenc et al., 2013). 14

Figure 2-18 SFRC strength at 28-day: a) Compressive strength, and b) Flexural strength (Acikgenc et al., 2013). 14

Figure 2-19 Effect of fiber reinforcement in peak differential displacement (Arnold et al., 2005). 15

Figure 2-20 Residual load characteristics of different shaped structural synthetic fibers (Bordelon, 2005). 17

Figure 2-21 Residual load capacities of FRC vs. fiber volume fraction for straight synthetic fibers (Bordelon, 2005). 17

Figure 2-22 Shrinkage vs. curing time for plain and FRC mixes (Alhassan and Ashur, 2012) (LMC = latex modified concrete; ARGF = alkali resistant glass fiber; SX= microtype polyolefin fiber; GF = micro type 100% virgin; NXL = macrotype polyolefin fiber; RSC = microtype polyvinyl alcohol fiber; RF = macrotype polyvinyl alcohol fiber). 18

Figure 2-23 (a) Compressive strength, (b) Modulus of elasticity, and (c) and (d) Modulus of rupture as a function of reinforcement index and fibers' volume fraction, respectively. 20

Figure 2-24 (a) RSR vs. Vf, (b) Correlation between RSR and V_f, (c) RS vs. V_f, (d) RSR as a function of V_f and fiber geometry. 21

Figure 2-25 Fibers used in the (Kevern et al., 2016) study: polypropylene fibrillated fiber (left), polypropylene macro fiber (left middle), carbon fiber (right middle), and steel fiber (right). 22

Figure 3-1. Fiber 1, Twisted on the left, Unfurled on the right 25

Figure 3-2. Photograph showing the length of Fiber 1 with Calipers 25

Figure 3-3. Fiber 2, straight embossed geometry. 26

Figure 3-4. Photograph showing the length of Fiber 2 with Calipers 26

Figure 3-5. Class A Aggregates, 3/4-inch and 1.5-inch (right side photograph) 27

Figure 3-6. Class B Aggregates 3/4-inch and 1.5-inch (right side photograph) 28

Figure 3-7. Class C Aggregates 3/4-inch and 1.5-inch (right side photograph) 28

Figure 3-8. Fine Aggregate 29

Figure 3-9. Gradations of the Individual Aggregates and Blends for Classes A, B, and C 30

Figure 3-10. Tarantula Curves for the three Aggregate Classes 31

Figure 3-11. Fiber Balling of Fiber 1 (Twisted Geometry) 33

Figure 3-12. Box Test in Progress 35

Figure 3-13. Surface Air Voids Ranking System for Box Test (Cook et al. 2016) 35

Figure 3-14. V-Kelly Test in Process 36

Figure 3-15. Compressive Strength Test 37

Figure 3-16. Modulus of Elasticity Test. 38

Figure 3-17. Four-Point Flexural Bend Test 39

Figure 3-18. Fibers Bridging a Crack 39

Figure 3-19. Freeze-Thaw Chamber 41

Figure 4-1. SAM Number vs. Air Content 48

Figure 4-2. Influence of Fiber Dosage on SAM Number (Air Content > 5.5%). 49

Figure 4-3. Influence of Fiber Type and Dosage on SAM Number (Aggregate A); A1 = aggregate A with fiber 1 (Twisted and bundled), A2 = aggregate A with fiber 2 (embossed geometry). 50

Figure 4-4. Influence of Fiber Type and Dosage on SAM Number (Aggregate B): B1 = aggregate B with fiber 1 (Twisted and bundled), B2 = aggregate B with fiber 2 (embossed geometry). 50

Figure 4-5. Influence of Fiber Type and Dosage on SAM Number (Aggregate C): C1 = aggregate C with fiber 1 (Twisted and bundled), C2 = aggregate C with fiber 2 (embossed geometry). 51

Figure 4-6. Box Test Rating vs Slump 52

Figure 4-7. Influence of Fiber Dosage on Box Test Rating 52

Figure 4-8. Influence Fiber Type on Box Test Rating (Aggregate Class A) 53

Figure 4-9. Influence of Fiber Type and Dosage on Box Test (Aggregate B) 53

Figure 4-10. Influence of Fiber Type and Dosage on Box Test (Aggregate C) 54

Figure 4-11. V-Kelly Slump vs Slump 55

Figure 4-12. V-Kelly Index vs Slump 55

Figure 4-13. Influence of Fiber Dosage on V-Kelly Index 56

Figure 4-14. Influence of Fiber Type on V-Kelly Index 56

Figure 4-15. Influence of Aggregate Type on V-Kelly Index (Aggregate A) 57

Figure 4-16. Influence of Fiber Type and Dosage on V-Kelly Index (Aggregate B) 57

Figure 4-17. Influence of Fiber Type and Dosage on V-Kelly Index (Aggregate C) 58

Figure 4-18. Compressive Strength vs. Air Content 59

Figure 4-19. Influence of Fiber Dosage on Compressive Strength 60

Figure 4-20. Influence of Fiber Type on Compressive Strength 60

Figure 4-21. Influence of Fiber Dosage on Modulus of Elasticity 61

Figure 4-22. MOR vs Air Content 62

Figure 4-23. Influence of Fiber Dosage on MOR 62

Figure 4-24. Influence of Fiber Type on MOR 63

Figure 4-25. Load vs. Displacement for Two Fiber Dosages (6 percent air voids) 64

Figure 4-26. Influence of Fiber Dosage on Toughness 64

Figure 4-27. Influence of Fiber Type on Toughness 65

Figure 4-28. Influence of Fiber Dosage on Residual Strength 66

Figure 4-29. Influence of Fiber Type on Residual Strength 66

Figure 4-30. Influence of Fiber Dosage on RSR 67

Figure 4-31. Influence of Fiber Type on RSR 67

Figure 4-32. Saturated Surface Resistivity vs Air Content 69

Figure 4-33. 28-day Saturated Surface Resistivity vs Air Content 71

Figure 4-34. Surface Resistivity vs. Air Content 72

Figure 4-35. Relative Dynamic Modulus (RDM) vs. Number of F/T Cycles 73

LIST OF TABLES

Table 2-1 Properties of structural synthetic fibers and FRC (Roesler et al. (2008)). 16

Table 2-2 Summary of fiber details (Barman and Hansen (2018)). 19

Table 2-3 Properties of fibers in Kevern et al. (2016) study. 22

Table 3-1. Description of fibers investigated in this task. 24

Table 3-2. Water Absorption and Bulk Specific Gravity of Aggregates. 29

Table 3-3. Mixture Design Details for Aggregate Class A (6% Air) 32

Table 4-1. Fresh Concrete Properties 42

Table 4-2. Hardened Concrete Test Results, Part 1 44

Table 4-3. Hardened Concrete Test Results Part 2. 46

Table 4-4. Performance Limits from the Rapid Chloride Permeability Test (RCPT), along with Equivalent Resistivity Values of a Saturated System (ASTM C1202) 68

Table 4-5. Resistivity Values of Calcium Hydroxide Saturated Specimens 70

Table 4-6. Chloride-ion Penetration Classification (AASHTO TP 95) 72

EXECUTIVE SUMMARY

The addition of structural fibers into concrete produces durable and ductile concretes with enhanced post-cracking performance. Minnesota has been using structural fibers in concrete pavements and overlays for decades and would like to increase the use of the same in thinner concrete overlays and bridge decks. On the other hand, Minnesota and many other states have implemented the performance engineered mixture (PEM) design for plain concrete. The concept of the PEM design procedure is to (i) assess the fresh properties of concrete using parameters representative of field conditions and (ii) produce concretes that are durable and long-lasting. Different types of concrete tests are recommended in the PEM design procedure, such as super air meter (SAM) (AASHTO TP 118), box (AASHTO PP-84), vibrating Kelly ball (V-Kelly) (AASHTO TP 129), and surface resistivity tests (AASHTO TP 95), etc. (Taylor, 2017). The SAM number provides an assessment of the concrete's resistance against freeze-thaw-related distresses. The box test rating assesses concrete's response to vibration and its ability to hold its shape without crumbling during slip-form paving application. The V-Kelly test examines the workability of concrete mixture and its response to vibration. While the different target parameters of the fresh concrete properties for the PEM procedure are known, they are unknown for fiber reinforced concrete (FRC).

The objective of this study was to conduct a laboratory investigation including various aggregates, fibers, and fiber dosages to determine the influence of the structural fibers on the fresh and hardened concrete test properties recommended for the PEM procedure.

The study began with a literature review focusing on the PEM, fibers, and fiber reinforced concrete for pavements. Then as many as 57 concrete mixes were designed and prepared with varying fresh concrete properties, fibers, fiber dosages, and coarse aggregate types. Two synthetic fibers were used: (i) Fiber 1 — twisted, bundled, 2.15 inches long; (ii) Fiber 2 — straight, embossed geometry, 2.15 inches long. Three different aggregates were used: Class A-granite, Class B-limestone, and Class C-gravel. Concretes were produced for three target design air voids, 4%, 6%, and 8%. Fresh and hardened concrete tests were conducted on each of the mixes, and the results were used to investigate the influence of the structural fibers on the fresh and hardened concrete properties. The major conclusions of the study were:

- The SAM number for the FRC mixes was not very different from the plain concrete; the average SAM numbers for FRC and plain concrete mixes were close to 0.2. Mixes with less than 5.5% air content consistently showed a very high SAM number. Between the three aggregates (Class A-granite, Class B-limestone, and Class C-gravel) used in this study, mixes with gravel showed a lower SAM number than those with the other two aggregate types.
- An increase in fiber dosage generally increased the box test rating. The influence of fiber dosage was more evident in mixes with a 0.50% V_f than in the other mixes. Some mixes with 0.5% V_f had visual ratings of more than 2 (high surface air voids). Aggregate C (gravel) mixes showed the least box test rating relative to the mixes with the other two aggregates.

- The addition of fibers in the mixture influences the V-Kelly index. Mixes with fiber dosage of 0.26% volume fraction had a V-Kelly index slightly below 0.8 in/√s (the recommended minimum value for plain concrete). Mixes with fiber dosage of 0.50% volume fraction were further below. Fiber type did not show a considerable influence on the V-Kelly index. Mixes with Aggregate C showed a higher V-Kelly index than the mixes with the other two aggregates.
- Structural synthetic fibers have a minimal effect on compressive strength and modulus of elasticity. Aggregate types had some influence on the compressive strength. Mixes with limestone Class B aggregate had higher compressive strength than identical mixes with granite Class A aggregate and gravel Class C aggregate due to the higher percentage of coarser aggregates and higher specific gravity. Aggregate C (gravel) resulted in the lowest compressive strength.
- The fiber dosage and type influenced the post-crack behavior and flexural toughness of hardened concrete. The average RSR improved from 20% to 36% when the fiber dosage increased from 0.26% to 0.50% V_f. The concrete mixes with Fiber 2 (embossed geometry) exhibited higher toughness than mixes with Fiber 1 for a given dosage. The embossed and deformed texture and higher stiffness of Fiber 2 likely contributed to the higher toughness. The types of aggregates used did not show any considerable variation in the concrete toughness.
- The resistivity and freeze-thaw test results indicated that synthetic fibers had no considerable effect on the resistivity readings, chloride-ion penetration, and freeze-thaw resistance, irrespective of the inclusion of fibers.

This study provides the following recommendations on the allowable range of the three fresh concrete properties mentioned above.

- As the concrete mixes prepared in this study do not show any considerable durability issues, at least in the laboratory condition, this study suggests that the SAM number of FRC mixes may be accepted above 0.2 (recommended for plain concrete mixes) when the mixes are designed as per the PEM method. This study recommends a maximum SAM number of 0.3 for the FRC mixes. The recommended SAM number 0.3 is approximately equal to the average of the SAM numbers of the FRC mixes plus one standard deviation (68% probability). As mentioned before, the standard deviations of the SAM number for the concrete mixes are pretty high (COV = 29% and 45% for FRC mixes); therefore, it will be challenging to achieve a strict target value close to the average of the results like 0.22 or 0.21. As the FRC mixes even with a higher SAM number (>0.3) produced in this study did not show any detrimental effect on the strength and durability, a SAM number of 0.3 may be considered acceptable and achievable (68% probability) and at the same time, mixes will assure sufficient freeze-thaw resistance.
- Based on the results of this study, it is recommended that when the fiber dosage is around 0.5% V_f or higher and crushed aggregates (e.g., Class A and Class B) are used in the mix, the additional amount of water reducer should be considered to adjust the workability.
- The study indicates that adding fibers to the mixture influences the V-Kelly index and workability of the concrete under vibration. Therefore, when fibers are used in the mixes, additional effort shall be given to improve the workability of the concrete so that the V-Kelly index can be improved to meet the target V-Kelly index of 0.8 in/√s or more. It may also happen that FRC does not need to meet the

0.8 in/√s criterion, as the fibers in the concrete offer resistance to the penetration of the Kelly-ball, which decreases the V-Kelly index. The hard concrete and durability test results for the FRC mixes indicate that FRC mixes with a lower V-Kelly index pass the strength and durability criteria. However, it is impossible to make any firm recommendation about the workability or finishability of the FRC mixes for the slip form paving if the V-Kelly index is lower than 0.8 in/√s. V-Kelly test results show that the fiber type has no significant influence on the V-Kelly index, at least for the two fibers used in this study, but the fiber dosage does. The V-Kelly indexes for mixes with granite and limestone aggregates are comparable; mixes with gravel aggregates result in a higher V-Kelly index among the three types of aggregates.

CHAPTER 1: INTRODUCTION

Structural or macro fibers are known to improve the long-term performance of concrete pavements and overlays. The addition of fibers into concrete mixtures produces more durable and ductile concretes with enhanced post-cracking performance and joint load transfer when sufficient dosage is implemented (Barman et al., 2021). Minnesota has been using structural fibers in concrete pavements and overlays, and bridge decks for decades (Burnham, 2015; Barman et al., 2010; Tanquist et al., 2013; Barman et al., 2018) and would like to increase the use of the same in thinner concrete overlays and bridge decks.

On the other hand, Minnesota and many other states have implemented the performance engineered mixture (PEM) design for plain concrete. The concept of the PEM design procedure is to (i) assess the fresh properties of concrete using parameters that are representative of field conditions and (ii) produce concretes that are durable and long-lasting. Different types of concrete tests are recommended in the PEM design procedure, such as super air meter (SAM) (AASHTO TP 118), box (AASHTO PP-84), vibrating Kelly ball (V-Kelly) (AASHTO TP 129), and surface resistivity tests (AASHTO TP 95), etc. (Taylor, 2017). The SAM number assesses the concrete's resistance against freeze-thaw-related distresses. The box test rating assesses concrete's response to vibration and its ability to hold its shape without crumbling during slip-form paving application. The V-Kelly test examines the workability of concrete mixture and its response to vibration. While the different target parameters of the fresh concrete properties for the PEM procedure are known, those for the fiber reinforced concrete (FRC) are unknown.

The objective of this study is to conduct a laboratory investigation including various aggregates, fibers, and fiber dosages to determine the influence of the structural fibers on the fresh and hardened concrete test properties recommended for the PEM procedure. The study will eventually recommend the allowable range for different fresh concrete properties: SAM number, box test rating, and V-Kelly index.

CHAPTER 2: LITERATURE REVIEW

2.1 INTRODUCTION

This chapter presents a comprehensive literature review on the performance engineered concrete mixture, fibers, and fiber reinforced concrete. The concept of the PEM and various important factors that affect the concrete as per the PEM design method are discussed in this chapter. Various types of fibers, with a particular emphasis on the fibers that are used in the pavements and bridge decks, such as steel and synthetic fibers, are discussed. The influence of the fibers on the various fresh and hard concrete properties related to the pavement application is discussed.

2.2 PERFORMANCE ENGINEERED CONCRETE MIXTURES

Advances in testing technology over the years have allowed the concrete pavement industry to recognize the strengths and weaknesses of concrete materials more efficiently and helped iron out many of the concrete's durability challenges that create obstacles to sustainability. In the concrete pavement context, sustainability focuses on developing concrete mixtures that are more efficient in their materials usage without compromising the engineering performance (Taylor et al., 2014). The PEM design procedure assesses the quality of concrete based on what it encounters in the field during pouring and its service life. The PEM mixture design procedure aims to produce concrete mixtures that resist climate- and material-related distresses, such as freeze-thaw damages and concrete degradation due to chloride-ion penetration. Some critical factors that affect the efficiency of the PEM design method are discussed below.

2.2.1 Aggregate Durability

The type of aggregates used in a concrete mixture can significantly impact concrete pavement's performance. The aggregates encounter distress when the concrete structure is exposed to extreme heat, cold, moisture, chemical deicers, and freeze-thaw (Cackler et al., 2017). To ensure the durability of aggregates in a concrete mixture, the PEM method specifies the following:

I. Coarse aggregates shall pass specific freeze-thaw requirements and are not prone to fracture/dilation when subjected to harsh winter conditions (Cackler et al., 2017).
II. Coarse aggregates are not prone to alkali-silica reactivity (ASR) or alkali-carbonate reactivity (ACR); supplementary cementitious materials (SCM) should be used, if necessary.

2.2.2 Fluid Transport Property

The transport properties of concrete pavement material help assess the resistance of materials against failure due to alkali-carbonate reaction (ACR), chloride penetration, and freeze-thaw. The PEM design requires that an electrical/surface resistivity test (AASHTO TP95, 2011) be conducted to evaluate the transport properties of concrete. The test method is based on the understanding that solid concrete is a poor conductor of electricity compared to concrete with fluid-filled pores. Therefore, the resistivity of

concrete is lower when the volume and connectivity of the pore system are higher (Cackler et al., 2017). Figure 2-1 shows the resistivity test in progress.

I. The fluid transport property in the PEM method is controlled by: Maintaining a water-cementitious material ratio between 0.40 and 0.45 to reduce capillary pore volume and void connectivity while avoiding undesired shrinkage.
II. Encouraging the use of SCMs at a specified dosage to improve the long-term transport performance.
III. Controlling concrete mixture hydration time and temperature, especially in cold climate regions, to resist freeze-thaw damage.

Figure 2-1 Resistivity test in progress.

2.2.3 Cold Weather Resistance

The PEM design uses the ASTM C666 test to determine the resistance of concrete against rapid freezing and thawing in cold climate regions. Figure 2-2 shows the critical saturation values of concrete and indicates that freeze-thaw damage is more likely when the concrete is saturated (Cackler et al., 2017). This figure illustrates that air-entrained concrete has a lower saturation rate and risk of freezing damage than the concrete mix with entrapped air voids.

The PEM method suggests the inclusion of an air-entraining admixture (AEA) in the mixture to protect concrete from freeze-thaw damage. The addition of AEA aids in stabilizing spherical air voids (0.0005 to 0.05 inches in diameter) and yields better workability while lowering segregation and bleeding (Ley, 2015). However, the compressive strength of concrete decreases by approximately 500 psi for every 1% increase in air content (Ley, 2015).

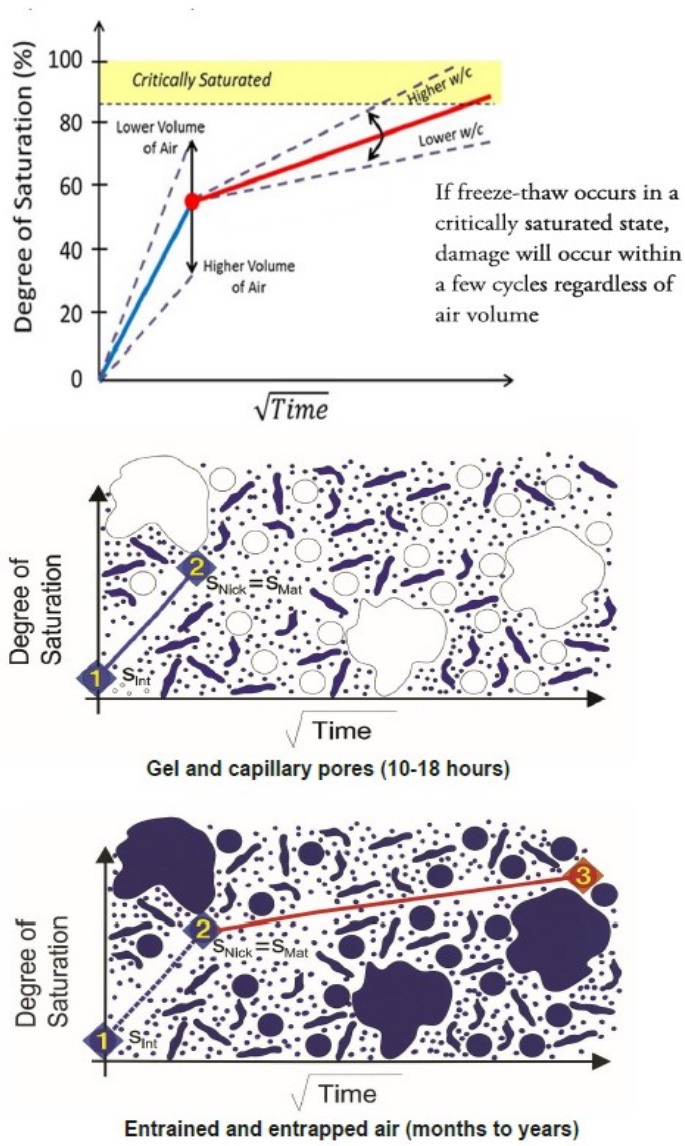

Figure 2-2 Illustration of the degree of saturation of concrete with time (Cackler et al., 2017).

Super Air Meter (SAM), developed by Oklahoma State University, is used to measure the quality of air void system in fresh concrete. As described by AASHTO TP 118, the SAM test provides the SAM number that defines air bubble spacing. Figure 2-3 and Figure 2-4 show results of 300 unique concrete mixtures (prepared in the laboratory and field) comparing the SAM number to spacing factor (bubble spacing) and durability factor in freeze-thaw testing, respectively (Ley, 2015). The spacing factor illustrates the air-void system quality, and the durability factor indicates the concrete performance in a freeze-thaw cycle. A SAM number of 0.20 (corresponding to the spacing factor = 0.008 inches and durability factor = 70%) or below is recommended for plain concrete mixtures subjected to harsh climate regions that include freezing and thawing. Barman and Hansen (2018) found that fiber reinforced concrete mixtures (not designed per the PEM method) can have a higher SAM number of more than 0.20 (Figure 2-5). It was observed that an

increase in entrained air content decreased the SAM number, and a large set of SAM numbers were above 0.2.

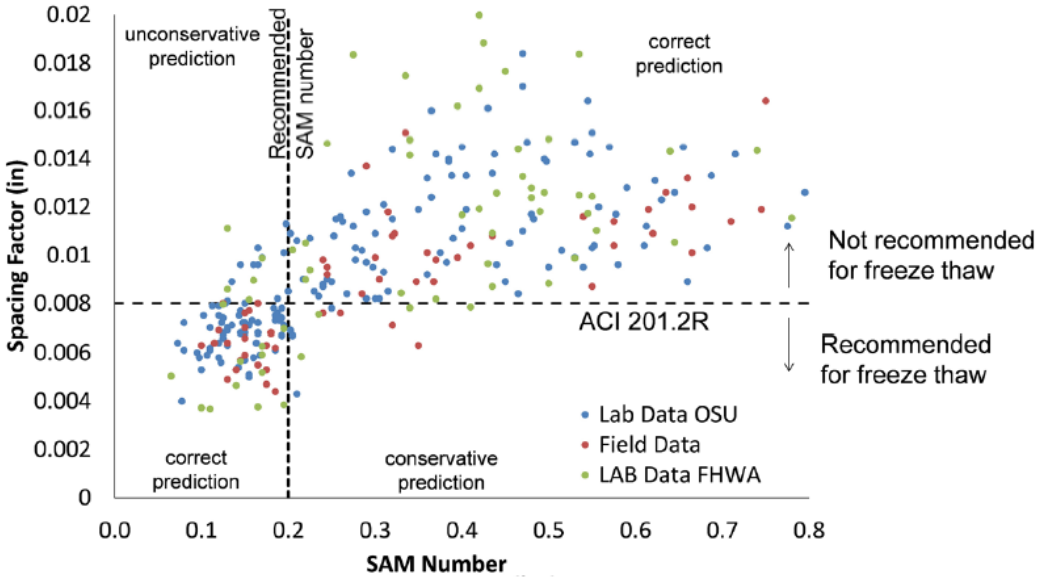

Figure 2-3 Spacing factor vs. SAM number (Ley, 2015).

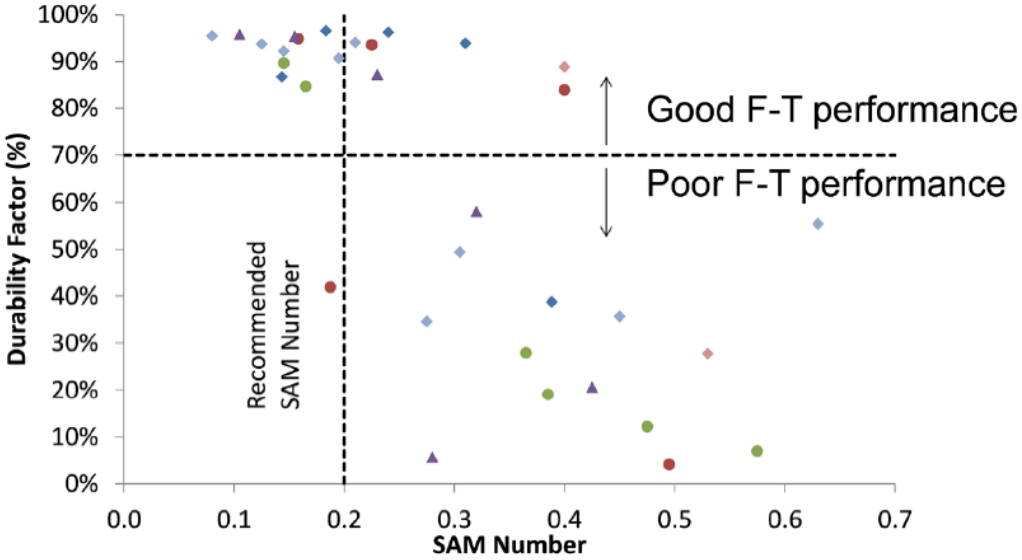

Figure 2-4 SAM number vs. durability factor (Ley, 2015).

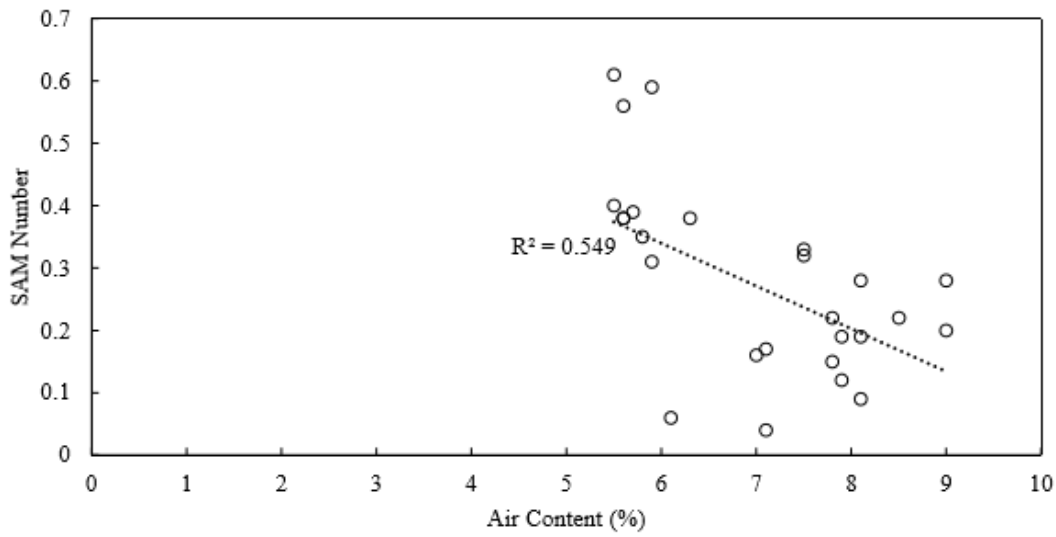

Figure 2-5 SAM number vs. air content (Barman and Hansen, 2018).

2.2.4 Shrinkage

Concrete pavements experience plastic and drying shrinkages due to moisture evaporation, uniform temperature change, temperature gradients, and moisture gradients. Upward and downward curvatures in pavement slabs are caused due to temperature gradients during the night-time (warmer bottom) and daytime (warmer surface) conditions, respectively (Cackler et al., 2017). Figure 2-6 depicts moisture warping and temperature curling in concrete pavements.

Figure 2-7 shows the drying shrinkage phases of a concrete structure as the bottom remains saturated and the surface undergoes a drying and wetting cycle (Mindess et al., 2008). Drying and wetting cycles allow concrete pavements to recover some shrinkages, but some remain irreversible. As shown in Figure 2-8, concrete swells when stored in water and shrinks when stored in air (Cackler et al., 2017). The swelling and shrinking continue until the concrete attains ultimate shrinkage.

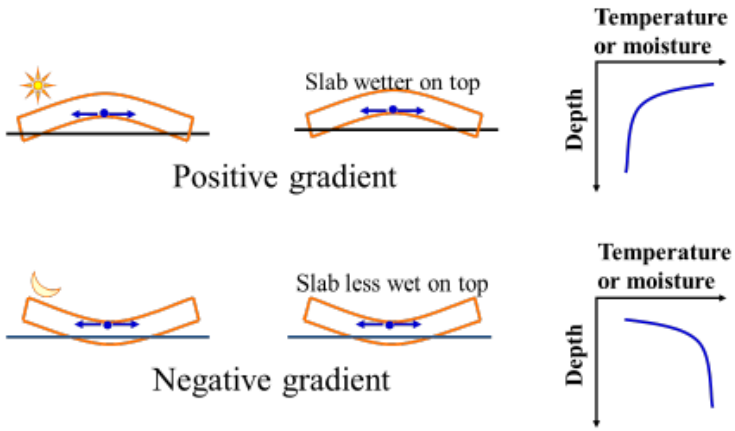

Figure 2-6 Moisture warping and temperature curling of concrete slab (Mack, 2009).

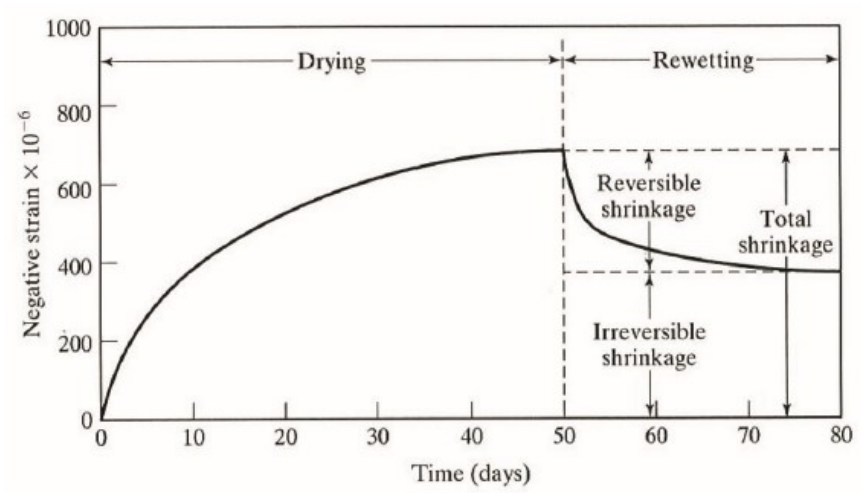

Figure 2-7 Strain vs. time graph of drying shrinkage components (Mindess et al., 2008).

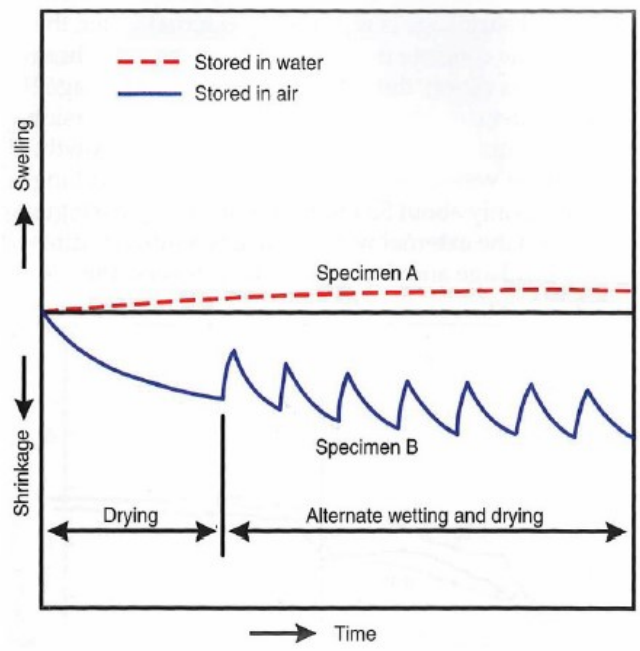

Figure 2-8 Long-term alternate wetting and drying shrinkage (Komatska and Wilson, 2016).

Destree et al. (2016) introduced a model to predict shrinkage cracking and curling of concrete slabs subjected to restraint by ground friction and fiber bridging. The model simulates the sequential development of multiple cracks and opening responses because of shrinkage. The model showed that an increase in fiber content, interfacial bond strength, and ground friction could reduce the average crack width (ACI.544.4R-18). In comparison with field data of several slabs, the simulated model results accurately predicted crack openings (ACI.544.4R-18). The PEM design recommends the following to reduce the effect of moisture warping and curling due to shrinkage (Cackler et al., 2017):

I. Sufficient curing.
II. Reduced permeability.
III. Low paste-volume or reduced cementitious material and increased aggregate volume.
IV. Good pore system in the concrete structure.

2.2.5 Strength

Concrete pavement strength is defined as its ability to carry static and dynamic loads (Taylor, 2017). Although concrete's strength is a crucial factor needed to assure structural performance, it does not fully measure concrete pavement's potential to sustain serviceable performance when subjected to harsh environmental conditions. The PEM design provides durable and workable concrete pavements that meet the strength criteria necessary to ensure satisfactory performance under local environmental conditions. The PEM method gives special attention to the aggregate gradation and paste-system to achieve the desired strength without compromising the workability.

2.2.5.1 Aggregate Gradation

Aggregate properties have more influence than cement content on the performance of concrete mixtures at a specific water-cement ratio (Dhir et al., 2006). Angular aggregates with rough textures are preferred (Taylor et al., 2014) as they can provide more strength. Determining the aggregate percentage in a concrete pavement mixture is critical for mixture consolidation and cohesiveness. A well-graded aggregate gradation is necessary to reduce water demand, provide sufficient workability, lower paste requirement, and increase the strength and durability of the pavement (Delatte, 2007; Taylor et al., 2014). The Tarantula Curve (Ley, 2014), shown in Figure 2-9, provides gradation limits to select the optimum aggregate gradation in the PEM design procedure. The theoretical optimum gradation is obtained by fitting the combined gradation of aggregates within the boundaries of the tarantula curve.

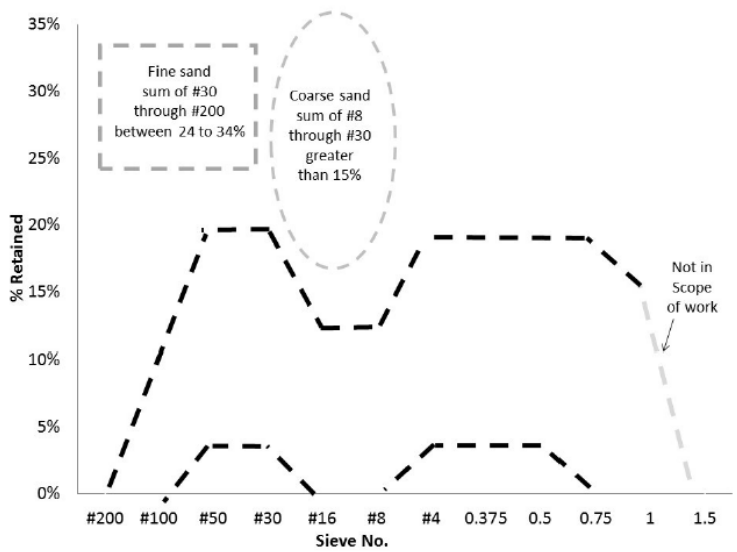

Figure 2-9 Tarantula curve showing recommended limits for aggregate gradation (Ley and Cook, 2014).

2.2.5.2 Paste System

The hydrated cement paste (HCP) requirement in a concrete mixture depends on the amount of paste needed to hold the aggregate particles together. Too much paste can reduce design strength and life (Cackler et al., 2017). SCMs (such as fly-ash) can be added to concrete mixtures to reduce Alkali-Silica Reaction (ASR) and mitigate calcium oxychloride formation. Figure 2-10 shows that the addition of fly-ash reduces calcium oxychloride formation. Other benefits of adding SCM to concrete mixtures are:

I. Reduced heat of hydration.
II. Increased chloride penetration resistance due to reduced permeability.
III. Less water needs to achieve workability.
IV. Increased overall strength of concrete after curing.

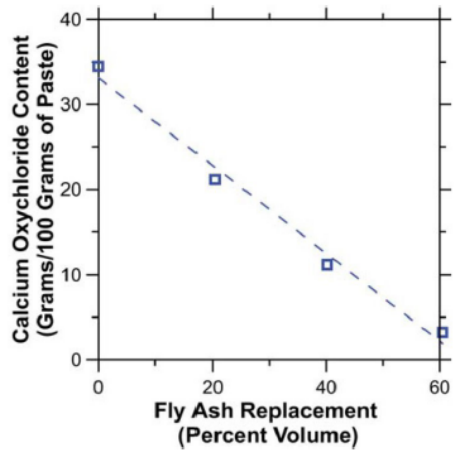

Figure 2-10 Influence of fly-ash in reducing calcium oxychloride content (Cackler et al., 2017).

2.2.6 Workability

The PEM design requires workable concrete mixtures that can be easily placed without compromising strength and durability. On the other hand, the concrete mixture needs to remain stable in shape after the consolidation process is finished. This requires that the aggregate volume and gradation of a concrete mixture be carefully selected to control the creep and stiffness of the mixture. The aggregate gradation meeting the tarantula gradation criteria will likely provide good workability.

The constructability of a concrete mixture is also critical. The addition of fibers into a concrete mixture can influence the workability of the mixture. It is recommended to add/increase water-reducing admixture or increase cementitious material (paste volume) to maintain workability without compromising the water-cement ratio (ACI.544.4R, 2018). The two newly developed tests, vibrating Kelly ball (V-Kelly) test and the box test are an upgrade from the slump test.

The V-Kelly test is used to assess the workability and response to vibration of the concrete mixture (Cackler et al., 2017). The box test is conducted to investigate the thixotropic properties of concrete mixtures, i.e., the impact of vibration on the concrete mixture and its ability to hold an edge after vibration (Cackler et al., 2017).

2.3 FIBERS

Fiber reinforced concrete is prepared by adding fibers to the concrete mixture. Unlike plain concrete, FRCs are more durable and ductile with a better post-crack performance. Structural fibers improve the post-crack performance of concrete by keeping cracks tight (Barman et al., 2018). Cracks held closer by fibers help reduce the panel fatigue crack severity and increase the load transfer between concrete slabs (Barman et al., 2018; Barman et al., 2021). This effect decreases joint deterioration and joint faulting.

Fibers are classified into two categories, micro (diameter < 0.3mm) and macro (diameter ≥ 0.3mm), and have varying lengths, geometries, and shapes. ASTM C1116 categorizes fibers into four types:

- Type I (Steel Fiber) – made with alloy, stainless, or carbon steel fibers.
- Type II (Glass Fiber) – made with glass fibers that resist alkali.
- Type III (Synthetic Fiber) – made with synthetic fibers.
- Type IV (Natural Fiber) – made with natural fibers.

Unlike plain concrete, FRCs do not fail immediately after a fracture upon cracking. Figure 2-11 shows the fibers bridging a crack. As illustrated in Figure 2-12, the fibers in FRC mixtures provide post-crack support and control crack propagation while allowing the concrete to withstand residual loads. It can be seen that FRC is able to hold some amount of load after crack development.

Figure 2-11 Crack control and bridging effect of fibers (Gaddam, 2016).

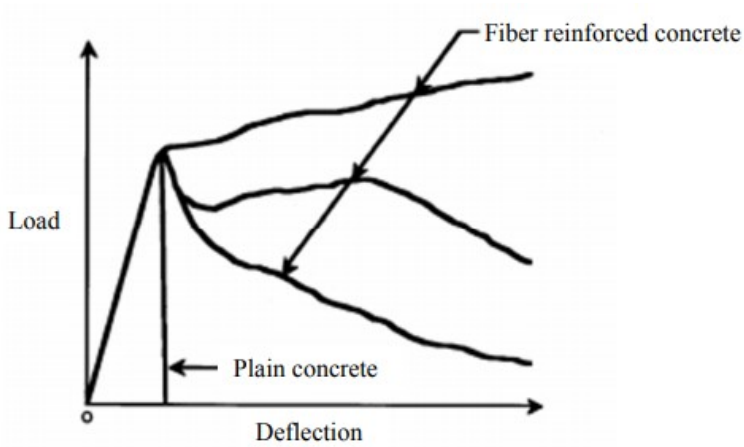

Figure 2-12 Illustration of load vs deflection in plain concrete and FRC (after ACI Committee 544, 2009).

The area under the load-deflection curve, depicted in Figure 2-12, is the toughness of the FRC. This is a representation of the energy absorbed by the FRC due to the load it had to withstand. Fiber failure occurs when fibers can no longer sustain loads (ACI 544.4R, 2018). As shown in Figure 2-13, it occurs through various phases such as debonding and sliding between fiber and matrix, frictional sliding, fiber pullout, and fiber rupture (ACI 544.4R, 2018).

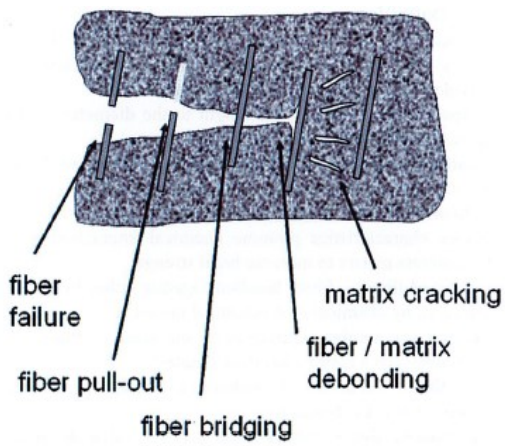

Figure 2-13 Stages of FRC failure (ACI.544.4R-18).

Strain softening occurs when the FRC residual strength decreases as crack width and deflection increase (ACI 544.4R, 2018). This occurs when a crack is held together by very few fibers, and the ultimate tensile strength is greater than post-cracking tensile stress. Whereas, during strain hardening, the residual strength of FRC increases as crack width and deflection increase (ACI 544.4R, 2018). Figure 2-14 shows that the number of fibers in a concrete mixture affects the strain-softening and -hardening behaviors of FRC.

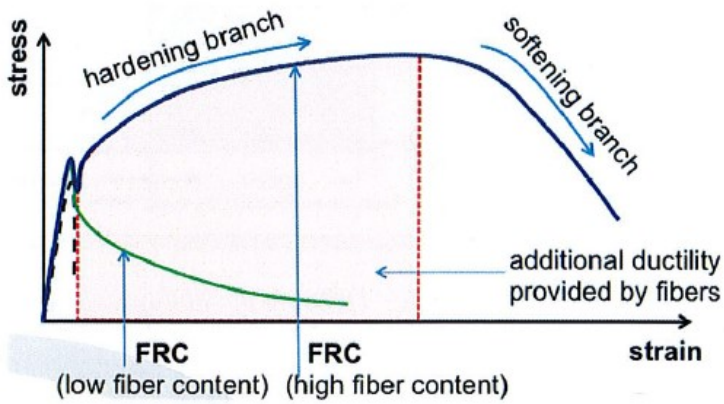

Figure 2-14 Strain softening and hardening behaviors (ACI.544.4R-18).

2.3.1 Steel Fiber Reinforced Concrete (SFRC)

Steel fibers are mostly used in industrial flooring with limited applications in concrete pavements. Figure 2-15 shows various geometries of commonly available commercial steel fibers. As shown in Figure 2-16, steel fibers with a hooked-end enhance the resistance to pullout from the concrete matrix (Komatska and Wilson, 2016).

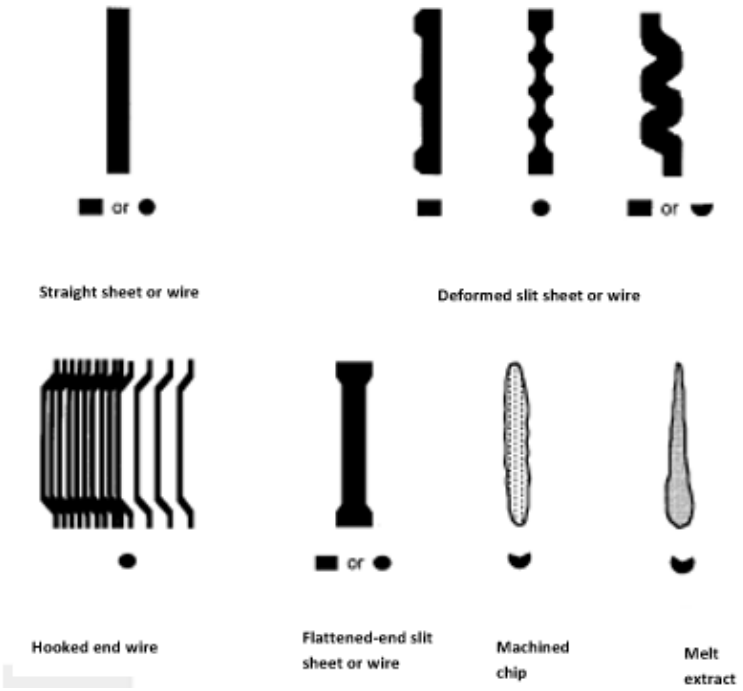

Figure 2-15 Various steel fiber geometries (Komatska and Wilson, 2016).

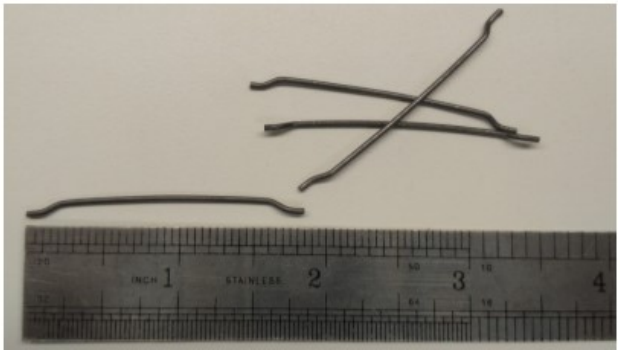

Figure 2-16 Photograph of steel fibers with hooked end (Barman, 2018).

Generally, the volume fraction of steel fibers varies from 0.25% to 2% of the total volume of the concrete mixture. The workability of SFRC is reduced when the fiber volume fraction is greater than 2%, and there is an uneven distribution of fibers in the concrete mixture (Komatska and Wilson, 2016). Acikgenc et al. (2013) observed that slump value reduced as the fiber dosage increased (Figure 2-17). The study also showed that mixture compactibility of steel fiber reinforced concrete was related to the aspect ratio (ratio of length to diameter) and fiber volume fraction of fibers (Acikgenc et al., 2013).

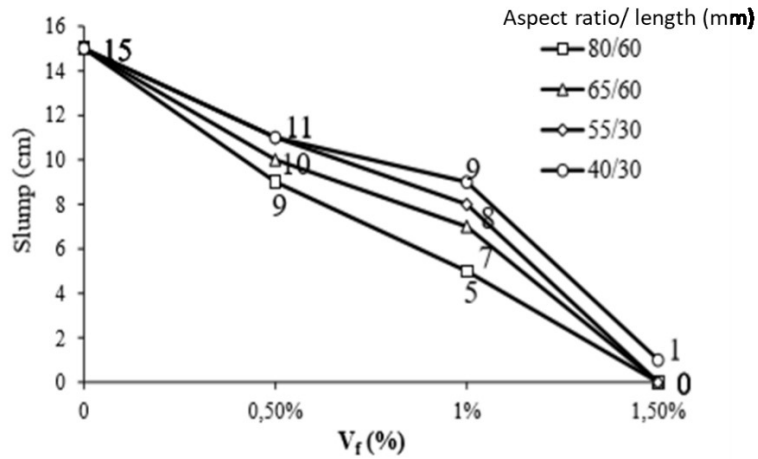

Figure 2-17 Slump test output (Acikgenc et al., 2013).

It was also found that fiber reinforcement has little to no impact on the free drying shrinkage of fresh concrete (Komatska and Wilson, 2016). Nevertheless, steel fibers slow down the fracture of restrained concrete during shrinkage and enhance the creep characteristics of concrete (Komatska and Wilson, 2016). Steel fibers in concrete cause more cracks due to internal stresses, but the crack widths are much narrower than conventional concrete.

Komatska and Wilson (2016) concluded that compared to concrete without steel fibers, the addition of 1.5% by volume of steel fibers increased the tensile strength and flexural strength by up to 40% and 150%, respectively. Figure 2-18 (a) indicates that the compressive strength of SFRC decreased beyond 1% fiber volume fraction, possibly due to higher voids in the specimen. It is also observed from Figure 2-18 (b) that longer steel fibers (60 mm) with a larger aspect ratio (80) were more effective in increasing the flexural strength of concrete mixtures.

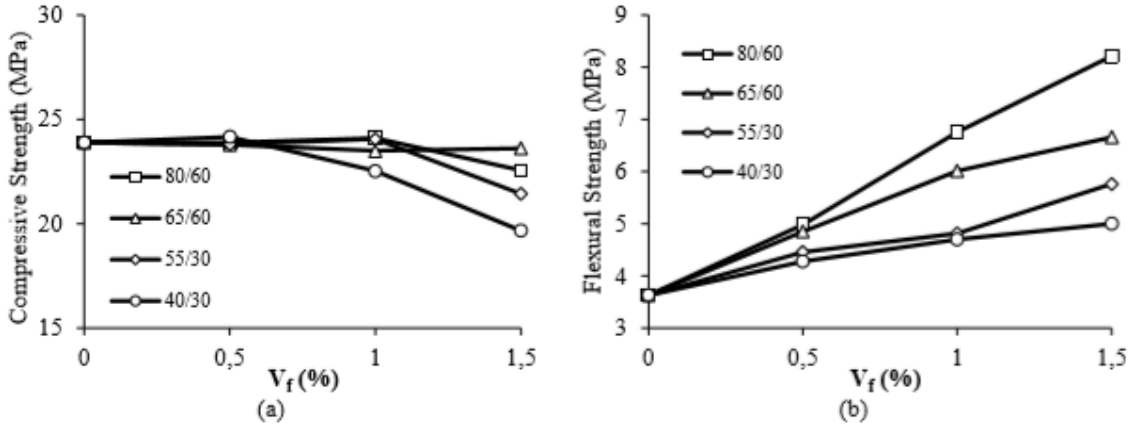

Figure 2-18 SFRC strength at 28-day: a) Compressive strength, and b) Flexural strength (Acikgenc et al., 2013).

Arnold et al. (2005) conducted a joint performance study of SFRC; it was found that an increase in fiber dosage resulted in a decrease in peak differential displacement. Figure 2-19 shows the effect of fiber reinforcement on peak differential displacement. It can be seen that when fiber was used in the concrete mixture, failure occurred at a wider crack width indicating the benefit of fibers in increasing the joint load transfer.

Sukontasukkul et al. (2018) found that SFRC showed a more consistent load-carrying capacity and reduced residual strength and toughness with an increase in temperature. The influence of fire on FRC residual strength may be less critical to the pavement, but it is crucial in the context of roadway bridges. The freeze-thaw durability of SFRC is comparable with that of plain concrete when the SFRC mixture is air-entrained, compacted adequately, and modified to integrate steel fibers (Komatska and Wilson, 2016). The bond between steel fibers and cement matrix can be improved with increased surface roughness or mechanical anchorage and can be protected from corrosion by the alkaline environment in the cement matrix, provided that the modulus of elasticity is relatively high (Komatska and Wilson, 2016).

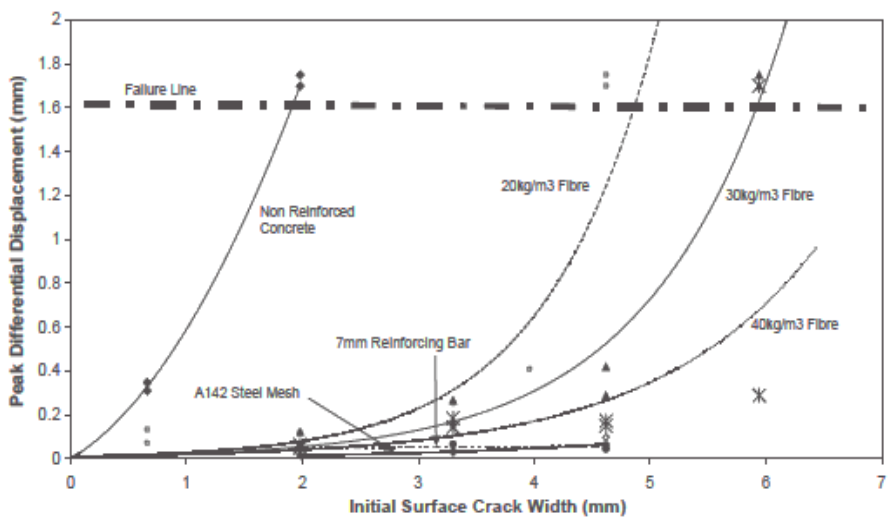

Figure 2-19 Effect of fiber reinforcement in peak differential displacement (Arnold et al., 2005).

2.3.2 Synthetic Fiber Reinforced Concrete (SyFRC)

Synthetic fibers are the most common fiber types used in concrete mixtures. A survey showed that 94% of FRC pavements in the United States included synthetic fibers, and the other 6% included steel fibers (Barman, 2018). Most FRC pavement overlays constructed in recent years have structural synthetic fibers. Several studies, exploring the properties and performance characteristics of synthetic FRC, were conducted in Illinois (Bordelon, 2011; Roesler et al., 2008; Bordelon, 2005). They considered the impact of certain factors on the performance of FRCs, such as the shape (straight, crimped, and twisted), type, dosage, length, diameter, and aspect ratio of fibers. Table 2-1 presents fibers' physical properties and a few hardened concrete test results for the FRC mixtures prepared with three different synthetic fibers in the Roesler et al. (2008) study. The peak flexural load and modulus of rupture (MOR) varied slightly with the fiber's dosage, shape, and aspect ratio, but an inevitable trend was not observed. Dosage of 4.5 lb/yd^3

in the straight synthetic fiber category and 4.6 lb/yd^3 in the twisted synthetic fiber category had the highest peak flexural load and MOR values, respectively.According to Figure 2-20, straight synthetic fibers performed better in terms of MOR values than the other two shapes. Bordelon (2005) found that the post-crack residual load capacity increased with the increase in fiber volume fraction (Figure 2-21). It was also observed that FRC with a 0.58% fiber volume fraction had a greater residual load capacity than the mixture with a 0.26% volume fraction.

Table 2-1 Properties of structural synthetic fibers and FRC (Roesler et al. (2008)).

Fiber type	**Straight synthetic**				**Twisted synthetic**		**Crimped synthetic**
Cross section	Rectangular				Rectangular		Rectangular
Length (in)	1.57				2.13		2.00
Thickness (in)	0.004				NA		0.03
Width (in)	0.05				NA		0.05
Aspect ratio	90				NA		46
Specific gravity	0.92				0.91		0.91
Volume fraction in the mix (%)	0.19	0.26	0.29	0.58	0.30	0.50	0.40
Dosage used (lb/yd^3)	3.00	4.00	4.50	8.90	4.60	7.70	6.10
Peak flexural load (lb)	6623	5472	9276	8939	8101	6487	8160
Modulus of rupture (psi)	556	456	733	745	675	541	673
Testing age (days)	14	14	14	14	14	14	14

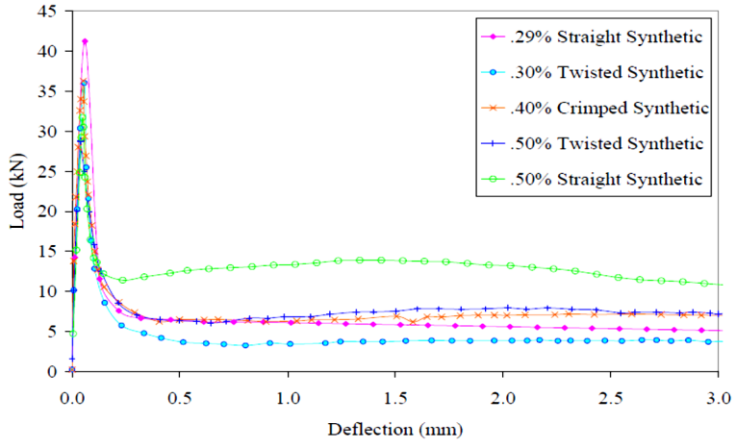

Figure 2-20 Residual load characteristics of different shaped structural synthetic fibers (Bordelon, 2005).

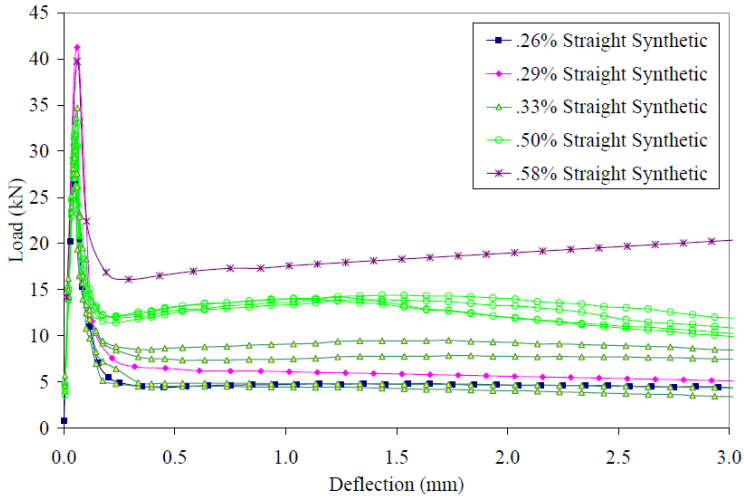

Figure 2-21 Residual load capacities of FRC vs. fiber volume fraction for straight synthetic fibers (Bordelon, 2005).

Macro-fibers form a mechanical bond with concrete due to friction. They are used to extend joints or produce jointless concrete slabs to reduce the maintenance cost of a concrete structure during its design life. Synthetic macro-fibers, with a volume fraction of 0.2 to 1% of concrete, enhance the concrete drying shrinkage crack control. Alhassan and Ashur (2012) reported that certain benefits of adding fibers in bridge overlays include a reduction in shrinkage cracking, an increase in toughness, additional post-crack strength, and an increase in crack resistance. Figure 2-22 shows the results of shrinkage vs. curing time for various combinations of plain and fiber reinforced concrete mixes. The FRC mixes showed less shrinkage than the plain concrete mix. On average, the drying shrinkage was found to be 17% lower for FRC mixes than the plain concrete mix. The study recommended a synthetic fiber content of 3 lb/yd^3 for bridge overlays. Drying shrinkage was reduced by 15% at this fiber dosage. It was also recommended that fibers should be held between 0.75 inches and 1.75 inches in length.

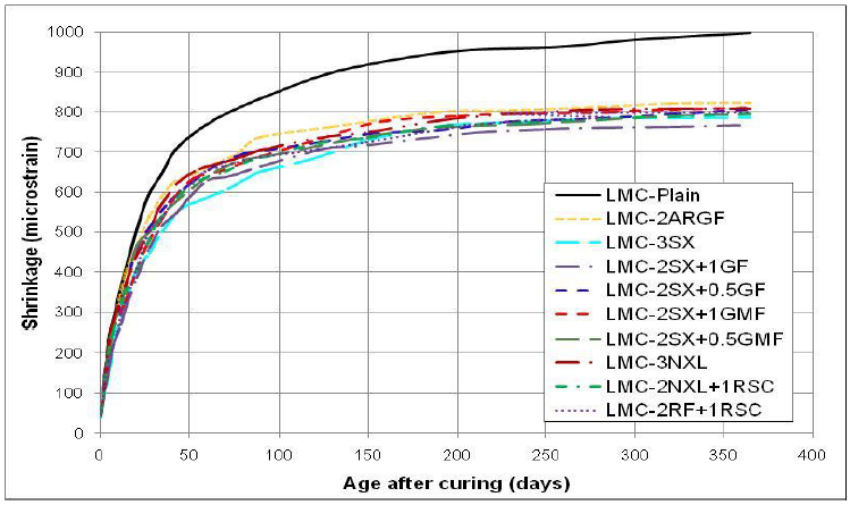

Figure 2-22 Shrinkage vs. curing time for plain and FRC mixes (Alhassan and Ashur, 2012) (LMC = latex modified concrete; ARGF = alkali resistant glass fiber; SX= microtype polyolefin fiber; GF = micro type 100% virgin; NXL = macrotype polyolefin fiber; RSC = microtype polyvinyl alcohol fiber; RF = macrotype polyvinyl alcohol fiber).

Synthetic macro fibers affect the hardened concrete mechanical properties in various ways depending on the type of synthetic fiber used in the mixture. The key impact of using synthetic macro fibers in hardened concrete is the increase in flexural toughness, which is defined as the measure of energy absorption capacity (Komatska and Wilson, 2016). This effect also improves the fatigue and shatter resistance of FRC and decreases crack propagation. The impact of synthetic fibers on the post-crack performance of concrete is an essential factor for their use in concrete pavements and overlays.

Acrylic fibers enhance post-crack toughness and ductility, aramid fibers improve the resistance to creep, static, and dynamic fatigue, and nylon fibers improve toughness, tenacity, and elastic recovery (Komatska and Wilson, 2016). There may be negligible effect on the hardened concrete compressive strength at a higher dosage of synthetic fibers (1.5% volume fraction).

Issa (2017) studied the effect of early-age properties of FRC on the fatigue damage of concrete pavements. Like many other studies, it was found that the synthetic fibers did not have a significant influence on the compressive and flexural strength of concrete mixes. However, flexural toughness increased with an increase in fiber dosage. The authors also observed that the fibers with embossed and deformed textures provided better bonding within the concrete mix. Relative dynamic modulus (RDM) tests were also performed, and it was concluded that fibers did not contribute significantly toward concrete durability against freeze-thaw cycles. ASTM C666 specifies a minimum RDM of 60% for concrete with good freeze-thaw durability. It was also noticed that the mixes with a higher dosage of synthetic fibers showed increased resistance to scaling by a higher degree.

Barman and Hansen (2018) conducted a laboratory study with nine synthetic fibers of different geometries, lengths, aspect ratios, and stiffness valu**es (**Table 2-2). The effect of low, intermediate, and high dosages (0.25, 0.50, and 0.75 percent volume fraction (V_f)) for each fiber type was studied.

It can be observed from Figure 2-23 (a), (b) and (c) that the compressive strength, modulus of elasticity and MOR of synthetic FRC were minimally influenced by the increase in the Reinforcement Index (RI). Note that the RI is the product of the aspect ratio (AR) and volume fraction (V_f) of fibers. Figure 2-23 (d) shows that the modulus of rupture varied inconsistently with the change in fiber property and V_f. The property of fibers 1 through 9 can be seen in Table 2-2.

Table 2-2 Summary of fiber details (Barman and Hansen (2018)).

Fiber Serial Number	Geometry / Type	Length (inch)	Aspect ratio, specific gravity, modulus of elasticity (ksi), tensile strength (ksi)
Fiber 1	Straight / Synthetic	1.5 or 2	*94, 0.91, N/A, 70
Fiber 2	Straight / Synthetic	1.5 or 2	*100, 0.91, N/A, 70
Fiber 3	Straight / Synthetic	1.55	90, 0.92, 1378, 90
Fiber 4	Straight / Synthetic	*1.63	96.5, 0.91, N/A, 70
Fiber 5	Twisted Straight / Synthetic	2	74, 0.92, 1380, 87-94
Fiber 6	Continuously Crimped / Synthetic	2.0	*60, 0.91, N/A, N/A
Fiber 7	Embossed / Synthetic	2.1	70, 0.91, N/A, 85
Fiber 8	Embossed / Synthetic	1.89	*66, 0.90-0.92, 1450, 93
Fiber 9	Embossed / Synthetic	2.1	70, 0.91, N/A, 85

**Measured, not found in manufacturer's sheet.*

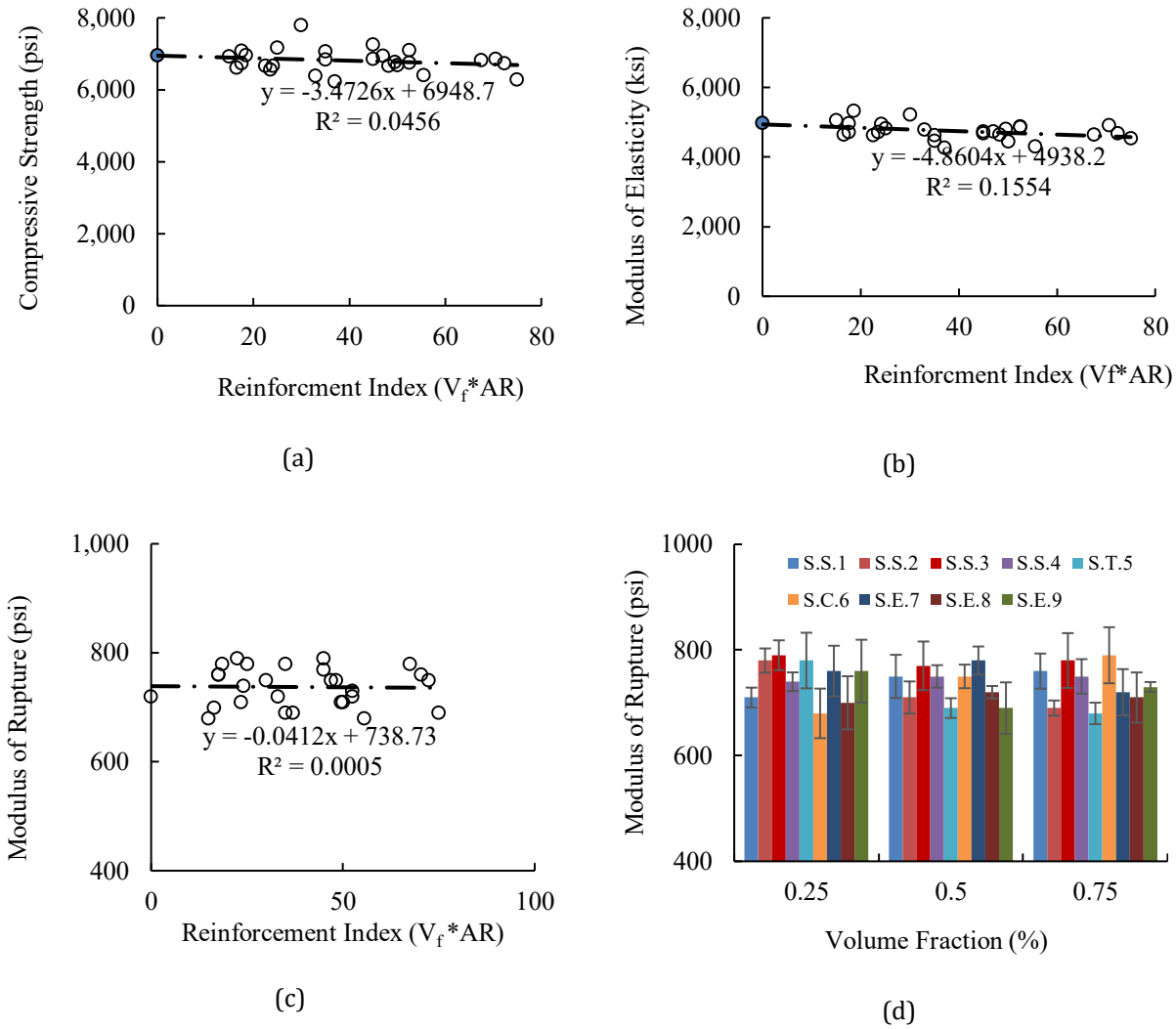

Figure 2-23 (a) Compressive strength, (b) Modulus of elasticity, and (c) and (d) Modulus of rupture as a function of reinforcement index and fibers' volume fraction, respectively.

It can be seen from Figure 2-24 (a) that the residual strength ratio (RSR) increased greatly with the increase in V_f for all fiber types. Overall, the RSR and V_f had an excellent correlation (R^2 = 0.86). It was concluded that embossed, twisted, and crimped fibers have better RSR and Residual Strength (RS) values than straight synthetic fibers (Figure 2-24 (d)).

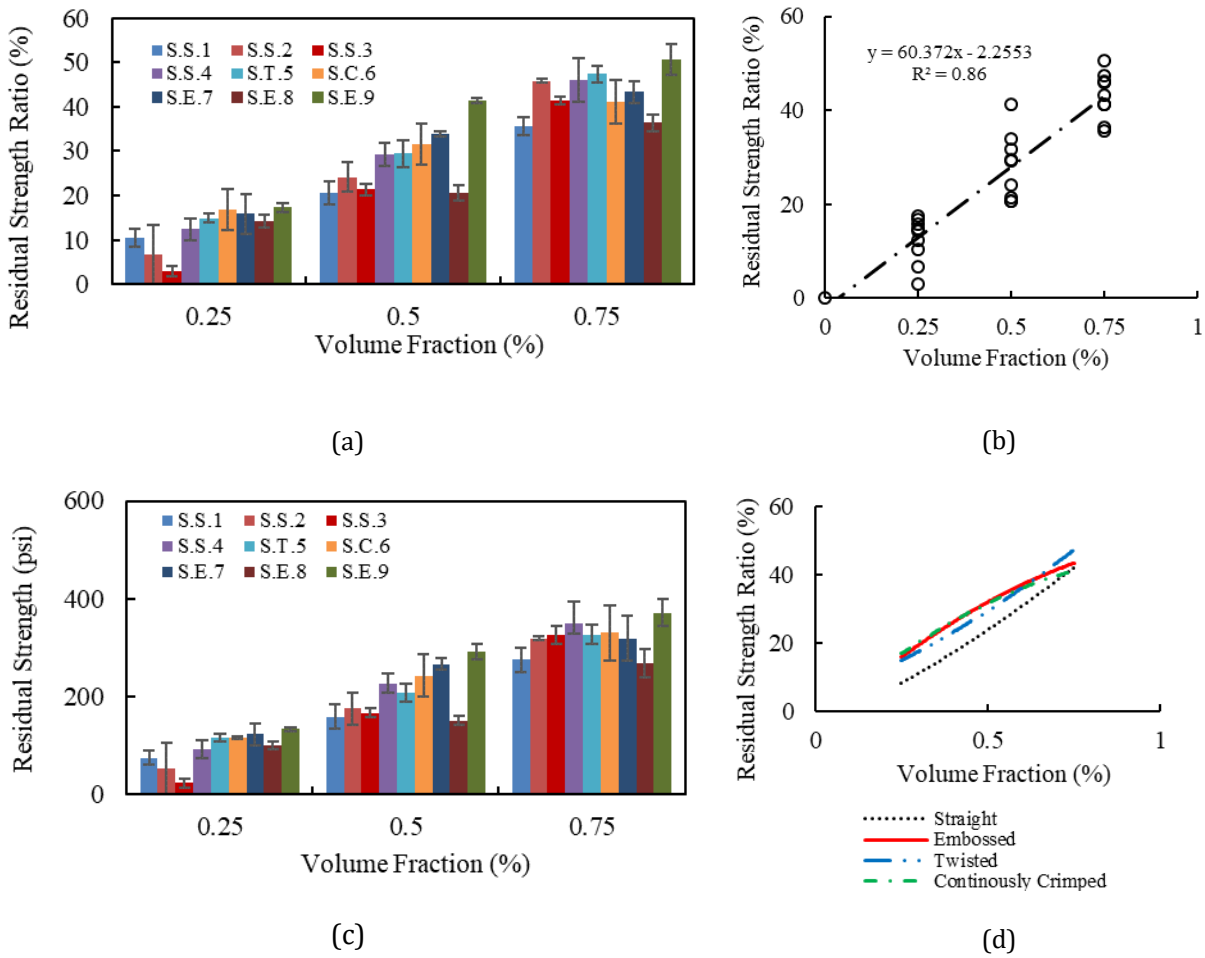

Figure 2-24 (a) RSR vs. Vf, (b) Correlation between RSR and V_f, (c) RS vs. V_f, (d) RSR as a function of V_f and fiber geometry.

Load Transfer Efficiency (LTE) measures the ability of concrete to transfer loads across adjacent slabs. Barman and Hansen (2018) found that FRC made with 5.25 to 6.5 lb/yd^3 structural synthetic fibers transferred 20% more load than plain concrete slabs. However, the LTE of FRC decreased with the increase in crack width and number of load applications due to abrasion of crack faces. Nevertheless, structural synthetic fibers did not experience significant fatigue even after millions of load repetitions in laboratory testing (Barman, 2014).

Minimal research was done to understand the freeze-thaw resistance of SyFRC. Similar to SFRC, SyFRC must be air-entrained and consolidated as it is susceptible to concrete degradation due to freeze-thaw damage (Vondran, 1987; Barman, 2014). Barman et al. (2019) stated that the inclusion of synthetic fibers in the concrete mixture could improve pavement durability against surface spalling.

The addition of synthetic fibers decreases the workability (slump) of the concrete mix. Although less workability is an issue in achieving required consolidation, a reduction in workability may increase the cohesiveness of concrete under the paver, which can improve slip-form characteristics (Ludirdja and

Yougn, 1992). Barman and Hansen (2018) found that the addition of certain synthetic fibers had a significant effect on the failure mode of specimens in various test procedures. For example, FRC specimens for compressive strength specimens failed in a ductile manner and rarely exhibited explosive failure.

The Louisiana Transportation Research Center (LTRC) investigated the fatigue and toughness characteristics of FRC prepared from polypropylene fibrillated, polypropylene macro, carbon, and steel fibers in concrete pavements (Kevern et al., 2016). The properties of fibers are provided in Table 3-1. Figure 2-25 shows pictures of different fibers used in that study. In general, it was found that polypropylene fibers performed better than steel fibers against fatigue when used in correct dosages. This study suggested that fibers with high tensile strength results in better residual load carrying capacity and carry a greater load at larger deflections.

Figure 2-25 Fibers used in the (Kevern et al., 2016) study: polypropylene fibrillated fiber (left), polypropylene macro fiber (left middle), carbon fiber (right middle), and steel fiber (right).

Table 2-3 Properties of fibers in Kevern et al. (2016) study.

Fiber type	Specific Gravity	Length (inches)	Tensile Strength (ksi)
Polypropylene Fibrillated	0.91	1.50	83 – 96
Polypropylene Macro	0.91	2.25	83 – 96
Carbon	1.70	4.00	600
Steel	7.85	2.00	152

The fatigue property of the concrete was studied by applying cyclic load on the pre-notched beam specimens as per the RILEM procedure developed by Jenq and Shah (1985). Pre-notched fatigue testing showed that both the tensile strength and length of fibers influence the fatigue properties of fibers. This study concluded that polypropylene fibrillated fibers offer increased fatigue performance but do not offer any significant post-crack performance.

2.4 CONCLUSIONS

This chapter introduced the PEM design procedure and described the application of fibers in concrete and their influence on the fresh and hardened concrete properties of concrete. The literature review discussed the key engineering parameters (aggregate durability, fluid transport property, cold weather resistance, shrinkage, strength, and workability) in PEM design procedure and the properties (geometry, strength,

durability, and physical characteristics) of steel and synthetic fibers. When discussing PEM, it was found that maintaining water to cementitious materials ratio between 0.40 and 0.45 reduces capillary pores volume; the Tarantula curve yields the optimum aggregate gradation; air-entraining admixture stabilizes spherical air voids. The PEM procedure suggests avoiding reactive aggregates prone to ASR, ACR, or fracture/dilation. The addition of fibers in concrete reduces workability while improving post-crack performance. Also, fibers with irregular geometry provide a better residual capacity to concrete, and long steel fibers are more effective in increasing the concrete's flexural strength. The literature review found no information on implementing the PEM design procedure for producing FRC and target value for PEM test parameters.

CHAPTER 3: MATERIALS AND MIXTURE DESIGNS

This chapter discusses the materials used in the laboratory investigation. Properties of fibers, cement, supplementary cementitious materials (SCM), aggregates (characteristics and gradations), and admixtures (air entrainer and water reducer) are discussed in this chapter. Descriptions of concrete mixture proportioning, batching, and the mixing procedure are included. Different tests conducted in this study are briefly introduced in this chapter.

3.1 FIBERS

Two different types of fibers were used based on the recommendation of the members of the technical advisory panel (TAP). The polypropylene-based macro synthetic fibers are the most common fibers used in pavements. The two fibers used in this research were synthetic fibers with different lengths, geometries, and manufacturers. More information about the fibers is given in Table 3-1. The geometry and length of Fiber 1 are illustrated in Figure 3-1 and Figure 3-2. The same for Fiber 2 is shown in Figure 3-3 and Figure 3-4. Two different fiber dosages were considered in terms of volume fractions (V_f), 0.26 % (4 lb/yd^3) and 0.5% (7.6 lb/yd^3) of the concrete volume. Fiber 1 is twisted and bundled, which unfurls during the concrete mixing; its effective diameter and aspect ratio are not uniform in the concrete mixture as a result. Fiber 2 has embossed geometry, and it holds its shape in the concrete mixture.

Table 3-1. Description of fibers investigated in this task.

Fiber Designation	Fiber 1	Fiber 2
Geometry	Twisted	Embossed
Length (in)	2.15	2.15
Aspect Ratio	Varies	70
Tensile Strength (ksi)	85	85
Specific Gravity	0.91	0.91

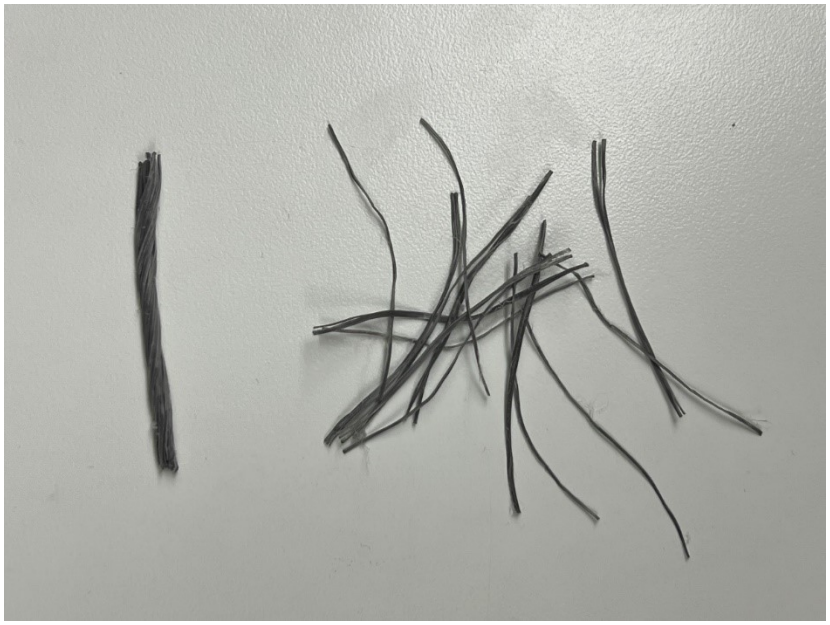

Figure 3-1. Fiber 1, Twisted on the left, Unfurled on the right

Figure 3-2. Photograph showing the length of Fiber 1 with Calipers

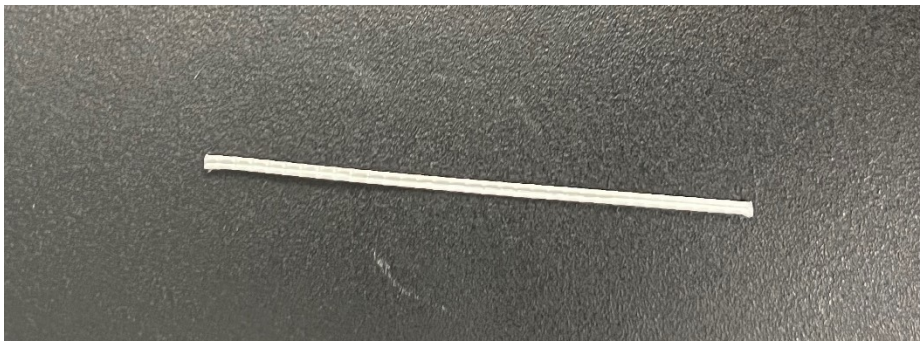

Figure 3-3. Fiber 2, straight embossed geometry.

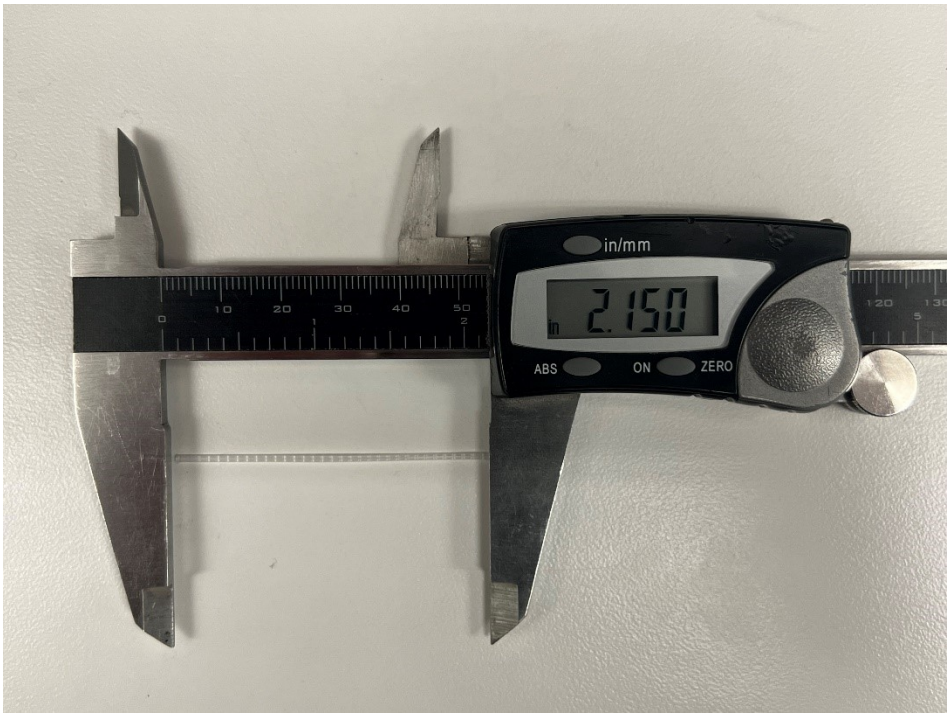

Figure 3-4. Photograph showing the length of Fiber 2 with Calipers

3.2 CEMENTITIOUS MATERIALS

ASTM C150 Type-I Portland cement and ASTM C618 Class-F fly ash were used for the concrete mixes. Fly-ash has been collected from Lakehead concrete plant, located in Duluth, MN. The Class-F fly ash was used at a 20% cement replacement for all mixtures. The composition of the fly ash can be found in the APPENDIX.

3.3 AGGREGATES

Three classes of coarse aggregates were used in this study: granite (Class A), limestone (Class B), and gravel (Class C) based on the MnDOT Standard Specifications for Construction (MnDOT 2020). The Class A and B aggregates, shown in Figure 3-5 and Figure 3-6 were quarried, then processed to reduce to desired sizes. Aggregate Class C is river gravels (Figure 3-7). For each class of aggregate, two different sizes of particles were collected. Aggregates were washed and tested for various aggregate volumetric and consensus properties such as water absorption and bulk specific gravity, as reported in Table 3-2. The water absorption percentage and bulk specific gravity tests were performed in accordance with ASTM C127. In addition, sieve analysis was also performed to determine the gradation of all the coarse aggregates collected. See Figure 3-9 for the gradations of the aggregates. Additional information can be found in the APPENDIX.

The fine aggregate was river sand, shown in Figure 3-8, collected from a gravel pit in Canyon, MN. The water absorption and bulk specific gravity of the fine aggregates are provided in Table 3-2. The gradation can be seen in Figure 3-9.

Figure 3-5. Class A Aggregates, 3/4-inch and 1.5-inch (right side photograph)

Figure 3-6. Class B Aggregates 3/4-inch and 1.5-inch (right side photograph)

Figure 3-7. Class C Aggregates 3/4-inch and 1.5-inch (right side photograph)

Figure 3-8. Fine Aggregate

Table 3-2. Water Absorption and Bulk Specific Gravity of Aggregates.

Coarse Aggregate	Absorption	Bulk Specific Gravity
Granite 3/4” Class A	0.35%	2.7
Granite 1.5" Class A	0.25%	2.7
Limestone 3/4" Class B	0.83%	2.74
Limestone 1.5"+ Class B	1.08%	2.73
Gravel 3/4" Class C	1.47%	2.67
Gravel 1.5" Class C	1.34%	2.7
Fine Aggregate		
River Sand	1.70%	2.68

The combined aggregate gradation for all the mixtures designed in this research is performance-engineered, using the Tarantula curve (Ley, 2015) to achieve the optimized aggregate gradation. Figure 3-9 below presents the gradation of the individual aggregates and the blended gradation for the Classes A, B, and C. The Tarantula gradations of the three aggregate blends are provided in Figure 3-10.

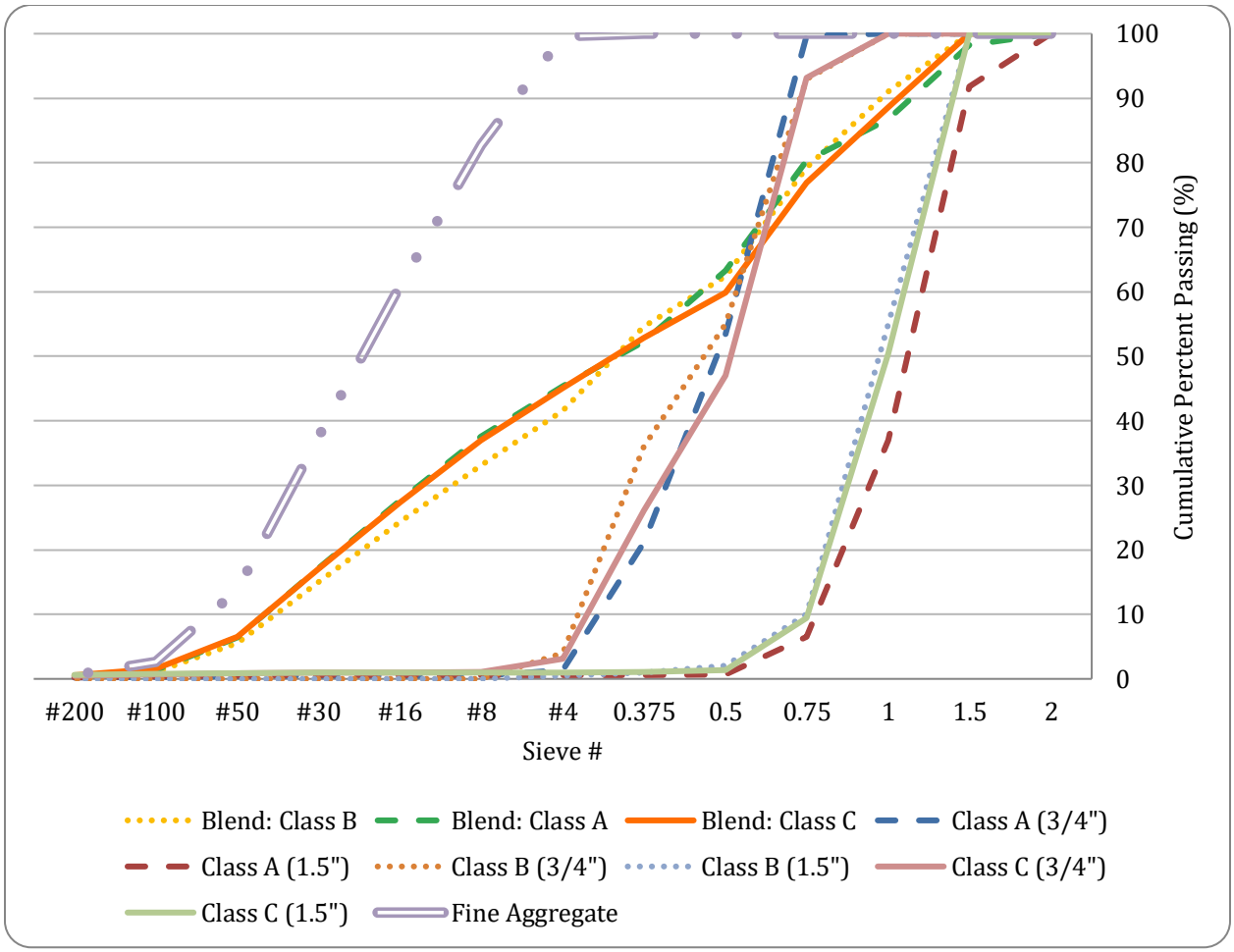

Figure 3-9. Gradations of the Individual Aggregates and Blends for Classes A, B, and C

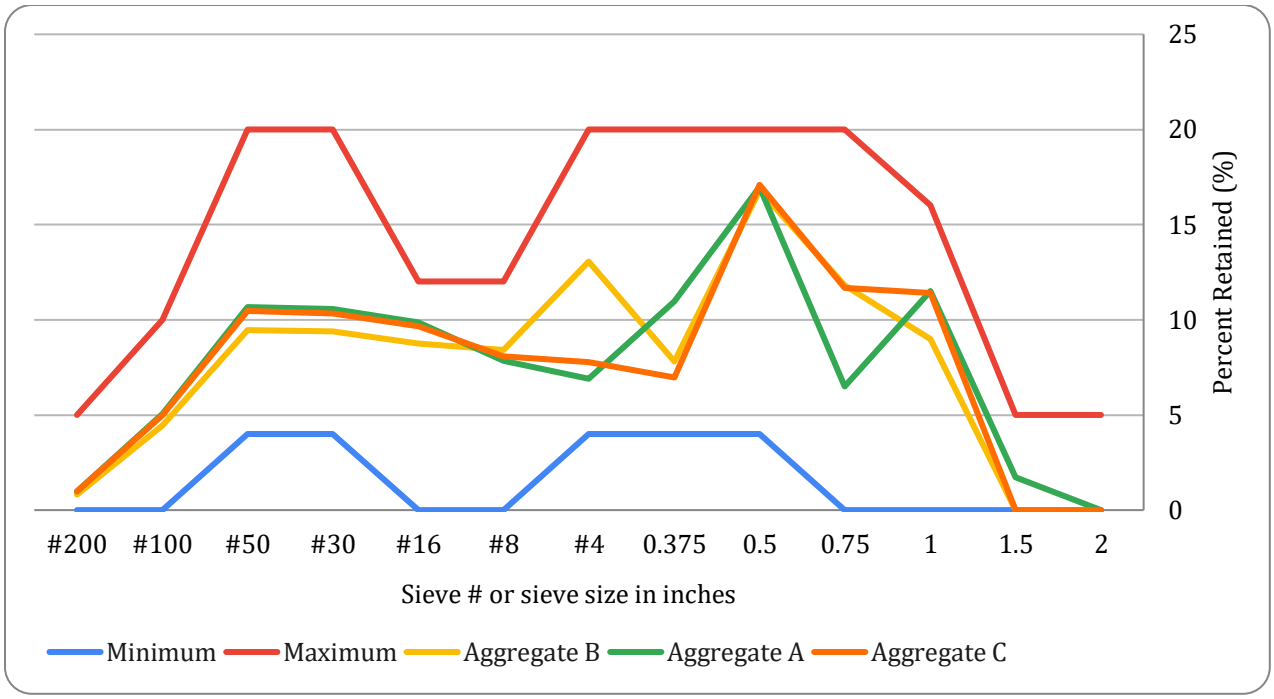

Figure 3-10. Tarantula Curves for the three Aggregate Classes

3.4 MIXTURE DESIGNS

Separate mixtures were designed for each of the three aggregate classes; each mixture contains two coarse aggregate samples and one fine aggregate sample to meet the Tarantula curve limits, as shown in Figure 3-10. Several trial batches were prepared to finalize the mixture designs. The trial batches were prepared with different dosages of admixtures to ensure that the air content and workability achieved were within the acceptable range of the target values. Three different target air contents (4%, 6%, and 8%) were considered. The cement content for all the mixes held a constant weight of 550 lb/yd^3. All mixtures also held constant water to cement ratio (w/c) of 0.42. Table 3-3 displays the batch weights for the Granite Class A aggregate (referred to as Class A, here onwards) mix with 6% air content. Batch weights for Class A mixes with 4% and 8% air contents, along with the batch weights for Class B and Class C mixes, can be found in the APPENDIX. It must be noted that the dosage of admixtures was varied as needed to achieve the required workability. The mix with the higher fiber dosage [0.5% (7.6 lb/yd^3)] required more water reducer to achieve the desired workability. The paste volume (cement, water, and air) of concretes produced in this research varies between 28.07% and 32.07%.

Table 3-3. Mixture Design Details for Aggregate Class A (6% Air)

Granite Class A Mixture Design (for 6% air content)			
	Volume (%)	**Mass (lb/Yd^3)**	**Aggregates Proportion by Volume (%)**
Cement (Type I)	8.29	440	-
Fly Ash	2.07	110	-
Class A (¾”)	23.7	1078	34%
Class A (1.5”)	14.64	666	21%
Fine Aggregate	31.6	1427	45%
Potable Water	13.71	231	-
Fibers	Varied	Varied	-
BASF MasterAir 400 (fl. Oz)	-	-	-
MasterPolyheed 1020 (fl. Oz)	-	-	-
Air	6	-	-
Paste	30.07	781	-

3.5 MIXING PROCEDURE

A mixing procedure was established for concrete mixtures involving fibers to efficiently and consistently produce fiber reinforced concrete that meets the required air content and workability requirement. The different steps are listed below.

a) Add all fine aggregates and air-entraining admixture (AEA) to the mixer with one-third of the mixing water and mix for 2 minutes.
b) Add all coarse aggregates to the stopped mixer.
c) Turn on the mixer and pour in all fibers in the mixer by hand with care to pull apart balls or mats. Mix for a total of 3 minutes.
d) Add the cement, remaining mixing water, and water reducer to the mixer and mix for 3 minutes.
e) Stop the mixer and allow the concrete to rest for 3 minutes.
f) Mix for a final two minutes, then perform fresh concrete tests.

Fibers tend to ball and mat when they are not appropriately dispersed, but the established mixing procedure ensures proper fibers dispersion to avoid fiber balling (Figure 3-11) or matting. Prior to mixing, aggregates were gathered from the barrel and poured onto the laboratory floor for at least 24 hours to achieve uniform moisture content in the aggregates. Then they were gathered into a pile and covered with a plastic sheet for 24 hours. Representative samples of each aggregate pile were used to determine the moisture contents, which were used for adjustment of the weights of the aggregates and water. Each batch of the concrete mixture was prepared after a butter batch. The butter batch is a small

batch of concrete, identical in composition to the designed concrete, used for the purpose of coating the inside of the mixer.

Figure 3-11. Fiber Balling of Fiber 1 (Twisted Geometry)

3.6 CONCRETE TESTS

Fresh concrete tests such as slump, Box, V-Kelly, and super air meter (SAM) tests were conducted for each mixture prepared in this study. Hardened concrete (cylinder and beam) specimens were tested for properties such as compressive strength (ASTM C39), modulus of elasticity (ASTM C469), modulus of rupture (ASTM C78), residual strength (ASTM C1609), freeze-thaw resistance (ASTM C666), and surface/electrical resistivity (AASHTO TP95). Cylindrical specimens were tested for compressive strength, modulus of elasticity, hard air content, and surface/electrical resistivity. Beam specimens were tested for rapid freeze-thaw and flexural behavior. The rapid freeze-thaw test was performed to study the resistance of concrete against the freeze-thaw cycles. Most of the test specimens were stored/cured in an environmental chamber at a relative humidity of 95% and a temperature of $23 \pm 2^{O}C$ unless the test needed a different curing condition.

3.6.1 Slump Test

The slump test is conducted to determine the workability of concrete mixtures. Following the completion of the concrete mixing procedure, a slump test was performed on the fresh concrete mixture in accordance with ASTM C143. Even though a constant water-cement ratio was maintained for

all the mixtures, the slump of the concrete varied between 1 and 5 inches. This is not surprising as the concretes produced in this study contained different dosages of fibers and air-entraining admixtures to produce concretes with three different air contents (4, 6, and 8%). An appropriate amount of water reducer was sometimes added to improve the workability of the concretes, especially for the mixes with lower air contents.

3.6.2 Air Content and SAM Test

The SAM test was performed in accordance with AASHTO TP 118 to determine air content (%) and SAM number. The SAM number determines the spacing factor and assesses the resistance of the concrete mixture against freeze-thaw-related distresses (Ley, 2015). The results from this test have been used to study the influence of adding fibers in the concrete mixture on SAM number.

3.6.3 Box Test

The Box test was conducted to investigate the concrete mixtures' thixotropic nature, which is defined as the impact of vibration on the concrete and its ability to hold an edge after vibration (Cackler et al., 2017). Figure 3-12 shows a box test in progress. The box test was performed in accordance with AASHTO PP84 on all the mixtures once the mixing procedure was complete and the mixture had been tested for slump and air. Figure 3-13 shows the surface air voids ranking system, which is based on the assessment of the air voids on the sides of the concrete sample during the box test. The visual inspection is conducted to determine the suitability of the concrete's resistance against edge collapse.

Figure 3-12. Box Test in Progress

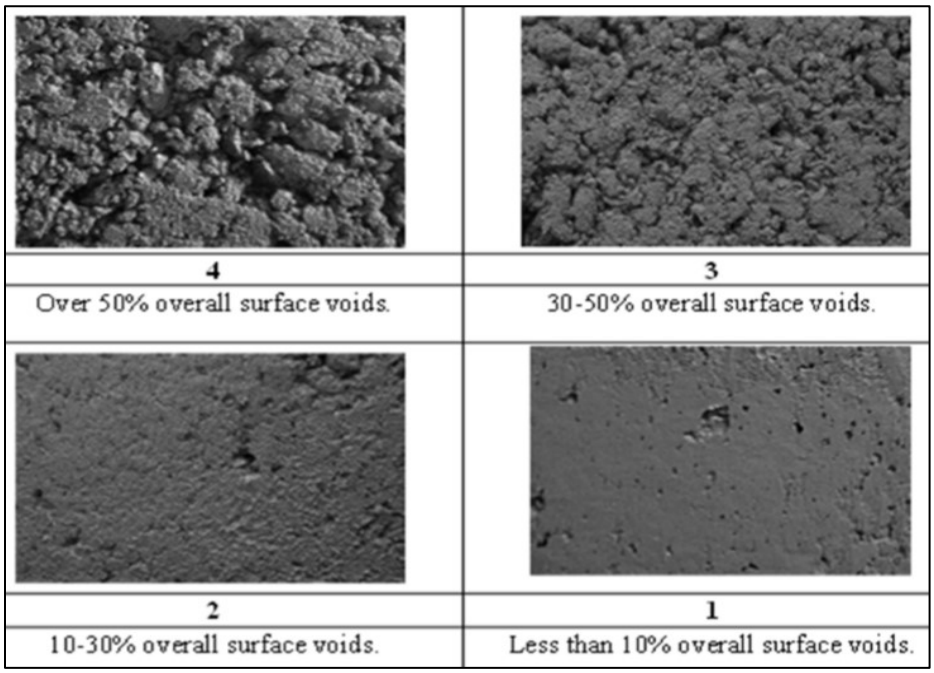

Figure 3-13. Surface Air Voids Ranking System for Box Test (Cook et al. 2016)

3.6.4 Vibrating Kelly Ball Test

The Vibrating Kelly Ball (V-Kelly) test was performed in accordance with AASHTO TP 129 on all the mixtures once the mixing procedure was complete and the mixture had been tested for slump and air content. The V-Kelly test examines the workability of concrete mixture and its response to vibration. The V-Kelly test, shown in Figure 3-14, is an advancement on the Kelly ball test and can be used to determine the workability and response to vibration on low slump concrete. The V-Kelly test is essential for the PEM design procedure because it helps explain the thixotropy of the concrete and is used to indicate static and dynamic characteristics.

Figure 3-14. V-Kelly Test in Process

The first part of the V-Kelly test (prior to turning ON the vibrator) is the Static Test. The second part (after turning the vibrator ON) is the Dynamic Test. The static test provides a measure of the concrete's consistency (V-Kelly slump), and the dynamic test provides the concrete's response to vibration (V-Kelly index).

3.6.5 Compressive Strength Test

The compressive strength test was conducted per ASTM C39, using 6-inch (diameter) × 12-inch (height) cylindrical specimens. Four cylinders were cast and tested for their compressive strength 28 days after casting. Figure 3-15 shows an ongoing compressive strength test; the cylindrical specimen is loaded along its longitudinal axis.

Figure 3-15. Compressive Strength Test

3.6.6 Modulus of Elasticity Test

The modulus of elasticity test was performed on 6-inch (diameter) × 12-inch (height) cylindrical specimens in accordance with ASTM C469M. Cylindrical specimens used in the modulus of elasticity test were later on tested for their ultimate compressive strength in accordance with ASTM C39. Figure 3-16 below shows an ongoing modulus of elasticity test.

Figure 3-16. Modulus of Elasticity Test.

3.6.7 Beam Flexural Test

The flexural strength test was performed in accordance with ASTM C 1609 on three 21-inch (length) × 6-inch (wide) × 6-inch (depth) beam specimens with a loading span length of 18 inches. The average flexural strength of the specimens was used to assess the mixture's flexural performance, toughness, and equivalent flexural strength ratio (also known as residual strength ratio (RSR)). Figure 3-17 illustrates an ongoing flexural performance test. Figure 3-18 shows fibers bridging a crack during a flexural performance test. The test data include the peak strength (load supported before cracking) and residual strength (load withstood by fibers after a mid-span displacement of 0.12 inches was reached). The test results were used to determine the Modulus of Rupture (MOR), Residual Strength (RS), RSR, and toughness of concrete. RSR is given by equation (1).

$$RSR = 100 * \frac{f_{e,3}}{MOR} \qquad (1)$$

Where, $f_{e,3}$ is the residual strength (RS) at mid-span for a deflection equal to 0.12 inches (120 mils). The area under the load vs displacement graph was used to determine the toughness of concrete.

Figure 3-17. Four-Point Flexural Bend Test

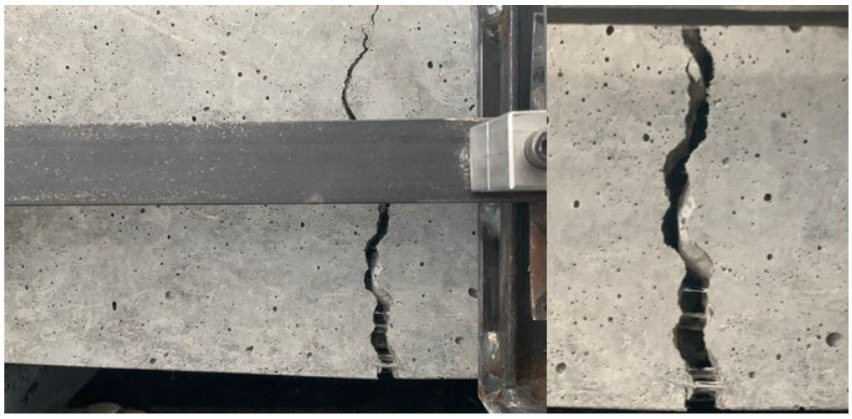

Figure 3-18. Fibers Bridging a Crack

3.6.8 Electrical/Surface Resistivity Test

The electrical surface resistivity test assesses the durability of concrete against the passage of water and aggressive fluids (e.g., chloride ions). Hard and low-impermeable concrete is a poor conductor of electricity compared to concrete with fluid-filled pores. Therefore, the resistivity of concrete is lower when the volume and connectivity of the pore system are higher (Cackler et al., 2017).

The electrical surface resistivity test method was performed following AASHTO TP95 on 4-inch (diameter) × 8-inch (height) cylindrical specimens by using a four-point Werner probe array (AASHTO TP95, 2014) and generating a current flow by applying an AC potential difference in the outer probes of the array. The inner probes measured the difference in the current flow.

In this study, two different sets of specimens were used to study the electrical resistivity of the concrete: (i) Set A- concrete specimens cured in a calcium hydroxide saturated simulated pore solution for 7 days (referred to as bucket test), and (ii) Set B- concrete specimens cured in a moist room for 28 days (20^0C and 95 relative humidity). Some specimens of Set A were also tested at 28 days.

The Werner probe array reading displays the apparent surface resistivity, and the uniaxial resistivity is calculated using equation (2):

$$R_{measured} = \frac{\rho_{Apparent}}{2\pi a \text{ or } 24} \qquad (2)$$

Where:

$$\rho_{Apparent} = Surface\ resistivity\ reading\ (ohm)$$

3.6.9 Rapid Freeze-Thaw Test

The rapid freeze-thaw test was performed following ASTM C666 to study the resistance of concrete to distresses caused by multiple freeze-thaw cycles (ASTM C666, 2008). This test evaluates the durability of concrete against shrinkage and expansive damages due to variations in temperature or weather conditions. Figure 3-19 shows the freeze-thaw chamber used to conduct this test.

Three beam specimens were exposed to freeze-thaw cycles inside a freeze-thaw chamber for each mix. The specimens were covered with wet burlaps for 24 hours before demolding and cured for 14 days prior to testing. The beams were put in aluminum containers surrounded by water and placed in the freeze-thaw chamber as per the test specification. The Relative Dynamic Modulus of Elasticity (RDME) was calculated at every 30 freeze-thaw cycles up to 300 cycles for each specimen. The average RDME of the specimens after 300 cycles was used to assess the durability of the concrete against distresses caused by multiple freeze-thaw cycles. The RDME was calculated using equation (3).

$$P_C = \frac{{E_C}^2}{{E_0}^2} * 100 \qquad (3)$$

Where:

$P_c = relative\ dynamic\ modulus\ of\ elasticity\ corresponding\ to\ c\ number\ of\ cycles,\ \%$

$E_C = dynamic\ modulus\ of\ elasticity\ after\ c\ number\ of\ freeze\text{–}thaw\ cycles, ksi$

$E_0 = dynamic\ modulus\ of\ elasticity\ after\ 0\ freeze\text{–}thaw\ cycles, ksi$

The durability factor was calculated as follows:

$$DF = \frac{PN}{300}$$

Where:

$$DF = durability\ factor, \%$$
$$P = relative\ dynamic\ modulus\ at\ N\ number\ of\ cycles, \%$$
N = number of cycles until specimen reaches 300 cycles or RDME reaches 60%.

Figure 3-19. Freeze-Thaw Chamber

3.6.10 Formation Factor Bucket Test

The formation factor bucket test evaluates the ability of concrete to prevent fluid transport through its pores, indicating concrete's resistance to chloride ion penetration. The test was conducted according to AASHTO TP 119-15 on two 4-inch (diameter) × 8-inch (height) cylindrical specimens. Immediately after demolding, the specimens were immersed in a 5-gallon bucket with calcium hydroxide saturated pore solution (consisting of 7.6g/L NaOH, 10.64g/L KOH, and 2g/L Ca $(OH)_2$). The specimens were kept in the solution for seven days before testing them using the Werner probe array. The specimens were tested at room temperature. Some specimens were also tested at 28 days.

CHAPTER 4: RESULTS AND DISCUSSIONS

This chapter presents the laboratory test results and discusses the influence of the fibers and aggregate types on the fresh and hardened concrete test results. First, the summary of the results is provided in tabular form, including key results for all mixes prepared in this study. All the fresh and hard concrete properties are discussed afterward, emphasizing the influence of the fiber type, dosage, and aggregate properties on the hard concrete properties.

4.1 RESULTS SUMMARY

The fresh concrete test results summary is given in Table 4-1. Along with the test results for mixes prepared in the lab, results for one plain and one fiber reinforced concrete field mixes are also provided. The two field mixes (Field_PC & Field_FRC) were used in a MnROAD test cell repair work (Cell 506) in the 2020 summer. It is assumed that these mixes were not designed according to the PEM requirements but are included in Table 4-1 for comparison purposes. All the results are analyzed and discussed in the next section of this chapter.

Table 4-1. Fresh Concrete Properties

Mixture Designation	Slump (in)	V-Kelly Slump (in)	V-Kelly Index (in)	Air (%)	SAM Number	Box Rating
Field_PC	5.50	NA	NA	7.80	0.09	NA
Field_FRC	NA	NA	NA	5.70	0.44	NA
6AP	2.50	2.50	1.23	7.00	0.19	1.50
8AP	3.25	1.80	1.24	9.00	0.27	1.00
4AP	2.00	0.80	1.03	4.00	0.16	2.50
8AP (2)	3.50	2.70	1.17	10.60	0.20	1.00
6AP (2)	2.00	2.30	1.21	6.00	0.23	2.00
8(4)A1.26	2.00	0.90	0.79	4.90	0.21	2.00
8A1.26	2.00	0.80	0.81	8.10	0.40	1.50
8A1.26(2)	3.50	2.50	1.17	9.70	0.17	1.00
4A1.50	1.25	0.50	0.46	2.90	0.84	3.50
6A1.50	1.75	0.40	0.71	5.90	0.30	3.13
4(6)A1.50	1.75	1.30	0.69	6.90	0.23	2.50
8A1.50	1.50	0.30	0.26	7.50	0.20	3.50
4A2.26	2.25	1.00	0.41	4.40	0.24	1.88
6A2.26	2.25	0.70	0.80	7.00	0.16	3.13
8A2.26	3.75	1.00	0.69	7.70	0.11	1.38
6(8)A2.26	3.25	0.90	0.57	7.60	0.14	1.06
4A2.50	0.25	0.50	0.42	2.80	0.74	3.75

6A2.50	3.25	1.10	0.62	6.30	0.15	1.75
8A2.50	3.75	1.30	0.28	8.90	0.12	1.00
8A2.50(2)	3.00	0.60	0.46	8.20	0.17	1.25
6BP	3.00	2.80	1.03	5.40	0.21	1.13
8(6)BP	3.50	2.70	0.98	5.60	0.19	1.00
8BP	2.75	2.00	1.32	7.50	0.23	1.00
4BP	2.25	2.00	0.92	3.00	0.80	1.50
4B1.26	2.00	1.50	0.61	3.50	0.67	3.25
6B1.26	1.75	1.80	0.88	6.90	0.18	1.88
8B1.26	4.00	2.50	0.79	8.50	0.14	1.13
4B1.50	1.00	0.60	0.35	4.00	0.72	3.25
6B1.50	3.00	1.50	0.47	6.40	0.24	1.88
8B1.50	2.50	1.90	0.61	8.90	0.12	1.25
8(6)B2.50	2.00	2.30	0.60	6.10	0.47	1.63
6B2.50	2.50	2.20	0.58	6.10	0.23	3.13
4B2.50	1.25	2.00	0.52	3.10	0.87	3.88
8B2.50	2.75	2.50	0.71	9.20	0.23	1.25
6B2.26	2.00	1.70	0.99	6.50	0.23	-
8B2.26	2.50	2.50	0.84	7.30	0.28	1.00
4B2.26	1.50	1.50	0.68	3.10	0.78	2.50
10C1.50	4.00	2.60	0.80	10.40	0.15	1.00
8C1.50	2.50	2.00	0.72	7.50	0.18	1.25
4C1.50	1.75	0.80	0.50	3.20	0.80	2.25
6C1.50	2.50	1.10	0.69	6.00	0.13	1.00
6C1.26	3.00	3.10	1.02	5.00	0.32	1.00
4C1.26	2.50	1.80	0.80	4.00	0.53	1.00
8(6)C1.26	3.00	1.70	0.90	6.10	0.17	1.00
8C1.26	2.50	1.70	0.90	7.80	0.18	1.00
8(6)CP	1.75	1.50	0.95	5.80	0.28	2.00
8CP	2.25	2.70	1.14	7.10	0.14	1.25
4CP	2.00	1.60	1.16	3.80	0.79	2.00
6C2.50	1.50	1.20	0.78	5.20	0.44	1.00
4C2.50	1.50	0.60	0.63	2.80	0.76	2.00
8C2.50	3.00	2.20	1.09	7.40	0.21	1.00
6C2.26	2.75	2.00	0.96	5.90	0.34	1.00
4C2.26	2.25	2.80	1.06	3.60	0.80	1.25
8C2.26	3.50	3.30	1.01	8.00	0.21	1.00
8C2.26 (2)	3.25	3.00	1.07	9.20	0.17	1.00

Mix designations listed in Table 4-1 provide information about the fiber, aggregate and target air voids of the mixes. For example, 8A1.50 represents a mix with a design air content of 8%, Granite class A aggregates (A), a fiber with a serial number of 1 (Fiber 1), and a fiber dosage of 0.50%, in terms of concrete's volume fraction. Field_PC represents Field Plain Concrete, and Field_FRC represents Field

Fiber-Reinforced Concrete. The hardened concrete test results are summarized in Table 4-2 and Table 4-3. The modulus of elasticity values obtained from the laboratory test and the ACI equation are included in Table 4-3. Note that 1 "mil" is equal to 1/1000 inches.

Table 4-2. Hardened Concrete Test Results, Part 1

Mixture	28-Day Compressive Strength (psi)	28-Day Surface Resistivity (kOhm-cm)	MOR (psi)	Toughness (in-lb)	Residual Strength (lbf)	RSR (%)	Deflection at Peak Load (mil)
Field_PC	4367	11	601	15	0	0	3.49
Field_FRC	4687	9	577	435	232	40	3.37
6AP	3730	23.6	560	74	0	0	3.6
8AP	3526	24	606	111	0	0	4.07
4AP	5891	20	717	20	0	0	3.94
8AP (2)	3458	22.6	540	88	0	0	3.25
6AP (2)	5245	21.7	696	118	0	0	4.19
8(4)A1.26	4535	20	684	351	130	19	3.88
6A1.26	4378	21	619	272	94	15	3.73
4A1.50	5195	17	746	484	234	32	4.40
6A1.50	4466	19	630	406	240	39	3.67
4(6)A1.50	4628	19	669	480	277	41	4.09
8A1.50	3954	22	605	359	161	26	3.63
4A2.26	5878	21	753	291	93	12	4.41
6A2.26	6271	23	735	367	156	21	4.64
8A2.26	4525	24	674	409	149	22	4.38
6(8)A2.26	5196	24	708	342	133	19	4.36
4A2.50	6629	19	817	467	213	26	4.75
6A2.50	5558	20	634	369	164	26	4.48
8A2.50	4932	23	664	452	219	33	4.88
8A2.50(2)	4947	23	682	537	294	44	4.82
6BP	5795	20	776	107	0	0	4.32
8(6)BP	5973	18.8	761	51	0	0	4.39
8BP	4566	19.1	675	45	0	0	3.89
4BP	6340	16.7	816	60	0	0	4.21
4B1.26	6928	18	809	339	91	11	4.83
6B1.26	5738	19	800	341	103	13	4.85
8B1.26	5074	19	647	306	83	13	4.74
4B1.50	5744	20	777	427	171	22	4.85
6B1.50	4857	19	760	462	210	28	4.83
8B1.50	4770	20	696	433	189	27	4.84
8(6)B2.50	4847	17.9	734	543	291	40	4.65
6B2.50	5539	18.5	771	599	343	45	4.80

4B2.50	6620	17.9	890	629	327	37	4.88
8B2.50	4108	19.9	654	489	275	42	4.37
6B2.26	4791	19.9	691	472	163	23	4.33
8B2.26	4321	19.9	697	408	190	27	3.88
4B2.26	6060	21.1	815	402	148	18	4.49
10C1.50	4107	22	629	462	225	36	4.42
8C1.50	4093	20	656	432	207	32	5.55
4C1.50	5252	18.4	739	514	246	33	4.93
6C1.50	4849	18.5	717	455	230	32	4.73
6C1.26	4806	18.4	695	322	139	20	4.72
4C1.26	5494	18.1	736	266	132	18	4.16
8(6)C1.26	4733	17.8	603	275	128	21	3.90
8C1.26	4773	17.8	671	314	143	21	4.70
6CP	5329	17.2	663	84	0	0	4.37
8(6)CP	4980	18	666	94	0	0	3.82
8CP	4384	17.8	618	54	0	0	4.35
4CP	5724	17.4	682	114	0	0	4.68
6C2.50	4321	20	692	546	325	47	4.41
4C2.50	5245	18.1	691	561	307	44	4.16
8C2.50	3949	18.2	635	582	355	56	4.35
6C2.26	4370	18.2	671	380	168	25	4.67
4C2.26	5325	17.9	627	350	158	27	4.38
8C2.26	3620	19	575	333	149	26	3.44
8C2.26 (2)	4235	19.8	541	345	177	33	4.17

Table 4-3. Hardened Concrete Test Results Part 2.

Mixture	Modulus of Elasticity (x10^6 psi)		Poisson Ratio	Average Density (lb/ft^3)
	Lab Test	ACI Equation		
Field_PC	3.84	3.83	0.21	148.0
Field_FRC	4.00	3.82	0.20	147.6
6AP	4.62	3.33	0.21	148.9
8AP	3.87	3.38	0.18	145.6
4AP	5.94	4.2	0.25	152.7
8AP (2)	4.00	4.45	0.21	143.4
6AP (2)	4.41	4.22	0.17	149.3
8(4)A1.26	4.05	3.93	0.22	150.3
6A1.26	4.08	3.87	0.23	148.9
8A1.26	4.21	3.59	0.25	147.9
4A1.50	4.77	4.01	0.21	151.8
6A1.50	4.38	3.77	0.20	148.0
4(6)A1.50	3.75	3.79	0.23	147.1
8A1.50	3.45	3.52	0.21	147.4
4A2.26	2.71	4.4	0.13	153.7
6A2.26	4.16	4.45	0.22	152.1
8A2.26	2.14	3.83	0.10	147.2
6(8)A2.26	4.92	3.96	0.40	148.8
4A2.50	3.13	4.67	0.06	153.7
6A2.50	4.68	4.26	0.26	153.5
8A2.50	2.06	4.15	0.09	147.7
8A2.50(2)	2.77	3.97	0.16	147.0
6BP	4.35	4.25	0.19	150.9
8(6)BP	4.37	4.41	0.22	150.3
8BP	4.48	3.71	0.21	149.3
4BP	5.55	4.52	0.21	154.6
4B1.26	4.80	4.75	0.26	153.9
6B1.26	4.32	3.91	0.24	150.8
8B1.26	4.34	3.95	0.22	148.5
4B1.50	4.80	4.32	0.20	152.7
6B1.50	4.04	3.92	0.22	147.3
8B1.50	4.70	3.95	0.22	148.1
8(6)B2.50	4.25	3.99	0.19	150.2
6B2.50	4.32	4.15	0.19	149.6
4B2.50	5.19	4.69	0.21	154.2
8B2.50	4.04	3.65	0.20	145.7
6B2.26	4.07	3.95	0.17	148.6

Mixture	Modulus of Elasticity (x10^6 psi)		Poisson Ratio	Average Density (lb/ft^3)
	Lab Test	ACI Equation		
8B2.26	4.05	3.68	0.18	147.7
4B2.26	4.9	4.49	0.2	153.2
10C1.50	3.47	3.70	0.16	144.4
8C1.50	3.76	3.64	0.24	145.8
4C1.50	4.29	4.08	0.30	152.3
6C1.50	4.16	4.04	0.27	148.7
6C1.26	4.53	3.97	0.22	150.1
4C1.26	5.27	4.13	0.19	152.7
8(6)C1.26	4.82	3.98	0.21	149.2
8C1.26	4.59	4.03	0.24	150.1
6CP	4.82	4.18	0.19	150.8
8(6)CP	4.29	3.97	0.19	151.3
8CP	4.06	3.72	0.17	149.1
4CP	5.86	4.32	0.19	153.6
6C2.50	4.29	3.76	0.19	150.8
4C2.50	4.76	4.20	0.19	153.4
8C2.50	4.53	3.58	0.23	148.0
6C2.26	4.38	3.92	0.18	150.3
4C2.26	4.43	4.12	0.20	152.2
8C2.26	3.37	3.36	0.17	148.0
8C2.26 (2)	3.87	3.74	0.20	145.0

4.2 DISCUSSIONS

4.2.1 Fresh Concrete Properties

4.2.1.1 SAM Test

A SAM number of 0.20 (corresponding to a spacing factor of 0.008 inches and durability factor of 70%) or below is recommended for plain concrete mixtures subjected to harsh weather conditions, including freezing and thawing (Ley, 2015). The SAM number results presented in Figure 4-1 show that increased entrained air content decreases the SAM number. A large set of SAM numbers is close to 0.20, the recommended SAM number value for plain concrete. It also appears that the SAM number can be as high as 0.5 to 0.8 when the concrete mixture contains less than 5.5% air voids.

The influence of fibers on SAM number was investigated by comparing the SAM numbers for all mixes with air content above 5.5%. Mixes with less than 5.5% air content were not included because they are not suitable for resistance against freeze-thaw-related distresses and are usually not recommended in Minnesota-like climates for pavements or bridge decks. Figure 4-2 shows the average SAM numbers for plain (no fiber) and two FRC mixes with 5.5% or more air contents. The average SAM numbers for mixes with no fiber, 0.26% V_f and 0.50% V_f were 0.22, 0.20, 0.21, with standard deviations of 0.05, 0.09, 0.06, respectively. It shall be noted that the workability (slump) and air content of the plain and FRC mixes presented in Figure 4-2 were comparable. FRC mixes needed additional water reducer admixture than plain concrete mixes to achieve comparable workability and air content.

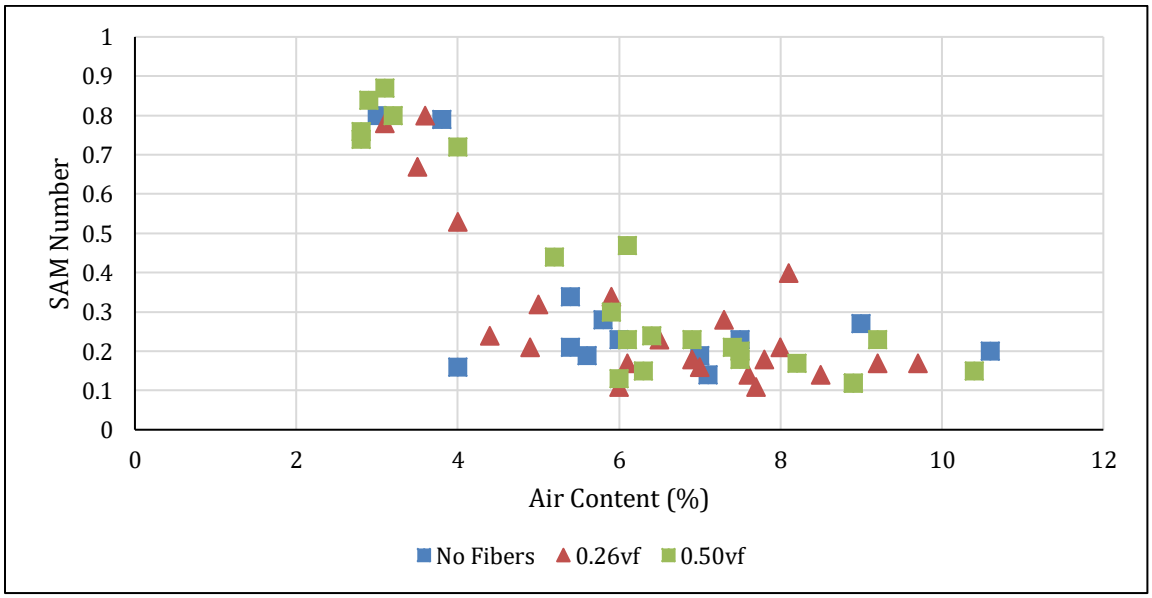

Figure 4-1. SAM Number vs. Air Content

Figure 4-3 shows that for aggregate type A (crushed granite), fiber 1 resulted in higher SAM numbers irrespective of the fiber dosages. Fiber type was more influential on the SAM number than the fiber dosages. Similar plots for aggregates B and C can be found in Figure 4-4 and Figure 4-5. In the case of Aggregates B and C, mixes with fiber 2 showed relatively higher SAM numbers than the mixes with fiber 1.

In conclusion, it can be stated that if the air content is 5.5% or more and the workability of the mixes is good for paving, the SAM numbers between the plain and FRC mixes are comparable, with a slightly higher value for the FRC mixes.

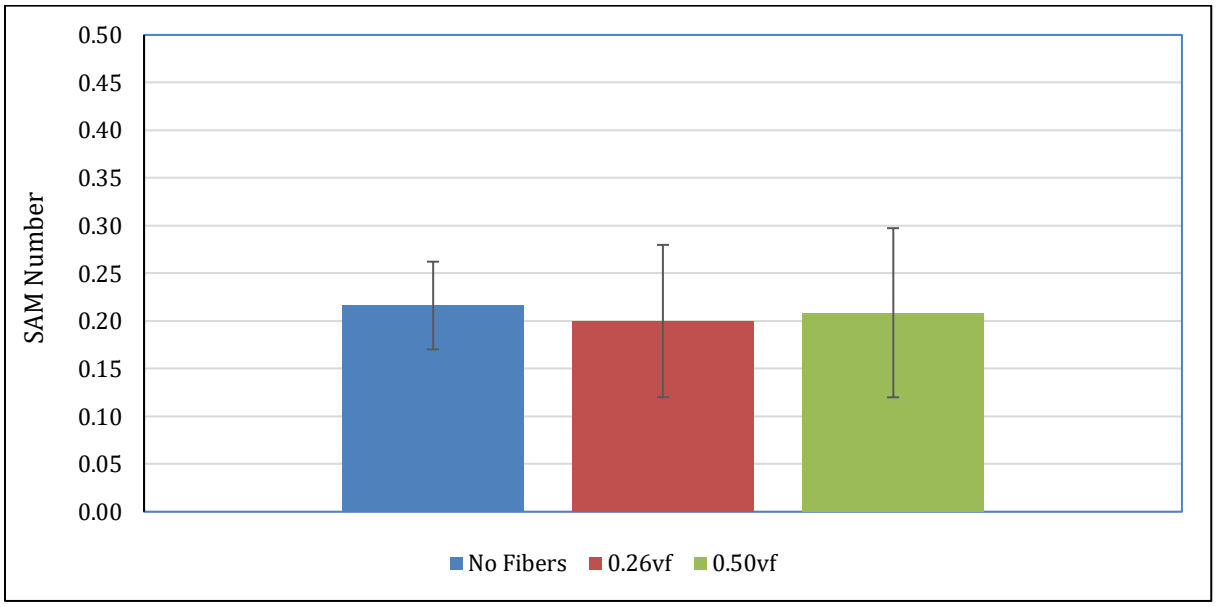

Figure 4-2. Influence of Fiber Dosage on SAM Number (Air Content > 5.5%).

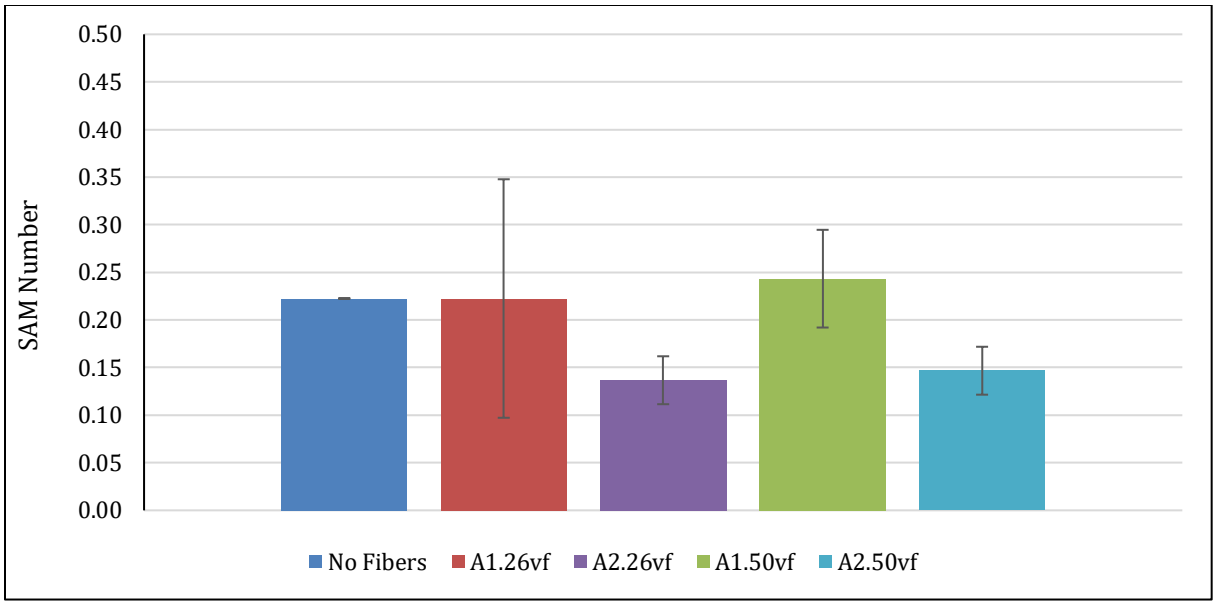

Figure 4-3. Influence of Fiber Type and Dosage on SAM Number (Aggregate A); A1 = aggregate A with fiber 1 (Twisted and bundled), A2 = aggregate A with fiber 2 (embossed geometry).

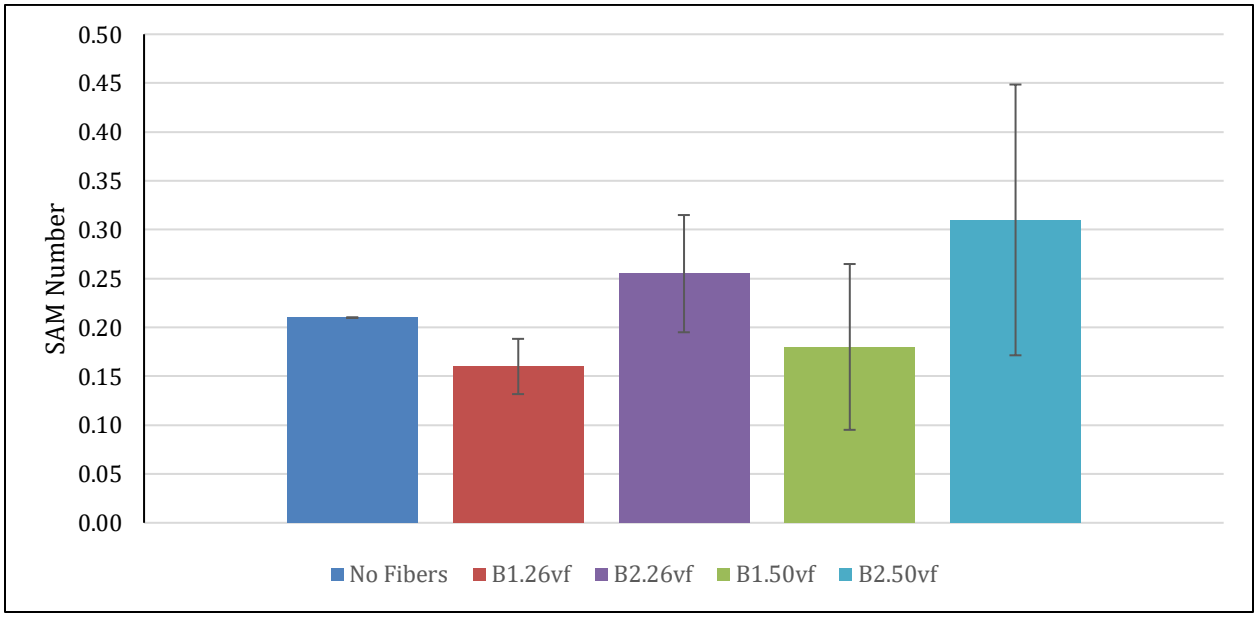

Figure 4-4. Influence of Fiber Type and Dosage on SAM Number (Aggregate B): B1 = aggregate B with fiber 1 (Twisted and bundled), B2 = aggregate B with fiber 2 (embossed geometry).

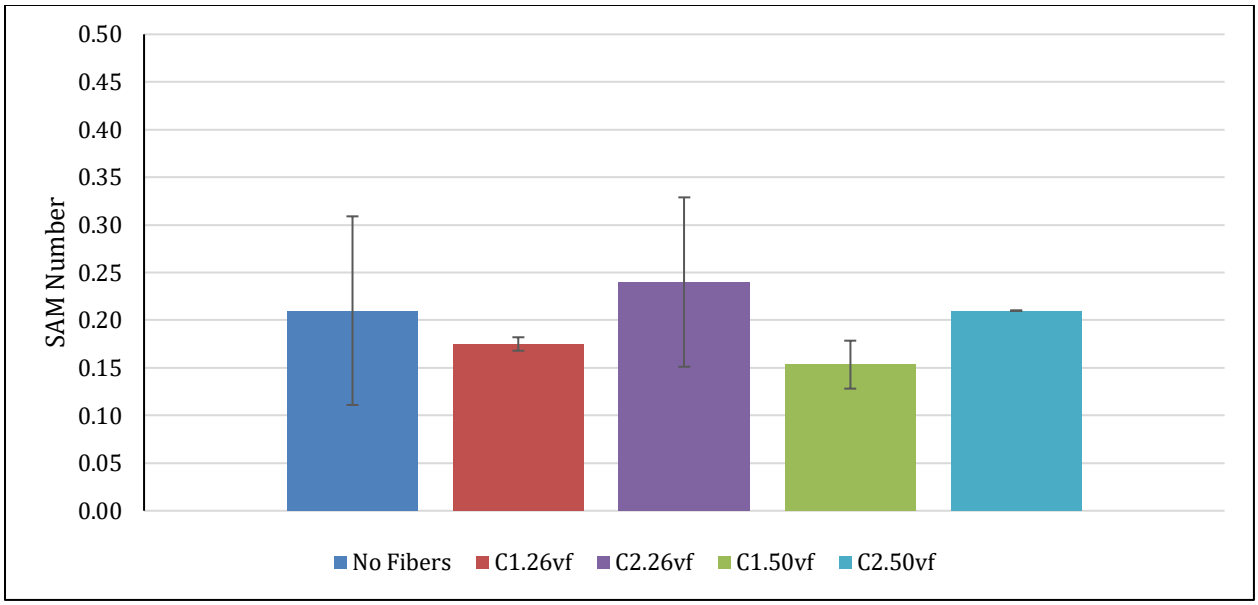

Figure 4-5. Influence of Fiber Type and Dosage on SAM Number (Aggregate C): C1 = aggregate C with fiber 1 (Twisted and bundled), C2 = aggregate C with fiber 2 (embossed geometry).

4.2.1.2 Box Test

As previously discussed, a Box test rating of 2 is ideal, which corresponds to 10 to 30 percent surface voids. A higher rating indicates more surface voids. Figure 4-6 shows the relationship of the Box Test rating with the slump for the mixes tested in this study. This figure indicates that the box test visual rating has an inverse relationship with the slump. As shown in Figure 4-7, the increase in fiber dosage increases the Box Test rating, indicating more voids on the surface. Some concrete mixtures with 0.5% V_f had visual ratings of more than 2. The results are reasonable as the box test rating depends on mixture workability; fiber usually decreases the workability. Figure 4-8 through Figure 4-10 show the relationships between fiber type, fiber dosage, and box test rating for aggregates A, B, and C. Mixes with 0.50% V_f had the highest average box test rating for all three types of aggregates. Aggregate C (gravel) mixes showed the least box test rating relative to the two other aggregates.

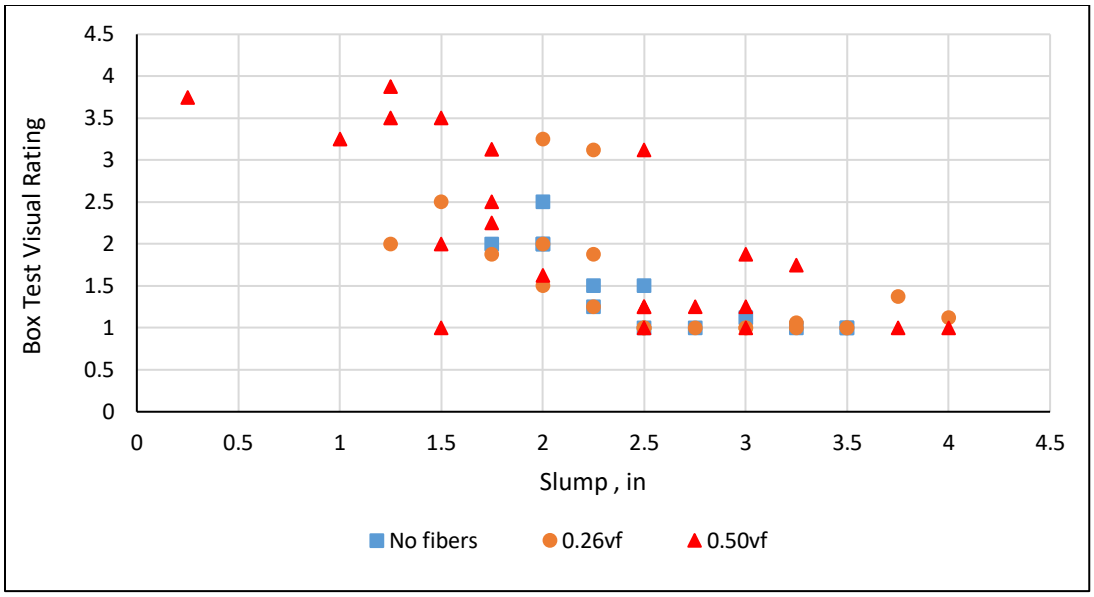

Figure 4-6. Box Test Rating vs Slump

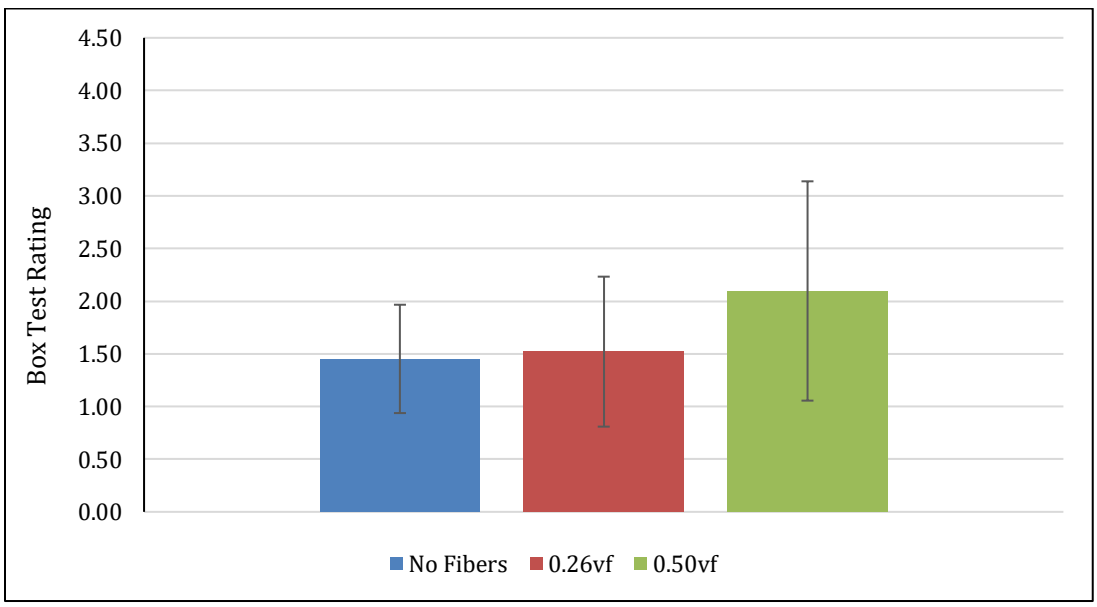

Figure 4-7. Influence of Fiber Dosage on Box Test Rating

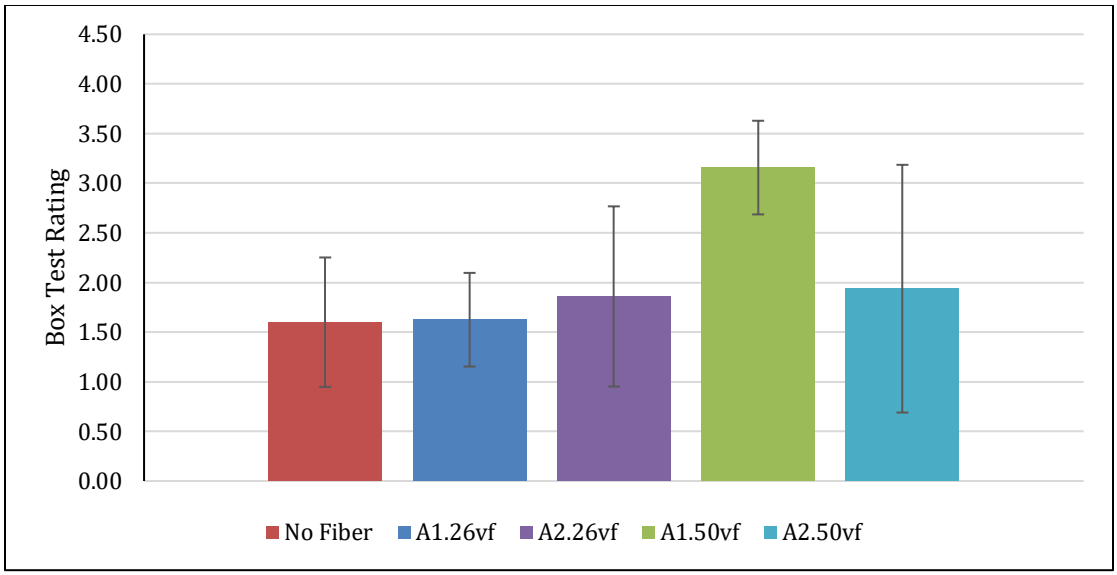

Figure 4-8. Influence Fiber Type on Box Test Rating (Aggregate Class A)

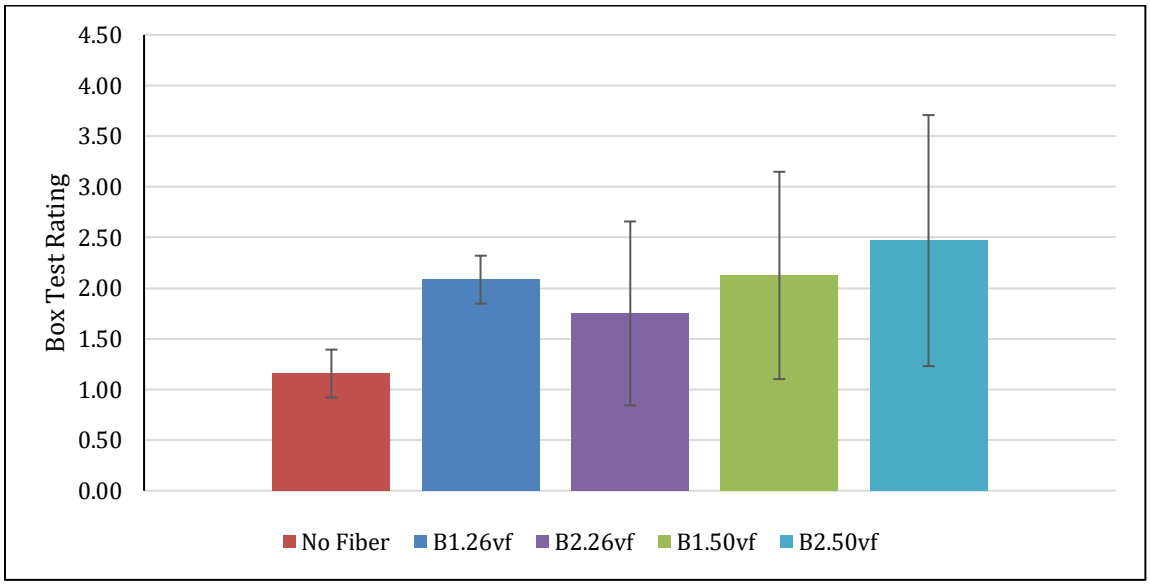

Figure 4-9. Influence of Fiber Type and Dosage on Box Test (Aggregate B)

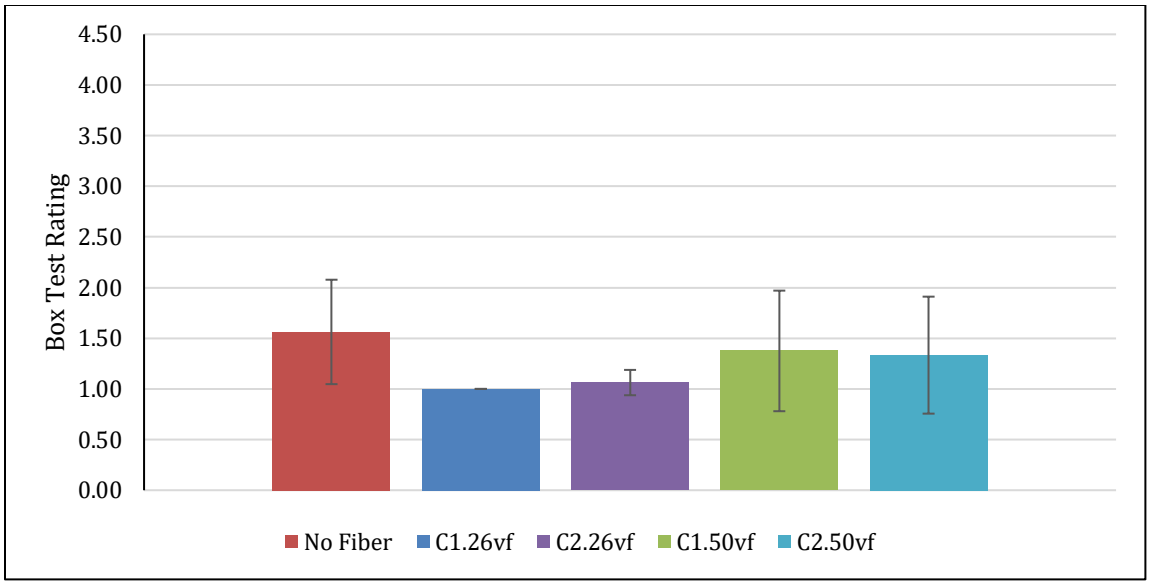

Figure 4-10. Influence of Fiber Type and Dosage on Box Test (Aggregate C)

4.2.1.3 V-Kelly Test

Figure 4-11 compares between V-Kelly slump and regular slump test results. Results show that the V-Kelly slump and regular slump test results (both are based on a static test) show a direct correlation. However, as both these slump test results do not quantify the workability of the concrete under vibration, the V-Kelly index result is more meaningful for investigating the fiber's influence on the pavement concrete's workability. The V-Kelly index decreases as fiber dosage increases for the same slump value. A V-Kelly index between 0.8 to 1.2 in/√s is recommended for the plain concrete mixture for slip-form paving. Figure 4-12 shows that the V-Kelly index and the regular slump test result do not yield a notable correlation. However, Figure 4-13 shows that the V-Kelly index decreases with increased fiber dosage. This was evident during mixing as the mixture became stiffer with increased fiber dosage due to a decrease in mixture workability. The average V-Kelly index for plain concrete was 1.11 in/√s, within the recommended range. The average V-Kelly index for mixtures with 0.26% V_f is 0.84 in/√s, which is at the low end of the recommended range. Mixtures with fiber dosage of 0.50% V_f showed an even lower V-Kelly index of 0.59 in/√s. This indicates that adding fiber to the mixture significantly influences the V-Kelly index and workability of the concrete under vibration in the slip-form paving. Therefore, it can be stated that when fibers are used in the mixtures, additional effort shall be given to improve the workability of the concrete so that the V-Kelly index can be improved to meet the target V-Kelly index of 0.8 in/√s or more. It may also happen that FRC does not need to meet the 0.8 in/√s criterion, as the fibers in the concrete offer resistance to the penetration of the Kelly-ball, which decreases the V-Kelly index. The hard concrete and durability test results for the FRC mixtures discussed in the following section may indicate whether FRC mixes with a lower V-Kelly index passes the criteria.

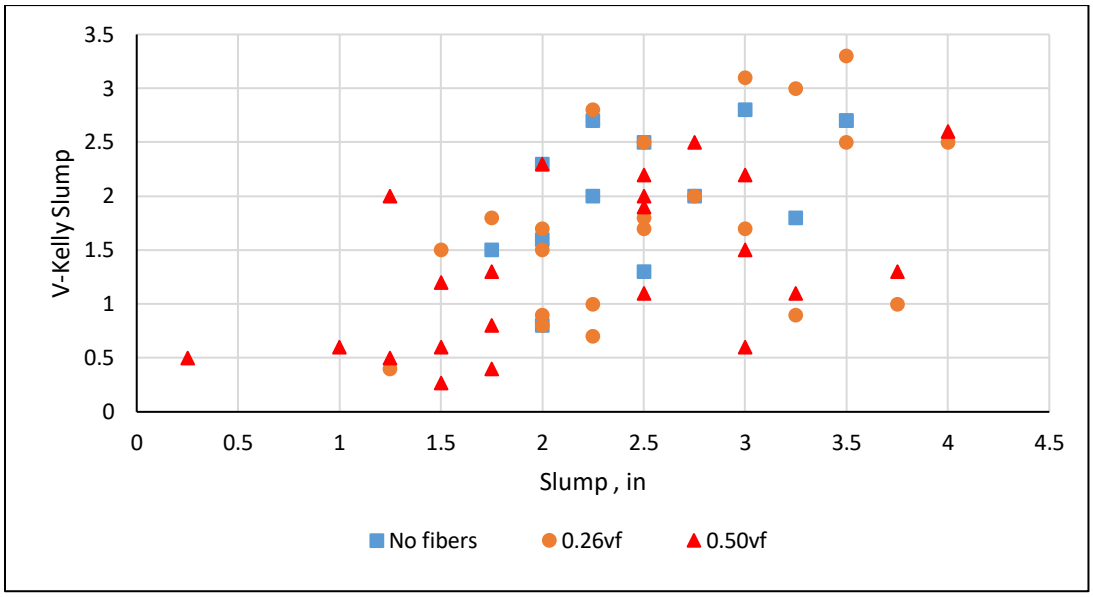

Figure 4-11. V-Kelly Slump vs Slump

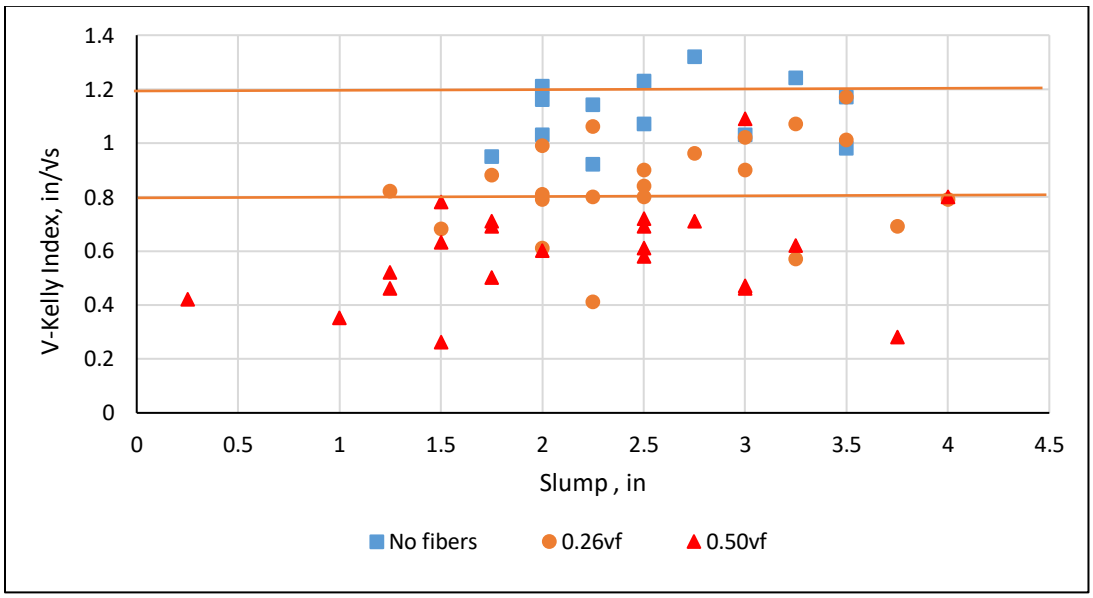

Figure 4-12. V-Kelly Index vs Slump

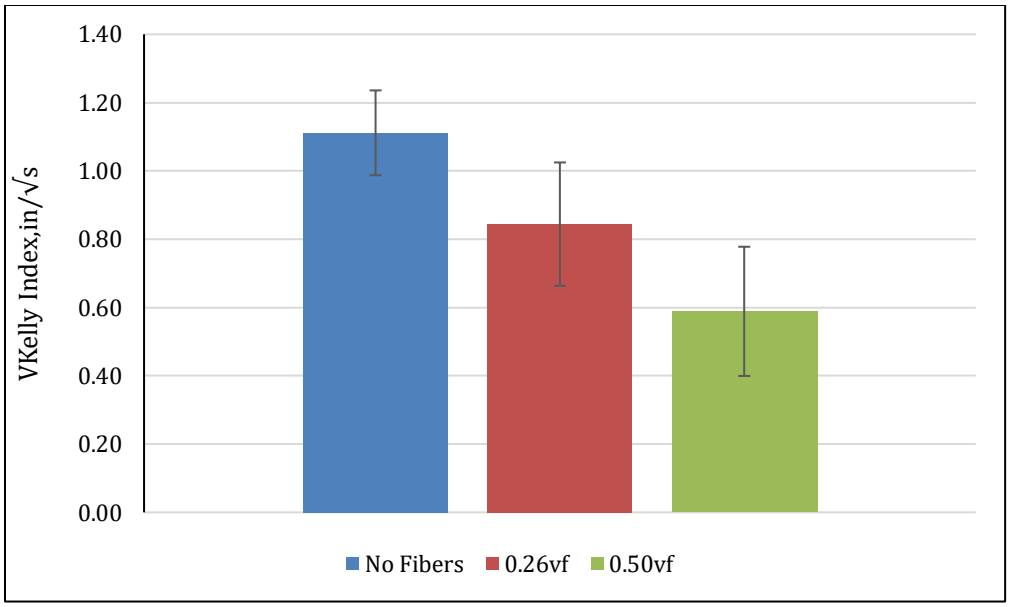

Figure 4-13. Influence of Fiber Dosage on V-Kelly Index

Figure 4-14 shows the influence of the fiber type and dosage on the V-Kelly index. The figure illustrates that the fiber type has no significant influence on the V-Kelly index, at least for the two fibers used in this study, but the fiber dosage does.

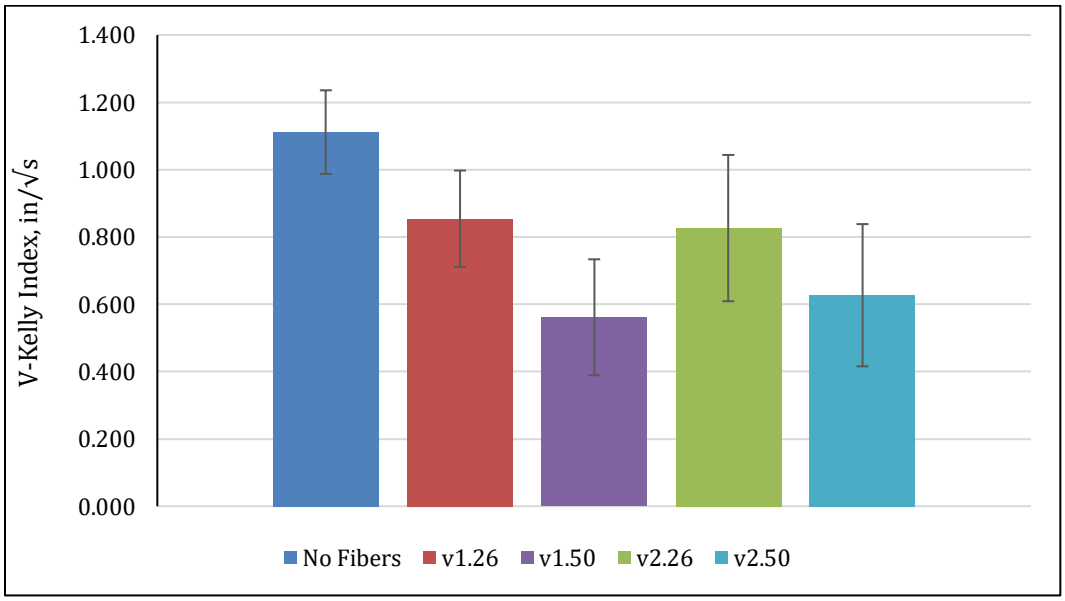

Figure 4-14. Influence of Fiber Type on V-Kelly Index

Figure 4-15 compares the V-Kelly index to fiber type and dosage for aggregate A. It seems fiber 2 resulted in a relatively lower V-Kelly index than fiber 1 for aggregate A. The same figures for aggregates B and C can be found in Figure 4-16 and Figure 4-17. The V-Kelly indexes for aggregates A and B are

comparable, while Aggregate C comparatively resulted in a higher V-Kelly index. The high workability of the mixes with gravel aggregates helped increase the V-Kelly index (less resistance to the Kelly-ball).

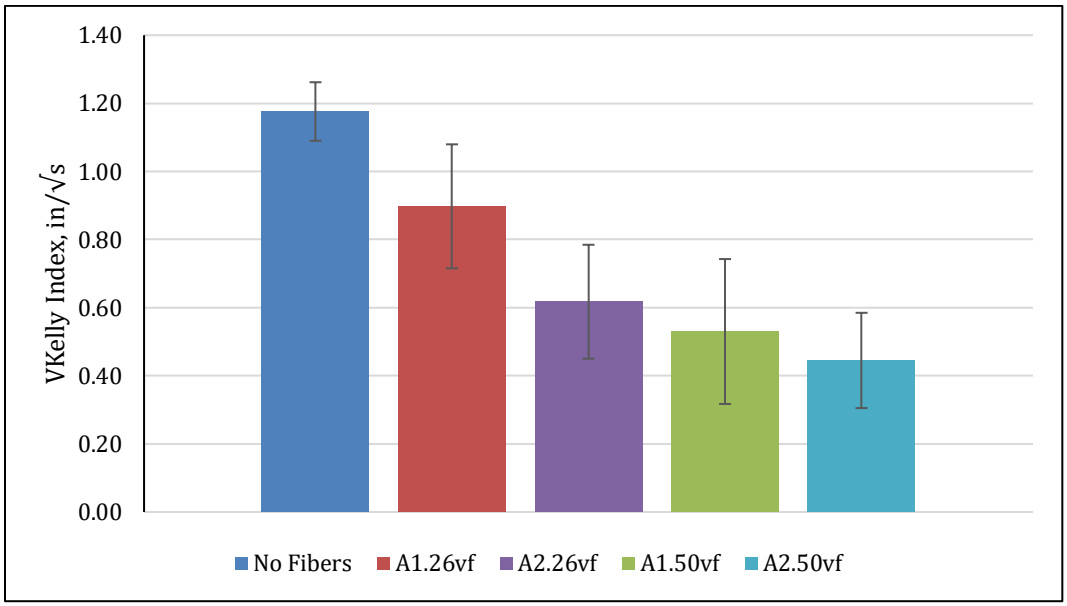

Figure 4-15. Influence of Aggregate Type on V-Kelly Index (Aggregate A)

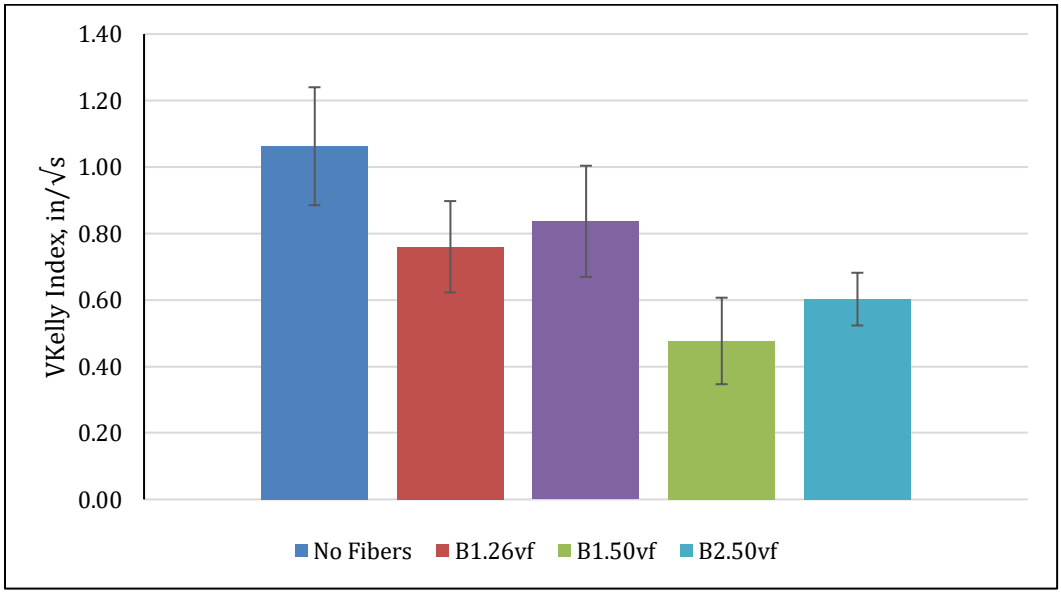

Figure 4-16. Influence of Fiber Type and Dosage on V-Kelly Index (Aggregate B)

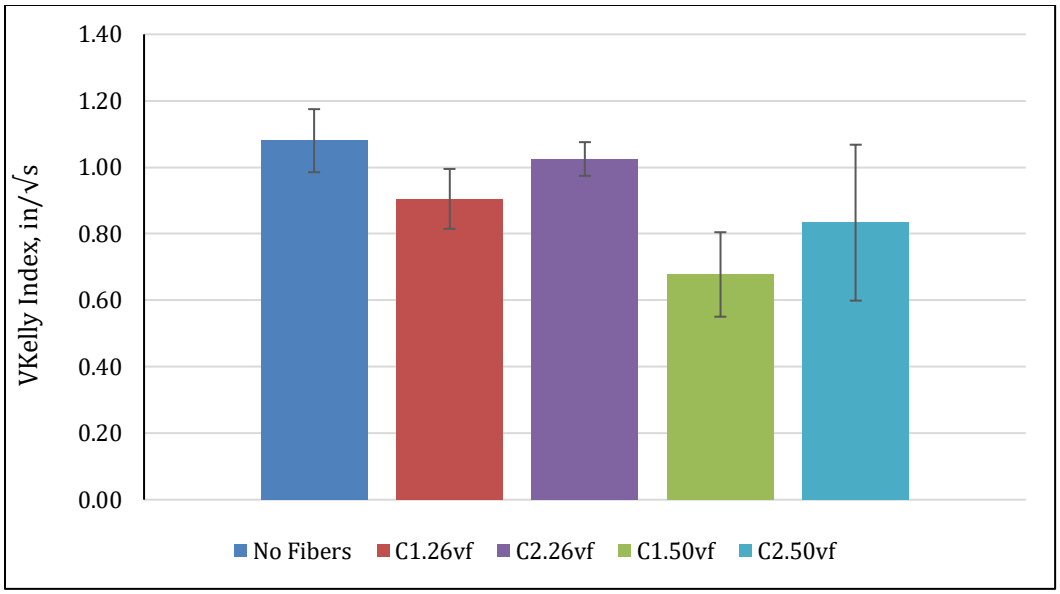

Figure 4-17. Influence of Fiber Type and Dosage on V-Kelly Index (Aggregate C)

4.2.2 Hardened Concrete Properties

4.2.2.1 Compressive Strength

Figure 4-18 shows that an increase in air content is inversely proportional to compressive strength. This finding is consistent with results from Ley (2015); concrete compressive strength decreases by approximately 500 psi for every 1% increase in air content. Aggregate class B showed the highest compressive strength. This could be because of its higher specific gravity value, angular shape, and rough texture. In addition, this observation can be attributed to a higher coarse aggregate to the cementitious material ratio in mixes with aggregate B (with 60% coarse aggregates) than those with aggregate A (with 55% coarse aggregates). Erntroy and Shacklock (1954) found that concrete mixtures with more coarse aggregates per unit volume had higher strength at a constant water-cement ratio. Neville (1996) concluded that the higher strength is due to less water per unit volume of concrete. Aggregate class C showed the lowest compressive strength, which is expected given its lower specific gravity and round shape, and smooth texture.

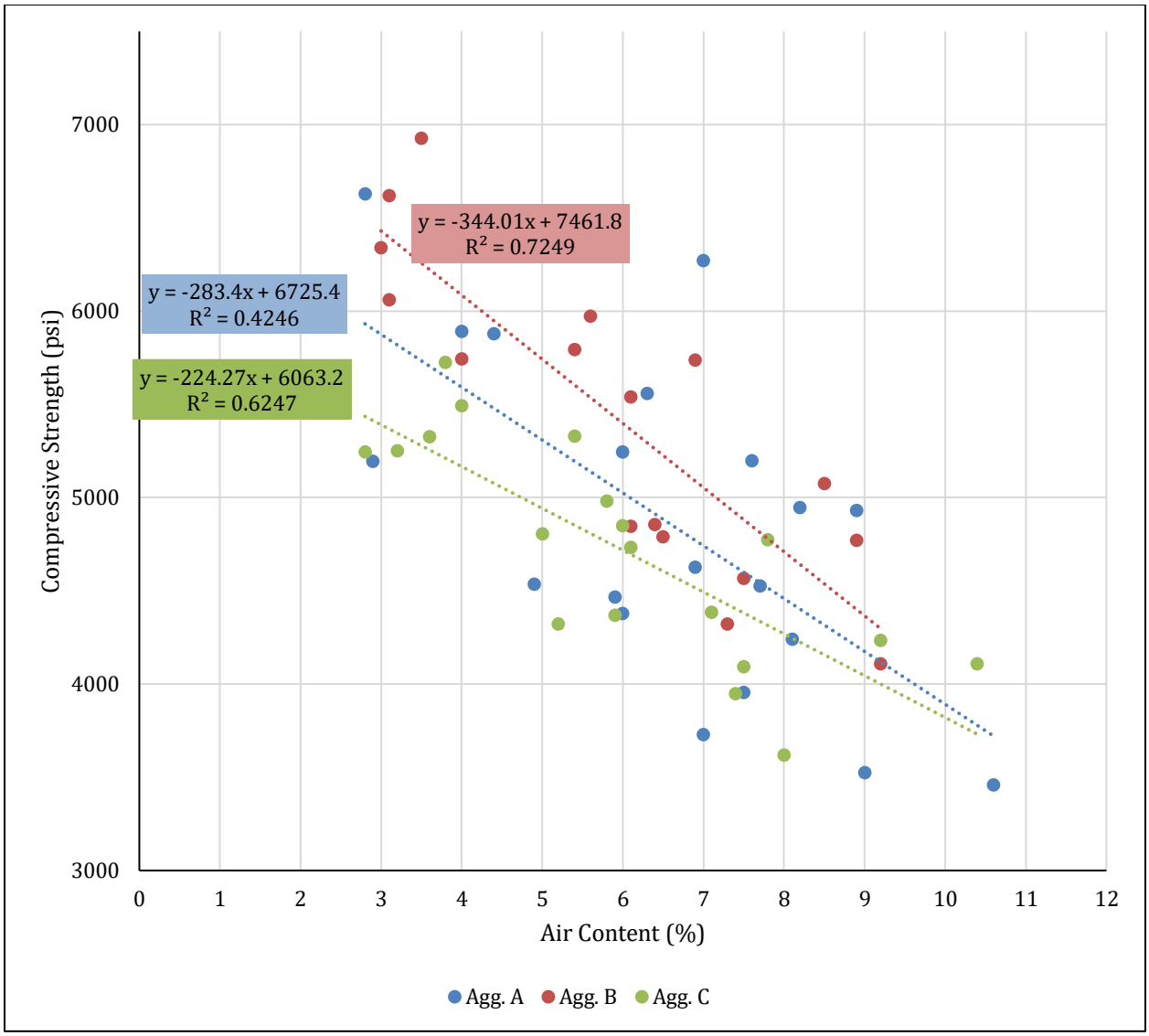

Figure 4-18. Compressive Strength vs. Air Content

Figure 4-19 indicates that the addition of macro synthetic fiber has little effect on the compressive strength of the concrete. The average compressive strengths for plain concrete and FRC mixes with 0.26% V_f, and 0.50% V_f were 4996 psi, 5014 psi, and 4937 psi, respectively. Figure 4-19 shows the compressive strength of mixes with different fiber types and dosages; the variation in compressive strength between the fiber types and dosages is minimal.

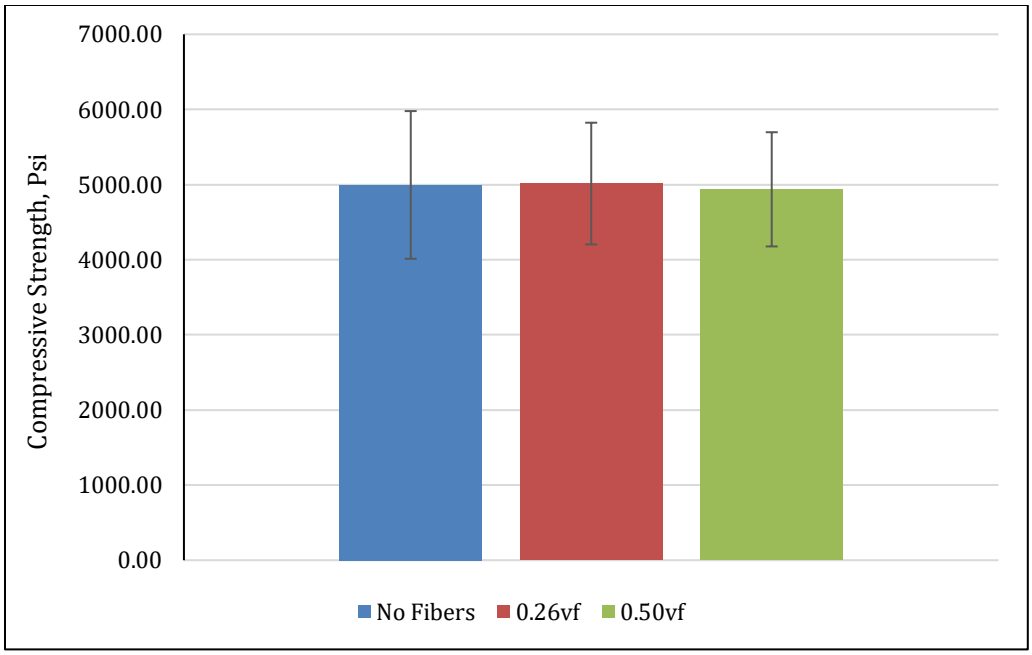

Figure 4-19. Influence of Fiber Dosage on Compressive Strength

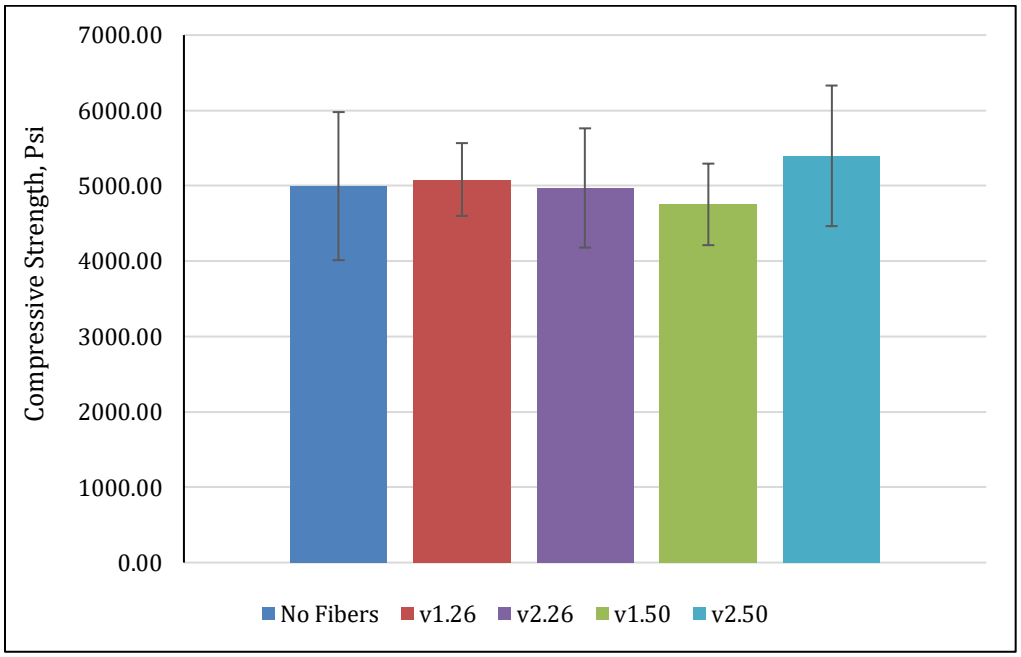

Figure 4-20. Influence of Fiber Type on Compressive Strength

4.2.2.2 Modulus of Elasticity

Figure 4-21 shows that the inclusion of synthetic fibers into the concrete mixture slightly lowers the modulus of elasticity of hardened concrete. Also, as observed in Figure 4-21**,** increasing the fiber dosage from 0.26% to 0.50% V_f does not influence the modulus of elasticity.

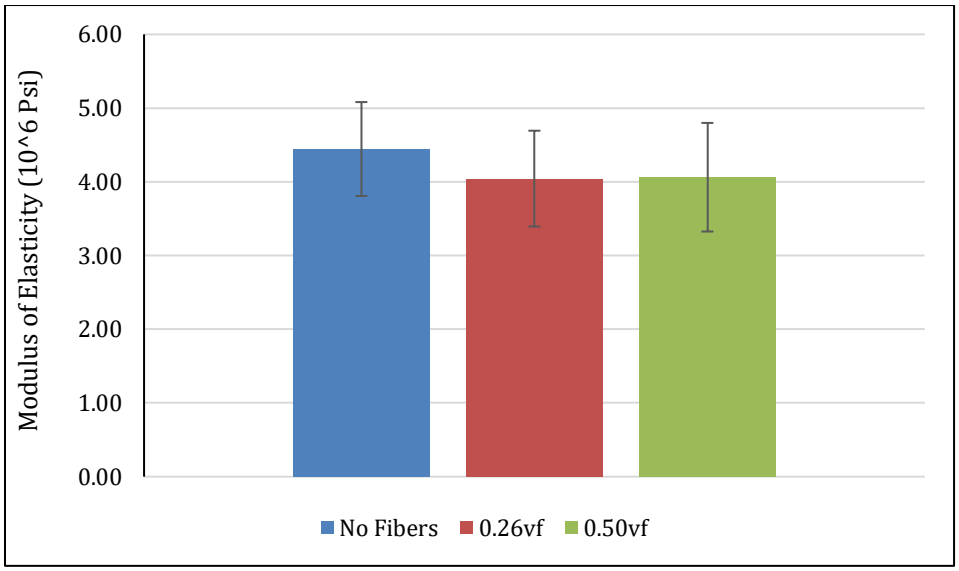

Figure 4-21. Influence of Fiber Dosage on Modulus of Elasticity

4.2.2.3 Flexural Strength

Figure 4-22 shows a decrease in modulus of rupture (MOR) with increased air content. The MOR is also influenced by the aggregate type, with the least MOR achieved for the mixes with aggregate C. As shown in Figure 4-23, the MOR is not influenced significantly by the addition of fibers. This finding agrees with Barman et al. (2018) study, which concluded that MOR remained minimally influenced by the volume fraction of macro synthetic fibers. Figure 4-24 shows that mixes containing Fiber 2 have slightly higher MOR values than the plain concrete (for both dosages) and fiber 1 mixes.

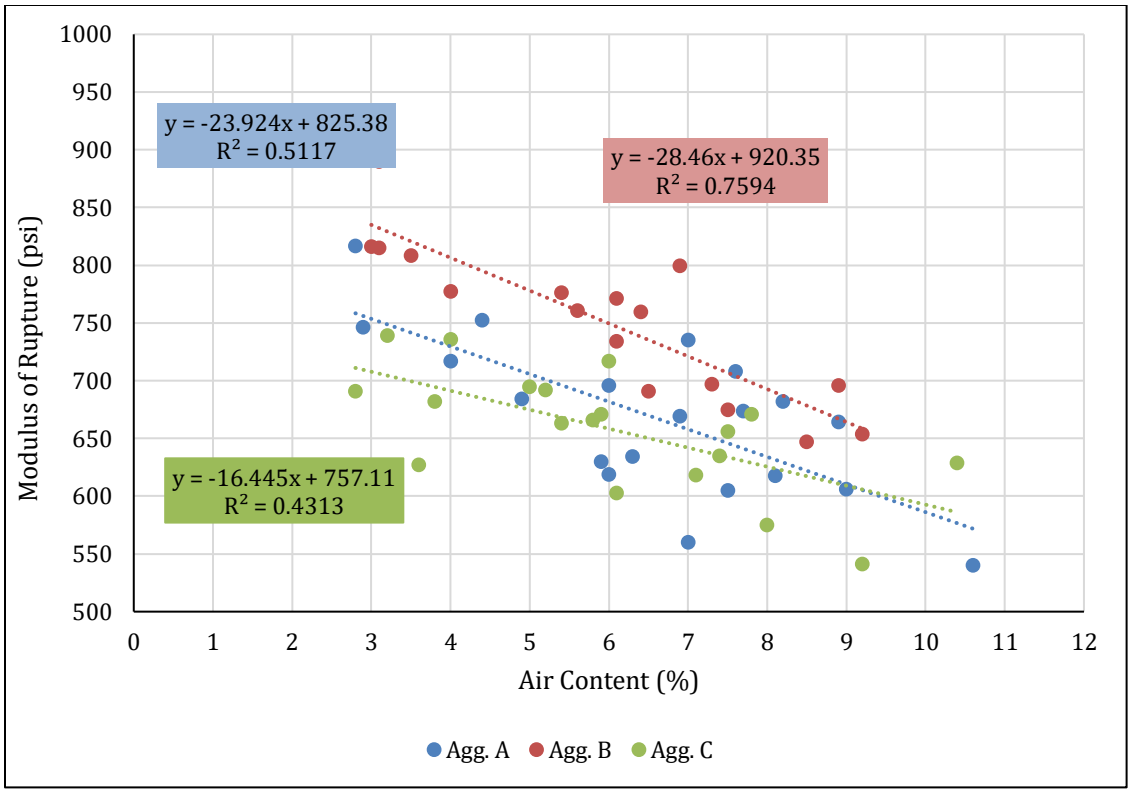

Figure 4-22. MOR vs Air Content

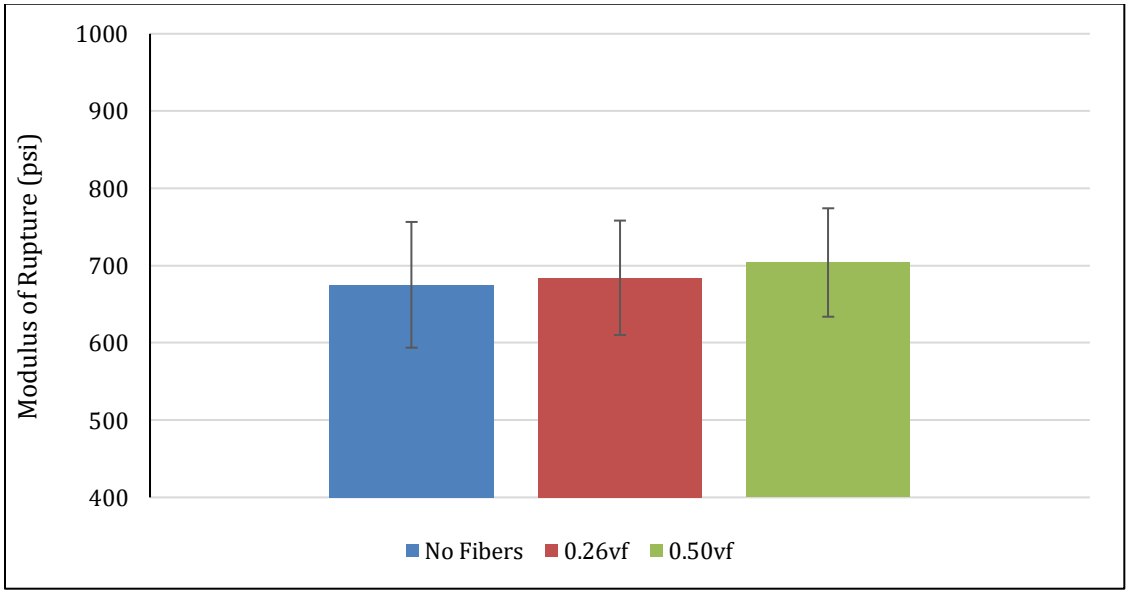

Figure 4-23. Influence of Fiber Dosage on MOR

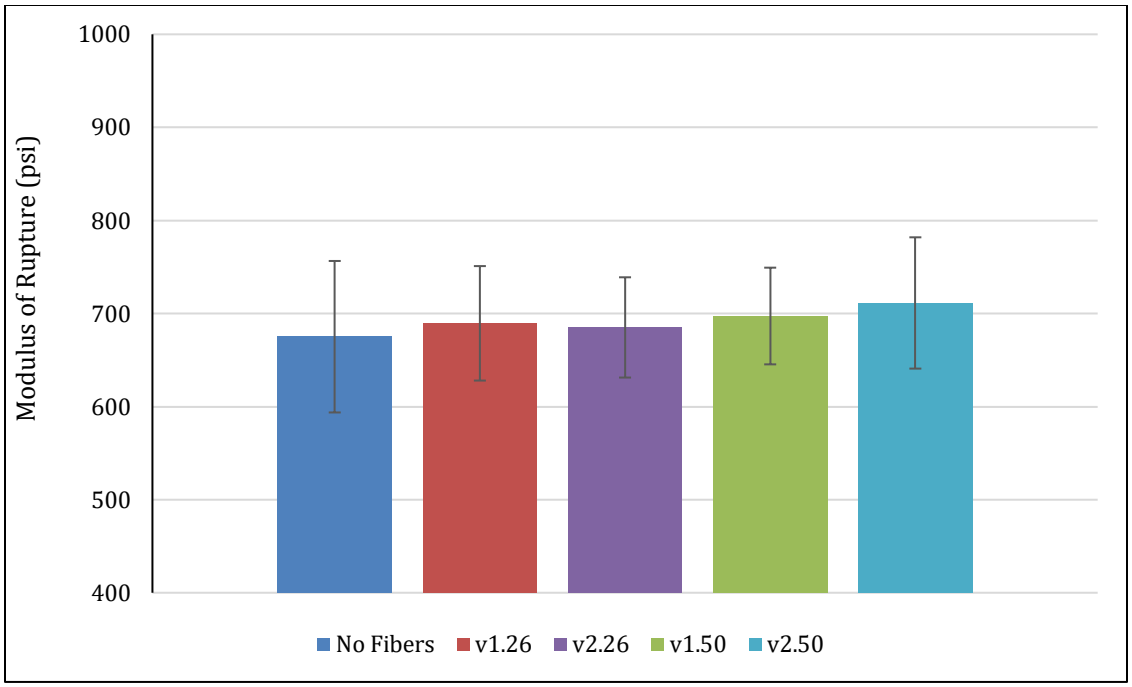

Figure 4-24. Influence of Fiber Type on MOR

4.2.2.4 Flexural Toughness from ASTM 1609 Test

Toughness values are computed from the load vs. displacement relationships obtained in the ASTM C1609 test. Figure 4-25 shows some example load vs. displacement curves for FRC beams. These curves are for five random specimens prepared of Fiber 1 (0.26% and 0.50% V_f fibers, 6% air content, aggregate A). The average toughness values for the two fiber dosages (all aggregate and fiber types) are shown in Figure 4-26. The effect of the fiber dosage on flexural toughness is evident. The average toughness improves by 42% by increasing the fiber dosage from 0.26% to 0.50% V_f.

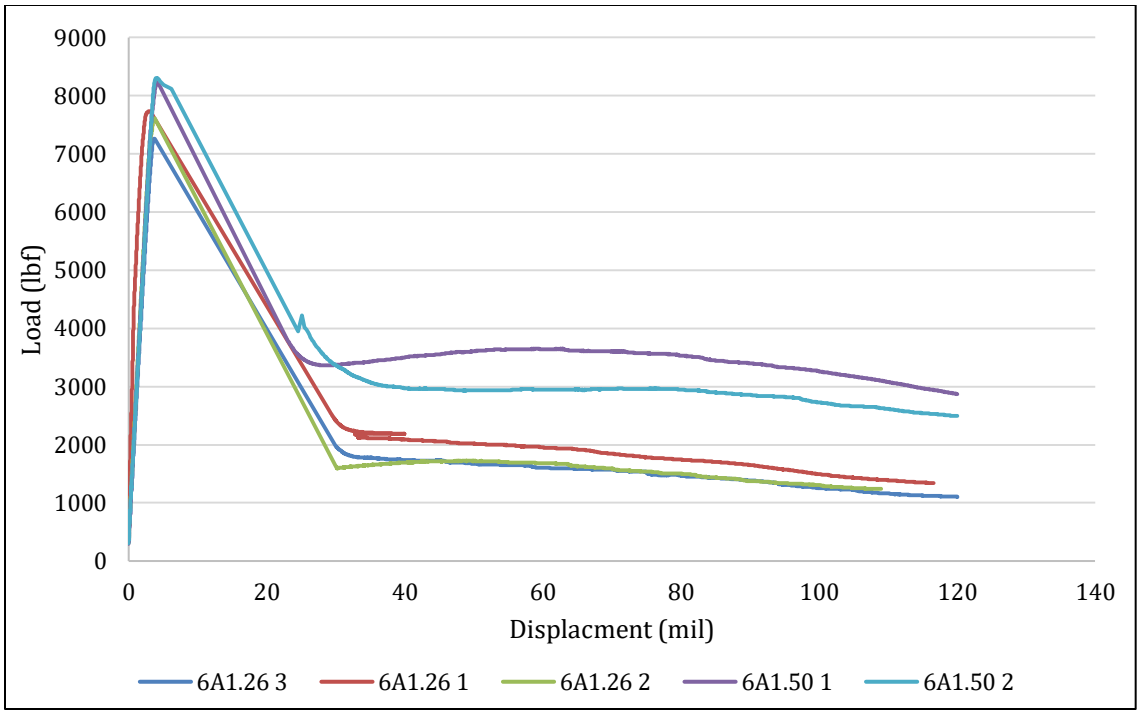

Figure 4-25. Load vs. Displacement for Two Fiber Dosages (6 percent air voids)

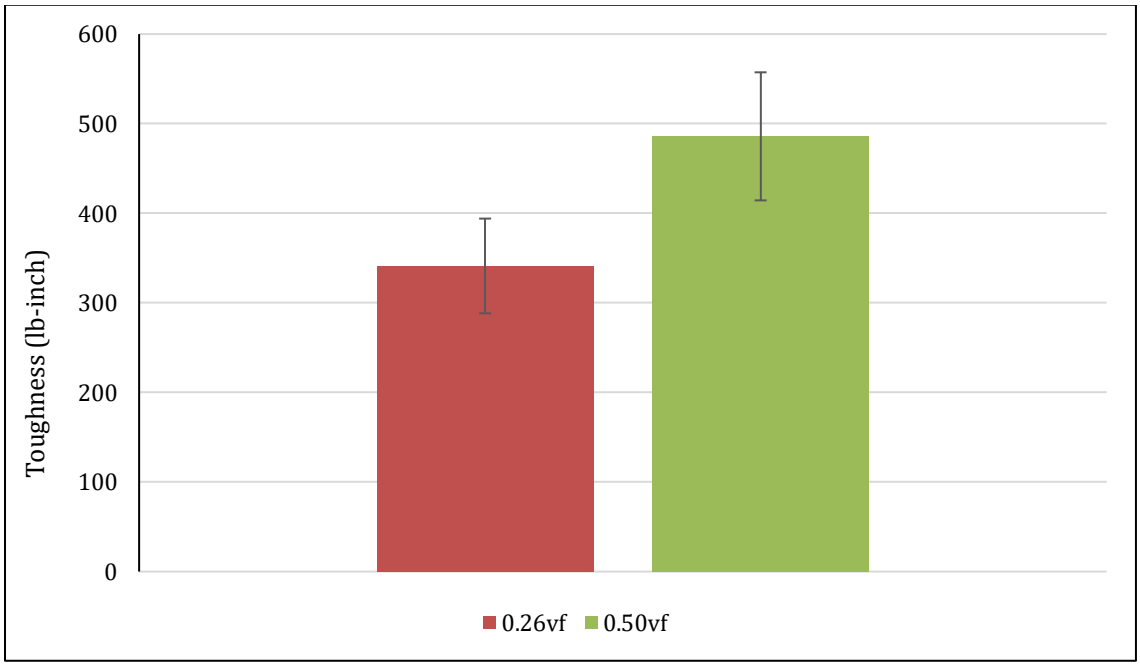

Figure 4-26. Influence of Fiber Dosage on Toughness

Figure 4-27 shows that concrete mixes with Fiber 2 exhibited higher toughness than mixes with Fiber 1. The embossed and deformed texture and higher stiffness of Fiber 2 likely contributed to the higher toughness.

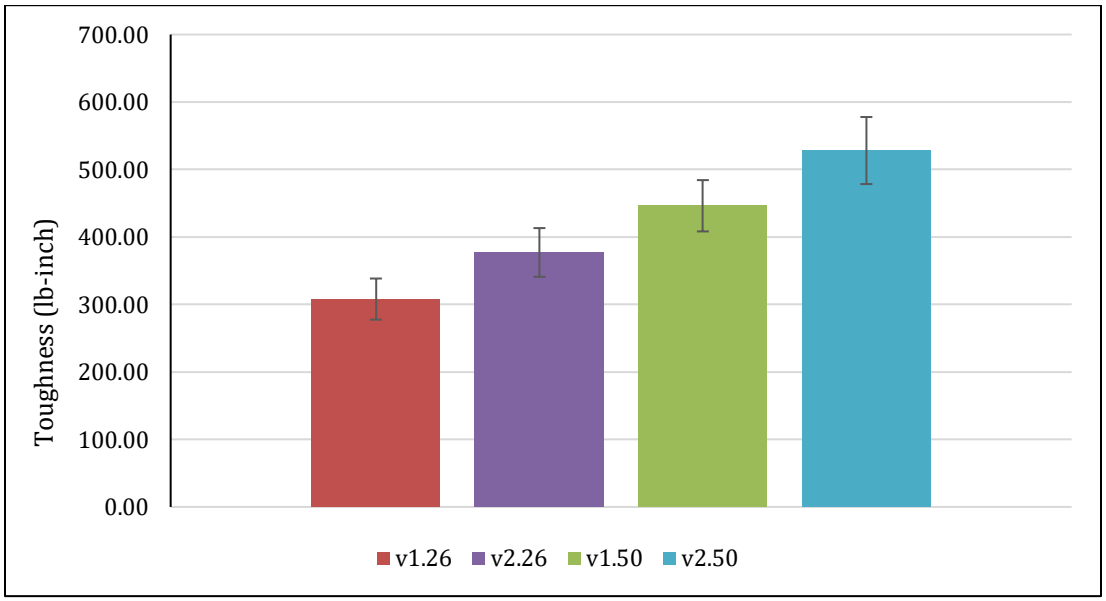

Figure 4-27. Influence of Fiber Type on Toughness

4.2.2.5 Residual Strength and Residual Strength Ratio (RSR)

Like the flexural toughness of concrete, the residual strength and RSR increased with the increase in fiber dosage (Figure 4-28 through Figure 4-31). The average RSR increased from 20% to 36% when the fiber dosage was increased from 0.26% to 0.50% V_f.

Fiber type also affects the residual strength and RSR values. At a dosage of 0.26% V_f, the RSR is slightly higher for Fiber 2 (23%) than Fiber 1 (17%). Increasing the dosage to 0.50% V_f improves the RSR of Fiber 1 and Fiber 2 to 31% and 41%, respectively.

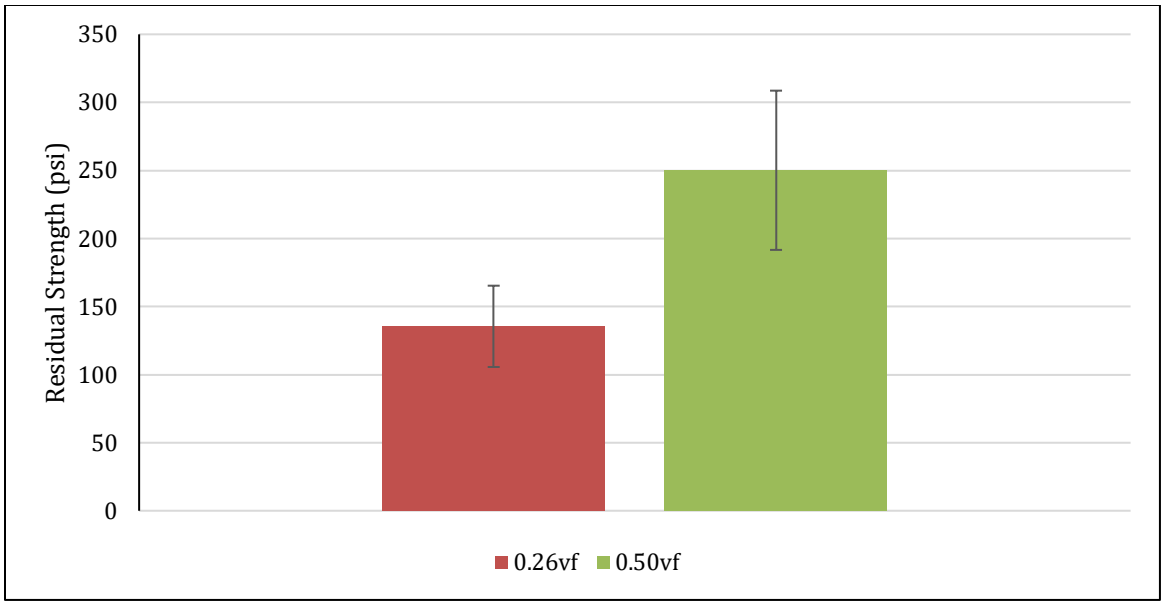

Figure 4-28. Influence of Fiber Dosage on Residual Strength

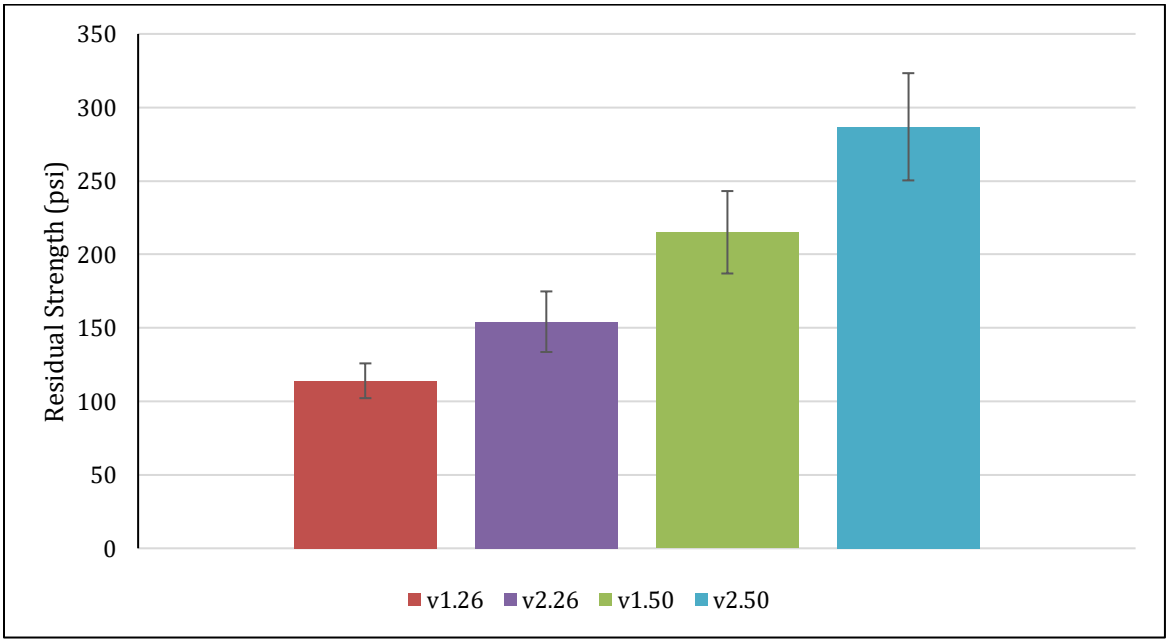

Figure 4-29. Influence of Fiber Type on Residual Strength

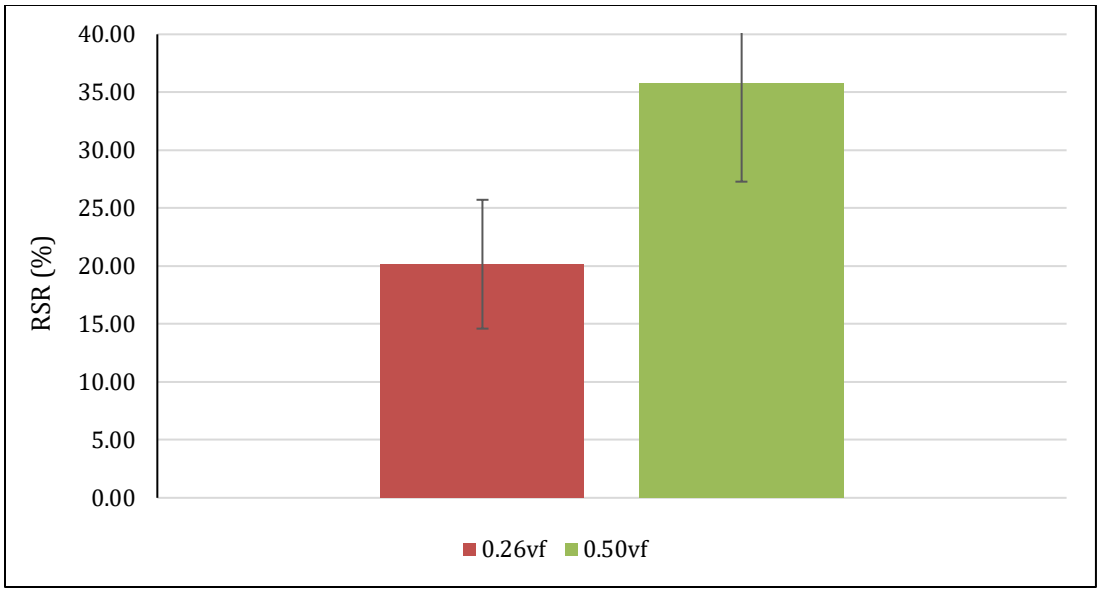

Figure 4-30. Influence of Fiber Dosage on RSR

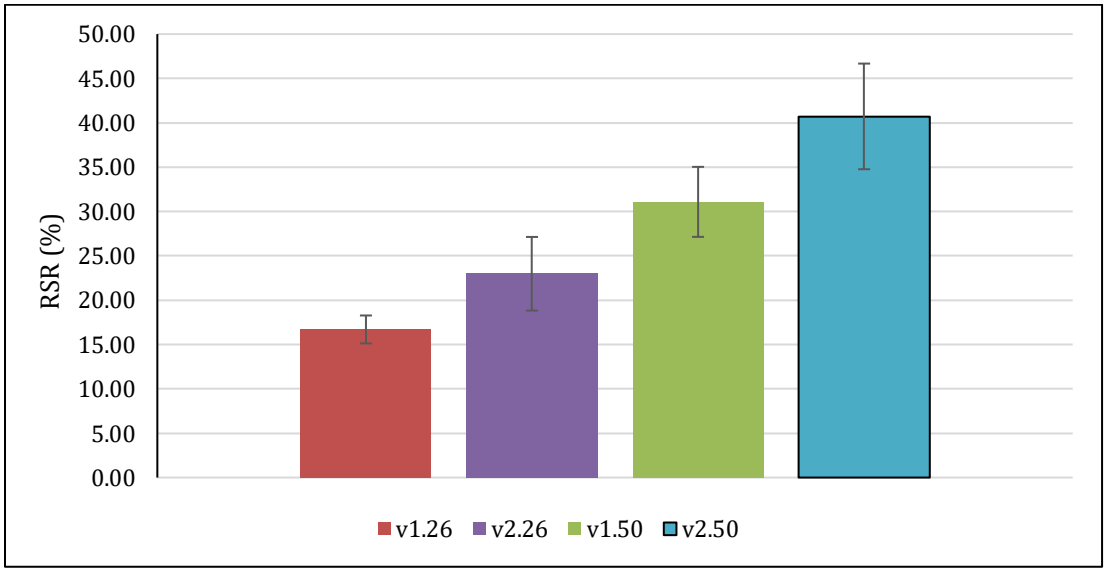

Figure 4-31. Influence of Fiber Type on RSR

4.2.2.6 Electrical Resistivity

The electrical resistivity of concrete provides an assessment of the resistance of concrete against the chloride-ion penetration. The factors such as specimen age, geometry, curing condition, and concrete properties can impact the resistivity of concrete. In this study, two different sets of specimens were used to study the electrical resistivity of the concrete: (i) Set A- concrete specimens cured in a calcium hydroxide saturated simulated pore solution for seven days (referred to as bucket test), and (ii) Set B-

concrete specimens cured in a moist room for 28 days (20^0C and 95 relative humidity). Some specimens of Set A were also tested at 28 days.

4.2.2.7 Set-A (Calcium Hydroxide Saturated Specimen)

Table 4-4 shows the resistivity limits for a saturated specimen (ASTM C1202) for different levels of permeabilities. A specimen is considered fully saturated after it is submerged in a pore solution for a minimum of 6 days. The electrical resistivity values shown in Table 4-5 are the 7-day and 28-day resistivity measurements for several mixes, with and without fibers. It is seen that after seven days of curing, concrete specimens have resistivity readings that correspond to moderate to the low penetrability of chloride ions. After 28 days of curing, concrete specimens have resistivity readings that correspond to the low penetrability of chloride ions. Figure 4-32 and Figure 4-33 show the penetrability according to ASTM C1202 (Table 4-4) of the specimens in Table 4-5.

Generally, concrete resistivity increases as the specimen ages until it reaches a nick point. All specimens tested showed low-to-moderate penetrability, which indicates that the concrete specimens produced in this study as per PEM will not be vulnerable to chloride ion penetration.

Table 4-4. Performance Limits from the Rapid Chloride Permeability Test (RCPT), along with Equivalent Resistivity Values of a Saturated System (ASTM C1202)

ASTM C1202 Classification[1]	Charge Passed (Coulombs)[1]	Resistivity (kOhm·cm)[2]
High	>4,000	<5.2
Moderate	2,000–4,000	5.2–10.4
Low	1,000–2,000	10.4–20.7
Very low	100–1,000	20.7–207
Negligible	<100	>207

[1]From ASTM C1202-12.
[2]Calculated using first principles.

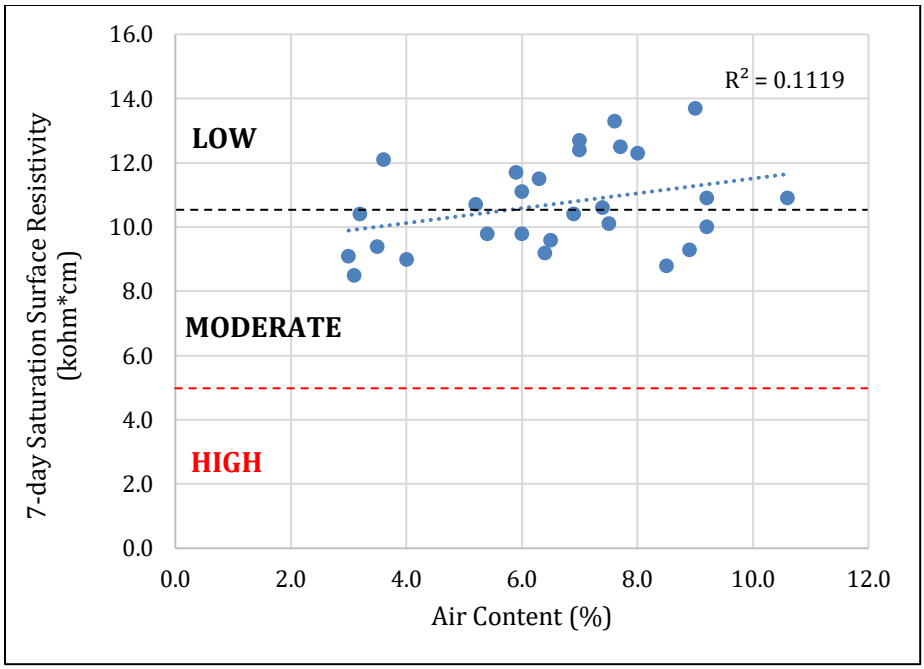

Figure 4-32. Saturated Surface Resistivity vs Air Content

Table 4-5. Resistivity Values of Calcium Hydroxide Saturated Specimens

Mixture	Air (%)	Resistivity values (kΩ/cm)		
		Initial	Final (after 7 days)	Final (after 28 days)
6A2.26	7.0	6.7	12.4	Not tested (NT)
8A2.26	7.7	7.3	12.5	NT
8A2.26 (2)	7.6	7.9	13.3	NT
6A2.50	6.3	7.5	11.5	NT
8AP	9.0	9.3	13.7	18.0
6AP	7.0	8.3	12.7	18.6
8AP (2)	10.6	8.7	10.9	NT
6AP (2)	6.0	9.5	9.8	NT
6BP	5.4	7.4	9.8	NT
4B1.26	3.5	7.4	9.4	NT
6B1.26	6.9	7.4	10.4	NT
8B1.26	8.5	5.3	8.8	NT
4B1.50	4.0	6.9	9.0	NT
6B1.50	6.4	5.8	9.2	NT
8B1.50	8.9	7.6	9.3	NT
8BP	7.5	9.0	10.1	13.3
4BP	3.0	7.4	9.1	11.6
8B2.50	9.2	7.2	10.9	13.1
6B2.26	6.5	7.7	9.6	13.2
4B2.26	3.1	9.0	8.5	11.1
6C1.50	6.0	6.2	11.1	NT
4C1.50	3.2	9.4	10.4	NT
6C2.50	5.2	10.4	10.7	14.8
8C2.50	7.4	8.9	10.6	13.7
6C2.26	5.9	9.2	11.7	13.6
4C2.26	3.6	7.4	12.1	13.1
8C2.26	8.0	12.5	12.3	16.2
8C2.26 (2)	9.2	7.0	10.0	NT

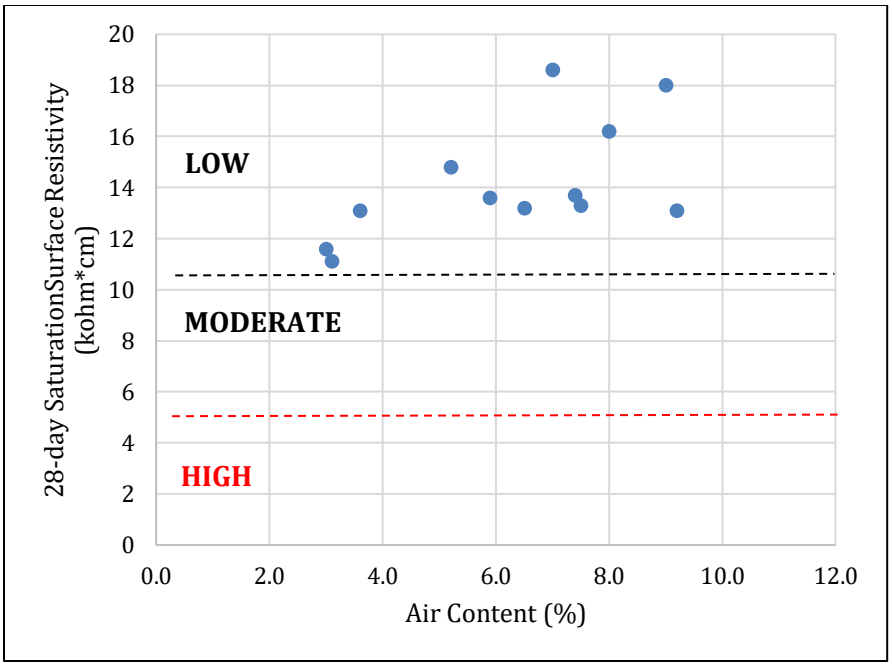

Figure 4-33. 28-day Saturated Surface Resistivity vs Air Content

4.2.2.8 Set-B (Moist Cured Samples)

Table 4-6 shows the 28-day resistivity classification of chloride-ion penetrability of specimens cured in a moist room based on the specimen geometry (AASHTO TP 95). Figure 4-34 shows that the concrete specimens tested in this study, irrespective of plain or fiber reinforced concretes, exhibited low chloride ion penetration. It is observed that the mixes designed in accordance with PEM requirements have better resistance to the penetration of chloride ions compared to the concrete mix, which was not designed according to the PEM method. For example, the two MnROAD samples included in this study showed high chloride ion penetration potential (<12 kohm.cm). Like the calcium hydroxide saturated specimen, the resistivity results for the moist cured specimen also indicate that the addition of macro synthetic fibers into the mixture has no significant effect on resistivity readings.

Table 4-6. Chloride-ion Penetration Classification (AASHTO TP 95)

Chloride Ion Penetrability	Surface Resistivity Test	
	4 inch X 8 inch Cylinder (KOhm-cm) a=1.5	6 inch X 12 inch Cylinder (KOhm-cm) a=1.5
High	< 12.0	< 9.5
Moderate	12.0 – 21.0	9.5 - 16.5
Low	21.0 – 37.0	16.5 – 29.0
Very Low	37.0 – 254.0	29.0 – 199.0
Negligible	> 254.0	> 199.0

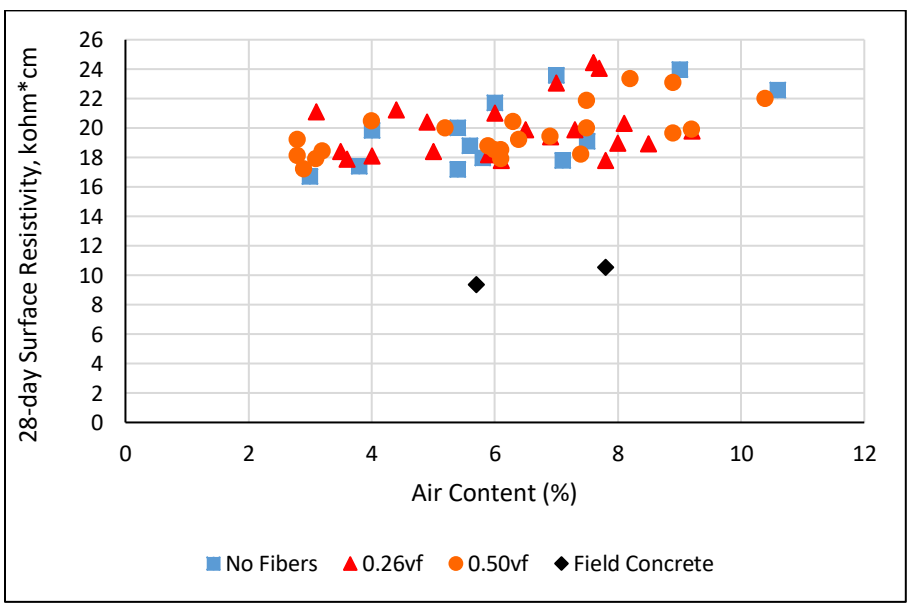

Figure 4-34. Surface Resistivity vs. Air Content

4.2.2.9 Freeze-Thaw Durability

Concrete with a Relative Dynamic Modulus (RDM) value greater than 60% after 300 freeze-thaw cycles is considered to have good resistivity against freeze-thaw exposure (ASTM C666). Figure 4-35 depicts that every specimen tested in the current study satisfies the 60% RDM minimum criterion by a large margin, indicating that the mixes prepared with the PEM method can produce mixes that can offer excellent resistance to freeze-thaw, irrespective of the plain or fiber reinforced concrete.

This finding agrees with Komatska and Wilson's (2016) study, which states that adding fibers does not compromise the concrete structure's freeze-thaw durability, provided that it is air-entrained, compacted adequately, and modified to integrate fibers. One surprising observation from the freeze-thaw test result is that the RDM did not decrease with the freeze-thaw cycles; this trend is not unique, and other researchers also observed a similar trend; for example, Al-Assadi et al. (2015) also did not observe a decrease in the RDM in their study.

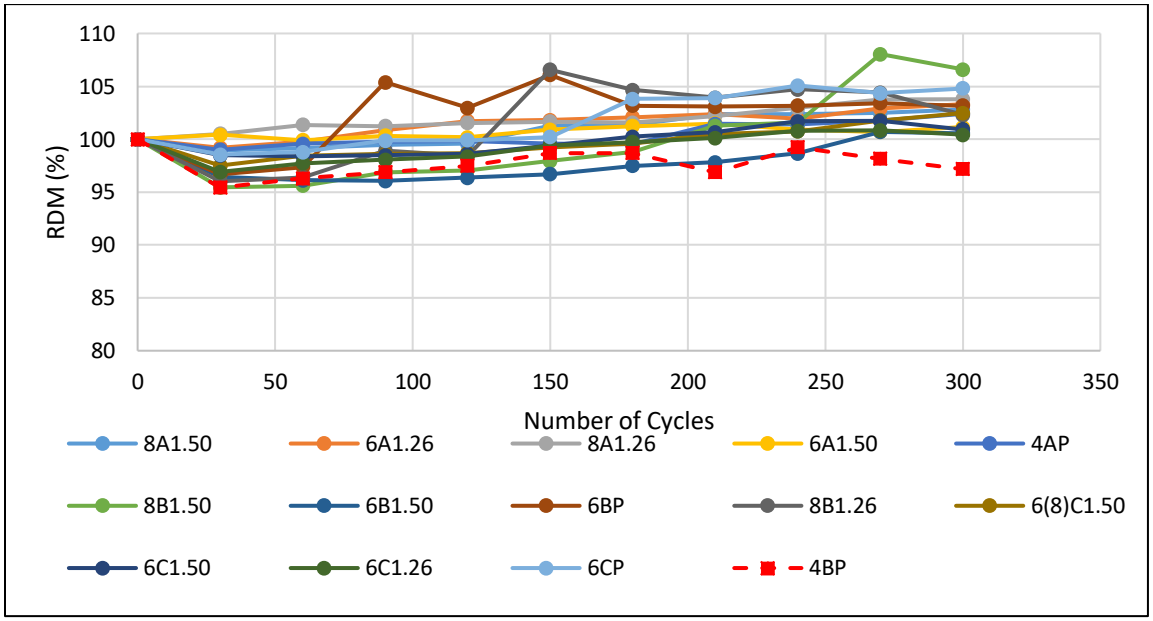

Figure 4-35. Relative Dynamic Modulus (RDM) vs. Number of F/T Cycles

CHAPTER 5: CONCLUSIONS AND RECOMMENDATIONS

5.1 CONCLUSIONS

Structural fibers are used in concrete mixtures to improve the long-term performance of concrete pavements and overlays. Fiber-reinforced concrete enhances the structural integrity of the concrete. In addition to using structural fibers in concrete pavements, this study implements the PEM procedure to assess the quality of concrete based on various factors affecting the performance of concrete in the field during pouring and throughout its service life. PEM mixture design produces concrete pavements that are resistant to weather- and material-related distresses by assessing key engineering parameters that determine the serviceability of concrete pavements. By studying the PEM design procedure with FRC through laboratory experiments, this research investigates the effect of fiber dosage, type, and geometry on SAM number, V-Kelly index, V-Kelly slump, box test visual rating, electrical surface resistivity, compressive strength, modulus of elasticity, modulus of rupture, residual strength, residual strength ratio, post-crack toughness, and freeze-thaw durability. Based on the test results, the following conclusions are made:

- This study's limited fiber dosage variation did not significantly influence the SAM number. A large set of SAM number values were close to 0.20, the recommended maximum value for plain concrete. An increase in entrained air content decreased the SAM number. Mixes with less than 5.5% air content consistently showed a very high SAM number. Between the three aggregates used in this study, mixes with Aggregate C-gravel showed a lower SAM number than the other two mixes.
- The addition of fibers in the mixture has a very significant influence on the V-Kelly index. Mixtures with fiber dosage of 0.26% volume fraction had a V-Kelly index slightly below 0.8 in/√s (the recommended minimum value for plain concrete). Mixtures with fiber dosage of 0.50% volume fraction were further below that.
- Fiber type did not show a significant influence on the V-Kelly index. Mixes with Aggregate Class C showed a higher V-Kelly index than the mixes with the two other aggregate types.
- An increase in fiber dosage generally increased the box test rating. The influence of fiber dosage was more evident in mixes with a 0.50% V_f than in the other mixes. Some mixes with 0.5% V_f had visual ratings of more than 2 (high surface air voids). Aggregate C (gravel) mixes showed the least box test rating relative to the two other aggregate types.
- Structural synthetic fibers have a minimal effect on compressive strength and modulus of elasticity. Aggregate types had some influence on compressive strength. Mixes with limestone Class B-aggregate had higher compressive strength than identical mixes with granite Class A-aggregate and gravel Class C-aggregate due to the higher percentage of coarse aggregates and higher specific gravity. Aggregate C-gravel resulted in the lowest compressive strength.
- MOR remained minimally influenced by the volume fraction of synthetic fibers.
- The fiber dosage and type influenced the post-crack behavior and flexural toughness of hardened concrete. The average RSR improved from 20% to 36% when the fiber dosage increased from 0.26% to 0.50% V_f. The concrete mixes with Fiber 2 (embossed geometry) exhibited higher toughness than mixes with Fiber 1 for a given dosage. The embossed and deformed texture and higher stiffness of

Fiber 2 likely contributed to the higher toughness. The types of aggregates used did not show any considerable variation in the concrete toughness.

- The resistivity results indicated that synthetic fibers had no considerable effect on the resistivity readings. All mixes prepared in this study, irrespective of the inclusion of fibers, resulted in concretes with low chloride ion penetrability.
- The relative dynamic modulus (RDM) values obtained from the rapid freeze-thaw test indicated that the addition of fiber did not influence the resistance of concrete to freeze-thaw durability issues.

5.2 RECOMMENDATIONS

This study aimed to determine the allowable range of fresh concrete properties such as SAM number, box test rating, and V-Kelly index for fiber reinforced concrete to be designed as per performance engineered mixture design procedure. This study provided the following recommendations on the allowable range of the three fresh concrete properties mentioned above.

5.2.1 SAM Number

Under this project's scope, concrete mixes were prepared with many variables, as discussed in Chapter 3 of this report. For comparison purposes, mixes were prepared for three design air contents, 4%, 6%, and 8%. The average SAM numbers for plain concrete, 0.26% V_f and 0.50% V_f FRC mixes are 0.22, 0.20, 0.21, with standard deviations of 0.05 (COV= 23%), 0.09 (COV= 45%), and 0.06 (COV= 29%), respectively. A comprehensive discussion of the SAM results with respect to the fiber type, fiber dosage, aggregate type, and air content was presented in Chapter 4. The aggregate type did not consistently affect the SAM number test results. In general, when the ingredients like aggregates and cementitious materials were kept the same, FRC mixes needed additional water reducer admixture compared to their plain concrete counterpart to achieve comparable workability and air content.

Based on the analysis of the SAM number test results for two different fiber types and dosages and aggregate types, it can be stated that if the air content is 5.5% or more and the workability of the mixes is acceptable for paving, the SAM numbers between the plain and FRC mixes (synthetic fibers) will be comparable, with a slightly higher value for the FRC mixes.

The electrical resistivity and freeze-thaw tests conducted in this study revealed that synthetic fibers have a negligible effect on concrete durability. Most of the plain and FRC mixes prepared in this study showed low to moderate permeability.

As the concrete mixes prepared in this study did not show any considerable durability issues, at least in the laboratory condition, this study suggests that the SAM number of FRC may be accepted above 0.2 (recommended for plain concrete mixes) when the mixes are designed as per the PEM method. This study recommends a SAM number value of 0.3 (maximum) for the FRC mixes. The recommended SAM number 0.3 is approximately equal to the average of the SAM numbers of the FRC mixes plus one standard deviation (68% probability). As mentioned before, the standard deviations of the SAM number for the concrete mixes are pretty high (COV = 29% and 45% for FRC mixes); therefore, it will be

challenging to achieve a strict target value close to the average of the results like 0.22 or 0.21. As the FRC mixes with even a higher SAM number (>0.3) produced in this study did not show any detrimental effect on the strength and durability, a SAM number of 0.3 may be considered acceptable and achievable (68% probability), and at the same time, mixes will assure sufficient freeze-thaw resistance.

5.2.2 Box Test Rating

It was found that the inclusion of fiber dosage by 0.5% V_f increased the box test rating, indicating more surface voids. The box test rating for plain concrete and 0.26% V_f FRC mixes were comparable. Some concrete mixes with 0.5% V_f had visual ratings of 3. The average box test results for the concrete mixes with gravel aggregate were lower than the mixes with crushed granite and limestone. Based on the results of this study, it is recommended that when the fiber dosage is around 0.5% V_f or higher and crushed aggregates are used in the mix, the additional amount of water reducer shall be considered to adjust the workability.

5.2.3 V-Kelly Test

The study revealed that the V-Kelly index is a good indicator to account for the influence of the fiber on the workability of the pavement concrete. A V-Kelly index between 0.8 to 1.2 in/√s is recommended for the plain concrete mixture for slip-form paving.

This study shows that the V-Kelly index decreases with increased fiber dosage. This is evident during mixing as the mixture becomes stiffer with increases in fiber dosage due to decreased mixture workability. The average V-Kelly index for plain concrete is 1.11 in/√s, within the recommended range. The average V-Kelly index for FRC mixes with 0.26% V_f fiber dosage is 0.84 in/√s, at the low end of the recommended range. Mixes with fiber dosage of 0.50% V_f show an even lower V-Kelly index of 0.59 in/√s. This indicates that the addition of fibers in the mixture influences the V-Kelly index and workability of the concrete under vibration. Therefore, when fibers are used in the mixes, additional effort should be given to improve the workability of the concrete so that the V-Kelly index can be improved to meet the target V-Kelly index of 0.8 in/√s or more. It may also happen that FRC does not need to meet the 0.8 in/√s criterion, as the fibers in the concrete offer resistance to the penetration of the Kelly-ball, which decreases the V-Kelly index. The hard concrete and durability test results for the FRC mixes indicate FRC mixes with a lower V-Kelly index pass the strength and durability criteria. However, it is impossible to make any firm recommendation about the workability or finishability of the FRC mixes for the slip form paving if the V-Kelly index is lower than 0.6 in/√s. V-Kelly test results also show that the fiber type has no significant influence on the V-Kelly index, at least for the two fibers used in this study, but the fiber dosage does. The V-Kelly indexes for mixes with granite and limestone aggregates are comparable; mixes with gravel aggregates result in a higher V-Kelly index for the three types of aggregates.

REFERENCES

1. ACI. (2018). *Guide to Design with Fiber-Reinforced Concrete.* American Concrete Institute Committee 544, Farmington Hills, MI.
2. Acikgenc, M., Alyamac, K. E., & Ulucan, Z. C. (2013). *Fresh and Hardened Properties of Steel Fiber Reinforced Concrete Produced with Fibers of Different Lengths and Diameters*. Paper presented at the 2nd International Balkans Conference on Challenges of Civil Engineering, BCCCE, 23-25 May 2013, Epoka University, Tirana, Albania.
3. Al-Assadi, G., Casati, M.J., Gálvez, J.C., Fernández, J., & Aparicio, S. (2015). *The Influence of the Curing Conditions of Concrete on Durability after Freeze-Thaw Accelerated Testing*. *Mater. Construcc. 65 [320], e067*. http://dx.doi.org/10.3989/mc.2015.06514
4. Barman, M. (2014). *Joint Performance Characterization of Bonded Concrete Overlay*, Ph.D. Dissertation, Department of Civil and Environmental Engineering, University of Pittsburgh, Pittsburgh, PA.
5. Barman, M., & Hansen, B. (2018). *Comparison of Performances of Structural Fibers and Development of a Specification for Using Them in Thin Concrete Overlays*. Minnesota Department of Transportation, St. Paul., MN.
6. Barman, M., Crick, C., & Burnham, T. (2019). *Performance Benefits of Fiber-reinforced Thin Concrete Pavement and Overlays* (Task-2: First Year Annual Cell Performance Report). Minnesota Department of Transportation, St. Paul, MN.
7. Barman M., Hansen B., & Arepalli, U. (2018). *Performance Benefits of Fibers-Reinforced Thin Concrete Pavement and Overlays* (NRRA Long-term Research Project). Minnesota Department of Transportation, St. Paul, MN.
8. Barman, M., Vandenbossche, J. M., & Li, Z. (2017). Influence of Interface Bond on the Performance of Bonded Concrete Overlays on Asphalt Pavements. *Journal of Transportation Engineering, Part B: Pavements, ASC*E, 143(3).
9. Cackler, T., Harrington, D., & Taylor, P. C. (2017). *Performance Engineered Mixture (PEM) for Concrete Pavement*, CP Road Map, National Concrete Pavement Technology Center, Ames, IA.
10. Cook D., Ghaeezadeh A., Ley T., & Russell, B. (2013). Investigation of Optimized Graded concrete for Oklahoma-Phase I. Oklahoma State University, Stillwater, OK.
11. Cook, D., Ghaeezadah, A., & Ley, T. (2014). A Workability Test for Slip Formed Concrete Pavements. *Construction and Building Materials, 68*, 376–383.
12. Delatte, N. (2007). *Concrete Pavement Design, Construction, and Performance*. CRC Press, Taylor & Francis.Boca Raton, FL
13. Dhir, R. K., McCarthy, M. J., Zhou, S., &Tittle, P. A. J. (2006). Discussion: Role of Cement Content in Specifications for Concrete Durability: Aggregate Type Influences. *Structures & Buildings, 159,* 361-363.
14. Issa, M., A. (2017). Effect of Early-Age Concrete Elastic Properties on Fatigue Damage in PCC Pavements Containing Fibers (Publication FHWA-ICT-17-019). Illinois Center for Transportation, Chicago, IL.
15. Kosmatka, S. H., & Wilson, M. L. (2016). *Design and Control of Concrete Mixtures*. Portland Cement Association, Skokie, IL.
16. Ley, T. (2015). *Producing Freeze-Thaw Durable Concrete* (pp. 1–3), CP RoadMap. National Concrete Pavement Technology Center, Ames, IA.

17. Ley, T., & Cook, D. (2014). *Aggregate Gradations for Concrete Pavement Mixtures*, CP Road Map. National Concrete Pavement Technology Center, Ames, IA.
18. MnDOT. (2017). MnROAD concrete special provision. (Table 2301). St. Paul, MN: MnDOT.
19. Superairmeter. (2015). *Operating Instruction*. Retrieved from https://myerstest.com/wp-content/uploads/2016/06/Super-Air-Meter-manual-vers-3-2_15-1.pdf
20. Taylor, P. C. (2013). *Long-Life Concrete: How Long Will My Concrete Last?* National Concrete Pavement Technology Center, Ames, IA.
21. Taylor, P. (2017). *Performance Engineering Mixtures Program*. National Concrete Pavement Technology Center, Ames, IA.
22. Taylor, P. C., Yurdakul, E., & Ceylan, H. (2014). *Performance Engineered Mixtures for Concrete Pavements in the US*. National Concrete Pavement Technology Center, Ames, IA.
23. Weiss, J. (2014). *Relating Transport Properties to Performance in Concrete Pavements*, CP RoadMap. National Concrete Pavement Technology Center, Ames, IA.
24. Erntroy, H., & Shacklock, B.W. (1954-May). Design of High-Strength Concrete Mixes. Paper presented at the Symposium on Mix Design and Quality Control of Concrete, London, Cement and Concrete Association.
25. Neville, A. M. (1996). *Properties of Concrete*. Hoboken, NJ: John Wiley & Sons.

APPENDIX A
MISCELLENIOUS DATA

Table A-1. Fly Ash Compositions

BORAL RESOURCES

Materials Testing & Research Facility
2650 Old State Hwy 113
Taylorsville, GA 30178
770-684-0102

ASTM C618 / AASHTO M295 Testing of Coal Creek Station Fly Ash

Sample Date: 2/25 - 3/1/19 **Report Date:** 4/17/2019
Sample Type: composite **MTRF ID:** 1284CC
Sample ID:

Chemical Analysis	Results		ASTM Limit Class F/C	AASHTO Limit Class F/C
Silicon Dioxide (SiO2)	52.75	%		
Aluminum Oxide (Al2O3)	15.44	%		
Iron Oxide (Fe2O3)	4.95	%		
Sum (SiO2+Al2O3+Fe2O3)	73.14	%	70.0/50.0 min	70.0/50.0 min
Sulfur Trioxide (SO3)	0.66	%	5.0 max	5.0 max
Calcium Oxide (CaO)	13.02	%		
Magnesium Oxide (MgO)	4.41	%		
Sodium Oxide (Na2O)	2.92	%		
Potassium Oxide (K2O)	2.30	%		
Sodium Oxide Equivalent (Na2O+0.658K2O)	4.43	%		
Moisture	0.04	%	3.0 max	3.0 max
Loss on Ignition	0.09	%	6.0 max	5.0 max
Available Alkalies, as Na2Oe	1.52	%	Not Required	1.5 max* *when required by purchaser
Physical Analysis				
Fineness, % retained on 45-µm sieve	25.07	%	34 max	34 max
Fineness Uniformity	3.18	%	±5 max	±5 max
Strength Activity Index - 7 or 28 day requirement				
7 day, % of control	85	%	75 min	75 min
28 day, % of control	82	%	75 min	75 min
Water Requirement, % control	93	%	105 max	105 max
Autoclave Soundness	0.01	%	0.8 max	0.8 max
Density	2.56			
Density Uniformity	1.85	%	±5 max	±5 max

The test data listed herein was generated by applicable ASTM methods. The reported results pertain only to the sample(s) or lot(s) tested. This report cannot be reproduced without permission from Boral Resources.

Doug Rhodes, CET
Facility Manager

AASHTO ACCREDITED

Table A-2. Coarse Aggregate Sieve Analysis Results

Sieves			Class A		Class B		Class C	
			¾-inch	1 ½-inch	¾-inch	1 ½-inch	¾-inch	1 ½-inch
mm	***in.***	***No.***	**Cumulative percent passing**					
50	2	2	100.00	100.00	100.00	100.00	100.00	100.00
37.5	1.5	1.5	100.00	91.77	00.00	99.81	100.00	99.81
25	1	1	100.00	36.99	100.00	62.93	100.00	62.93
19	0.75	0.75	99.71	6.57	91.00	18.07	91.00	18.07
12.5	0.5	0.5	53.40	0.69	53.03	0.97	53.03	0.97
9.5	0.375	0.375	21.15	0.63	32.42	0.56	32.42	0.56
4.75	0.187	No.4	1.34	0.62	2.91	0.56	2.91	0.56
2.36	0.093	No.8	0.50	0.61	0.60	0.55	0.60	0.55
1.18	0.046	No.16	0.49	0.59	0.58	0.54	0.58	0.54
0.6	0.024	No.30	0.46	0.56	0.55	0.53	0.55	0.53
0.3	0.012	No.50	0.40	0.49	0.50	0.51	0.50	0.51
0.15	0.006	No.100	0.33	0.38	0.45	0.47	0.45	0.47
0.075	0.003	No.200	0.21	0.23	0.35	0.40	0.35	0.40

Table A-3. Fine Aggregate Sieve Analysis Results

Sieves			Cumulative percent passing
mm	***in***	***No.***	
50	2	2	100.00
37.5	1.5	1.5	100.00
25	1	1	100.00
19	0.75	0.75	100.00
12.5	0.5	0.5	100.00
9.5	0.375	0.375	100.00
4.75	0.187	No.4	99.60
2.36	0.093	No.8	82.80
1.18	0.046	No.16	60.90
0.6	0.024	No.30	37.45
0.3	0.012	No.50	13.80
0.15	0.006	No.100	2.65
0.075	0.003	No.200	0.60

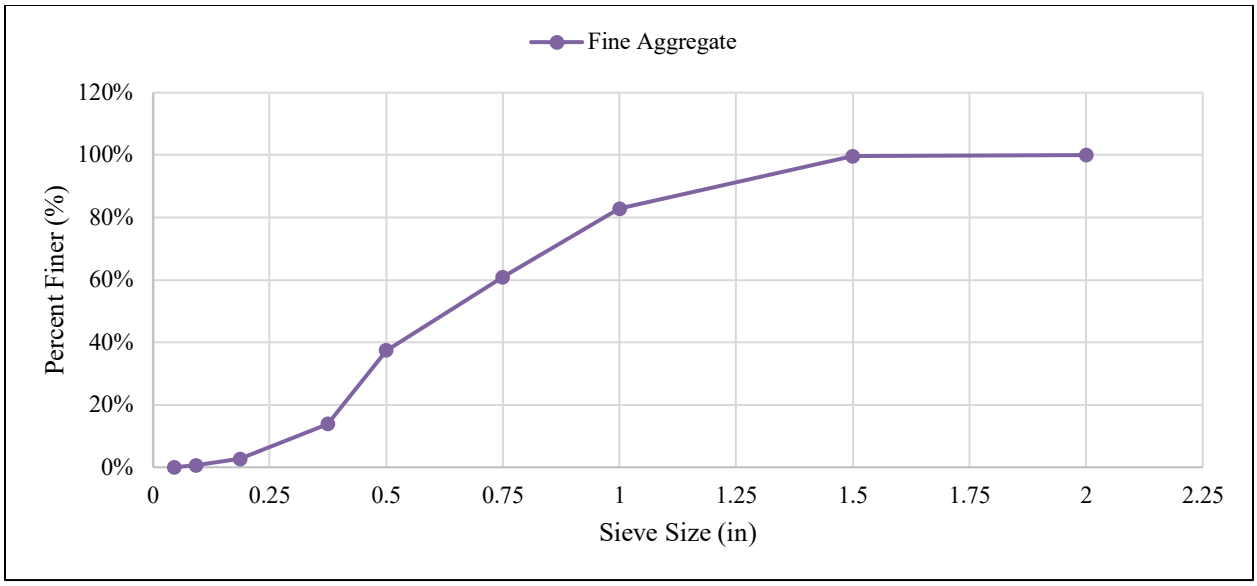

Figure A-1. Gradation for Fine Aggregate

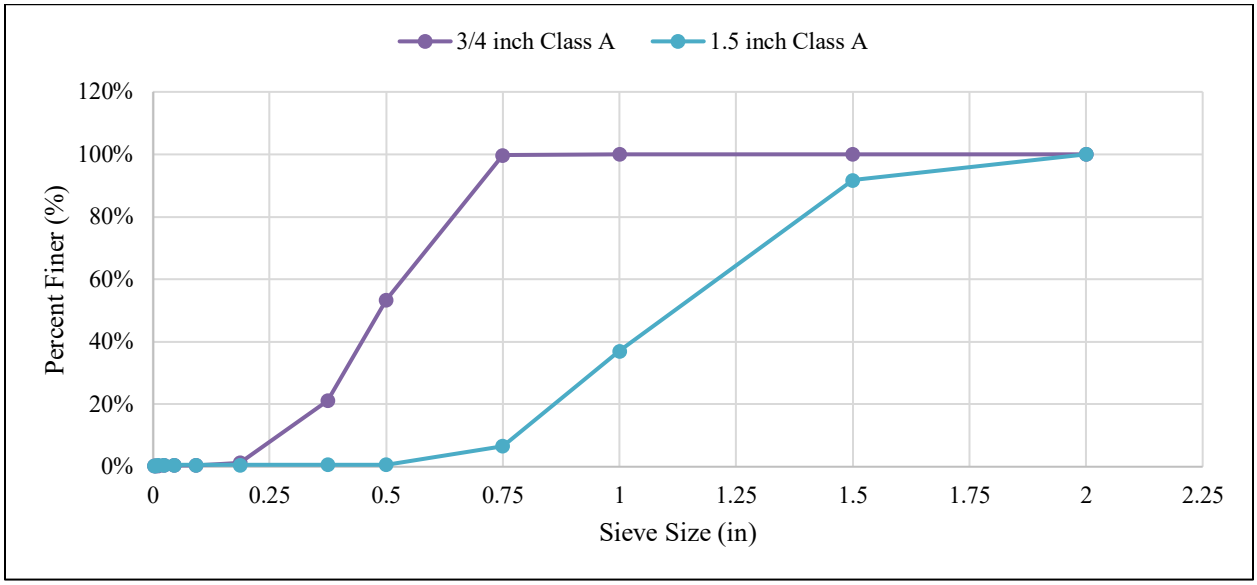

Figure A-2. Gradation for Class A Coarse Aggregates

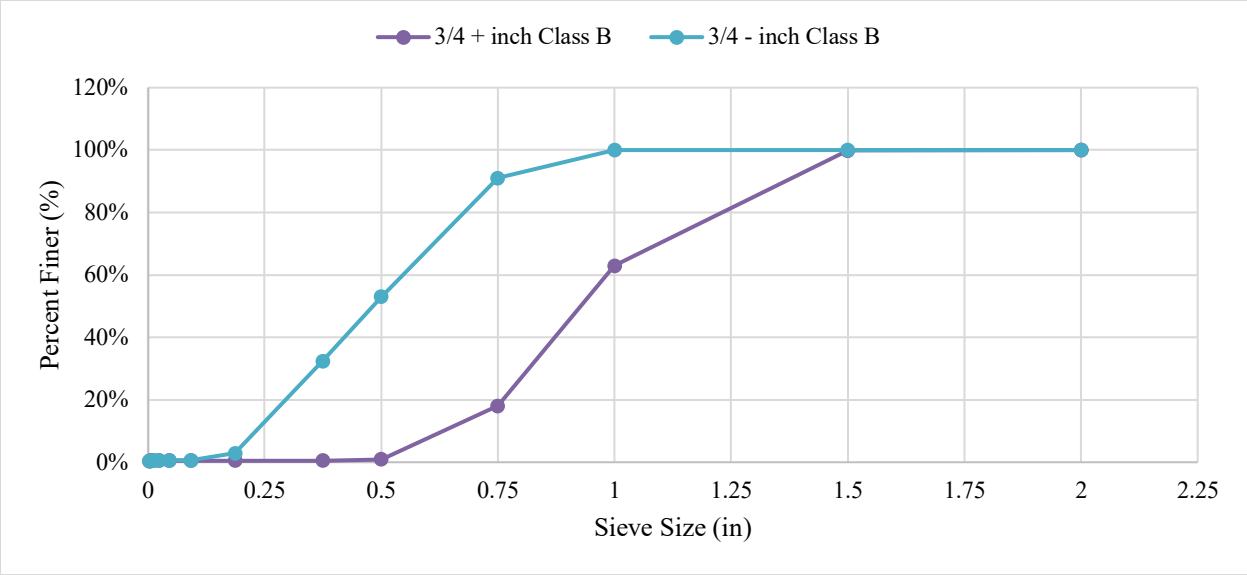

Figure A-3. Gradation for Class B Coarse Aggregates

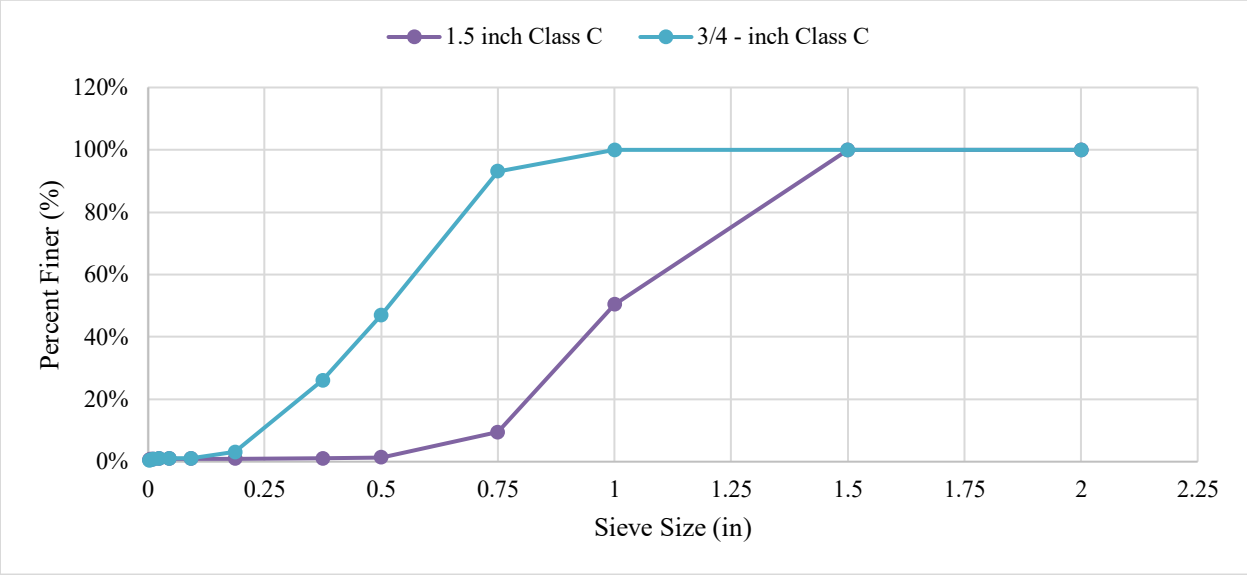

Figure A-4. Gradation for Class C Coarse Aggregates

Table A-4. General Mix Design for Aggregate A (8% Air)

Granite Class A Mixture Design (8% Air)			
	Volume (%)	**Mass (lb/Yd^3)**	**Aggregates Proportion by Volume (%)**
Cement (Type I)	8.29	440	-
Class A (¾”)	23.02	1047	34%
Class A (1.5”)	14.22	647	21%
Fine Aggregate	30.69	1386	45%
Potable Water	13.71	231	-
Fibers	Varied	Varied	-
Fly Ash	2.07	110	-
BASF MasterAir 400 (fl. Oz)	-	2.20	-
MasterPolyheed 1020 (fl. Oz)	-	8.80	-
Air	8	-	-
Paste	32.07	781	-

Table A-5. General Mix Design for Aggregate A (4% Air)

Granite Class A Mixture Design (4% Air)			
	Volume (%)	**Mass (lb/Yd^3)**	**Aggregates Proportion by Volume (%)**
Cement (Type I)	8.29	440	-
Class A (¾”)	24.37	1109	34%
Class A (1.5”)	15.05	685	21%
Fine Aggregate	32.50	1467	45%
Potable Water	13.71	231	-
Fibers	Varied	Varied	-
Fly Ash	2.07	110	-
BASF MasterAir 400 (fl. Oz)	-	0.45	-
MasterPolyheed 1020 (fl. Oz)	-	8.80	-
Air	4	-	-
Paste	28.07	781	-

Table A-6. General Mix Design for Aggregate B (8% Air)

Limestone Class B Mixture Design (8% Air)			
	Volume (%)	**Mass (lb/Yd^3)**	**Aggregates Proportion by Volume (%)**
Cement (Type I)	8.29	440	-
Class B (¾”)	26.99	1241f	40%
Class B (1.5”)	13.45	621	20%
Fine Aggregate	27.49	1241	40%
Potable Water	13.71	231	-
Fibers	Varied	Varied	-
Fly Ash	2.07	110	-
BASF MasterAir 400 (fl. Oz)	-	2.15	-
MasterPolyheed 1020 (fl. Oz)	-	10.00	-
Air	8	-	-
Paste	32.07	781	-

Table A-7. General Mix Design for Aggregate B (6% Air)

Limestone Class B Mixture Design (6% Air)			
	Volume (%)	**Mass (lb/Yd^3)**	**Aggregates Proportion by Volume (%)**
Cement (Type I)	8.29	440	-
Class B (¾”)	27.78	1278	40%
Class B (1.5”)	13.84	639	20%
Fine Aggregate	28.30	1278	40%
Potable Water	13.71	231	-
Fibers	Varied	Varied	-
Fly Ash	2.07	110	-
BASF MasterAir 400 (fl. Oz)	-	1.15	-
MasterPolyheed 1020 (fl. Oz)	-	13.20	-
Air	6	-	-
Paste	30.07	781	-

Table A-8. General Mix Design for Aggregate B (4% Air)

Limestone Class B Mixture Design (4% Air)			
	Volume (%)	**Mass (lb/Yd^3)**	**Aggregates Proportion by Volume (%)**
Cement (Type I)	8.29	440	-
Class B (¾”)	28.58	1314	40%
Class B (1.5”)	14.24	657	20%
Fine Aggregate	29.11	1314	40%
Potable Water	13.71	231	-
Fibers	Varied	Varied	-
Fly Ash	2.07	110	-
BASF MasterAir 400 (fl. Oz)	-	0.45	-
MasterPolyheed 1020 (fl. Oz)	-	10.00	-
Air	4	-	-
Paste	28.07	781	-

Table A-9. General Mix Design for Aggregate C (8% Air)

Gravel Class C Mixture Design (8% Air)			
	Volume (%)	**Mass (lb/Yd^3)**	**Aggregates Proportion by Volume (%)**
Cement (Type I)	8.29	440	-
Class C (¾”)	22.51	1013	33%
Class C (1.5”)	15.51	706	23%
Fine Aggregate	29.90	1350	44%
Potable Water	13.71	231	-
Fibers	Varied	Varied	-
Fly Ash	2.07	110	-
BASF MasterAir 400 (fl. Oz)	-	2.20	-
MasterPolyheed 1020 (fl. Oz)	-	8.80	-
Air	8	-	-
Paste	32.07	781	-

Table A-10. General Mix Design for Aggregate C (6% Air)

Gravel Class C Mixture Design (6% Air)			
	Volume (%)	**Mass (lb/Yd^3)**	**Aggregates Proportion by Volume (%)**
Cement (Type I)	8.29	440	-
Class C (¾”)	23.17	1042	33%
Class C (1.5”)	15.97	727	23%
Fine Aggregate	30.78	1390	44%
Potable Water	13.71	231	-
Fibers	Varied	Varied	-
Fly Ash	2.07	110	-
BASF MasterAir 400 (fl. Oz)	-	1.50	-
MasterPolyheed 1020 (fl. Oz)	-	8.80	-
Air	6	-	-
Paste	30.07	781	-

Table A-11. General Mix Design for Aggregate C (4% Air)

Gravel Class C Mixture Design (4% Air)			
	Volume (%)	**Mass (lb/Yd^3)**	**Aggregates Proportion by Volume (%)**
Cement (Type I)	8.29	440	-
Class C (¾”)	16.43	1072	33%
Class C (1.5”)	16.43	747	23%
Fine Aggregate	31.66	1430	44%
Potable Water	13.71	231	-
Fibers	Varied	Varied	-
Fly Ash	2.07	110	-
BASF MasterAir 400 (fl. Oz)	-	0.45	-
MasterPolyheed 1020 (fl. Oz)	-	8.80	-
Air	4	-	-
Paste	28.07	781	-